Supramolecular Fullerene Chemistry: A Comprehensive Study of Cyclophane-Type Mono- and Bis-Crown Ether Conjugates of C_{70}

by **Maurice J. van Eis**, **Paul Seiler**, **Liya A. Muslinkina**, **Martin Badertscher**, **Ernö Pretsch***, and **François Diederich***

Laboratorium für Organische Chemie, ETH-Hönggerberg, HCI, CH-8093 Zürich

Robert J. Alvarado and **Luis Echegoyen***

Department of Chemistry, Clemson University, Clemson, SC 29634, USA

and

Ignacio Pérez Núñez

Departamento de Química Fundamental, Universidade da Coruña, E-15071 A Coruña

Dedicated to Professor *Friedrich Bickelhaupt* on the occasion of his 70th birthday.

The covalently templated bis-functionalization of C_{70}, employing bis-malonate **5** tethered by an *anti*-disubstituted dibenzo[18]crown-6 (DB18C6) ether, proceeds with complete regiospecificity and provides two diastereoisomeric pairs of enantiomeric C_{70} crown ether conjugates, (±)-**7a** and (±)-**7b**, featuring a five o'clock bis-addition pattern that is disfavored in sequential transformations (*Scheme 1*). The identity of (±)-**7a** was revealed by X-ray crystal-structure analysis (*Fig. 6*). With bis-malonate **6** containing a *syn*-disubstituted DB18C6 tether, the regioselectivity of the macrocylization *via* double *Bingel* cyclopropanation changed completely, affording two constitutionally isomeric C_{70} crown ether conjugates in a *ca.* 1:1 ratio featuring the twelve (**16**) and two o'clock ((±)-**15**) addition patterns, respectively (*Scheme 3*). The X-ray crystal-structure analysis of the twelve o'clock bis-adduct **16** revealed that a H_2O molecule was included in the crown ether cavity (*Figs. 7* and *8*). Two sequential *Bingel* macrocyclizations, first with *anti*-DB18C6-tethered (**5**) and subsequently with *syn*-DB18C6-tethered (**6**) bis-malonates, provided access to the first fullerene bis-crown ether conjugates. The two diastereoisomeric pairs of enantiomers (±)-**28a** and (±)-**28b** were formed in high yield and with complete regioselectivity (*Scheme 9*). The cation-binding properties of all C_{70} crown-ether conjugates were determined with the help of ion-selective electrodes (ISEs). Mono-crown ether conjugates form stable 1:1 complexes with alkali-metal ions, whereas the tetrakis-adducts of C_{70}, featuring two covalently attached crown ethers, form stable 1:1 and 1:2 host-guest complexes (*Table 2*). Comparative studies showed that the conformation of the DB18C6 ionophore imposed by the macrocyclic bridging to the fullerene is not particularly favorable for strong association. Reference compound (±)-**22** (*Scheme 4*), in which the DB18C6 moiety is attached to the C_{70} sphere by a single bridge only and, therefore, possesses higher conformational flexibility, binds K^+ and Na^+ ions better by factors of 2 and 20, respectively. Electrochemical studies demonstrate that cation complexation at the crown ether site causes significant anodic shifts of the first reduction potential of the appended fullerene (*Table 3*). In case of the C_{70} mono-crown ether conjugates featuring a five o'clock functionalization pattern, addition of 1 equiv. of KPF_6 caused an anodic shift of the first reduction wave in the cyclic voltammogram (CV) by 70 to 80 mV, which is the result of the electrostatic effect of the K^+ ion bound closely to the fullerene core (*Fig. 14*). Addition of 2 equiv. of K^+ ions to C_{70} bis-crown ether conjugates resulted in the observation of only one redox couple, whose potential is anodically shifted by 170 mV with respect to the corresponding wave in the absence of the salt (*Fig. 16*). The synthesis and characterization of novel tris- and tetrakis-adducts of C_{70} are reported (*Schemes 5* and *6*). Attempts to prepare even more highly functionalized derivatives resulted in the formation of novel pentakis- and hexakis-adducts and a single heptakis-adduct (*Scheme 7*), which were characterized by ^{1}H- and ^{13}C-NMR spectroscopy (*Fig. 10*), as well as matrix-assisted laser-desorption-ionization mass spectrometry (MALDI-TOF-MS). Based on predictions from density-

functional-theory (DFT) calculations (*Figs. 12* and *13*), structures are proposed for the tris-, tetrakis-, and pentakis-adducts.

1. Introduction. – The first higher fullerene C_{70} [1] (*Fig. 1*) features, in many respects, similar reactivity to that displayed by the more-abundant buckminsterfullerene, C_{60} [2]. However, there are also marked differences. Whereas the more-symmetric I_h-C_{60} possesses only one type of C-atom and two different bond types (shorter 6-6 bonds at the junction between two hexagons and longer 6-5 bonds within pentagons), D_{5h}-C_{70} with lower symmetry features five types of C-atom (*a*–*e* in *Fig. 1,a*) and eight different bonds (four 6-6 and four 6-5 bonds). The different 6-6 bonds in C_{70} have been classified according to their local curvature as α-, β-, ε-, and $\varkappa$-type bonds (*Fig. 1,c*), with the degree of local curvature decreasing from α-type bonds located near the poles (*e.g.*, C(1)–C(2) (for the numbering, see [3])) to $\varkappa$-type bonds located at the equator of the C-sphere (*e.g.*, C(21)–C(22)) [4]. Increasing degree of local curvature correlates with increasing reactivity in nucleophilic attacks and cycloadditions to C_{70}: thus the *Bingel* monocyclopropanation [5a] occurs regioselectively at the α-type 6-6 bond C(1)–C(2) to give **1** (*Fig. 2*) [5b][6], whereas azomethine ylide 1,3-dipolar cycloadditions afford, as the major products, regioisomeric mono-adducts originating from attacks at α- (C(1)–C(2)) and β-type (C(5)–C(6)) bonds [7][8]. In addition to local curvature (the degree of pyramidalization of C-atoms can be quantified by the π-*o*rbital *a*xis *v*ector (POAV) angles introduced by *Haddon*; see [9–11]), high π-bond order is another factor favoring reactivity (in C_{70}, the C(5)–C(6) bond has the highest π-bond order, followed by the C(1)–C(2) bond; see [3a][12][13]).

Double *Bingel* cyclopropanations of C_{70} with diethyl malonate occur on opposite hemispheres at the most curved α-type bonds, yielding the three constitutional isomers **2**, (±)-**3**, and (±)-**4**, two of which are pairs of enantiomers due to the chirality of the addition pattern [5][6][14]. The isomeric ratio **2**/(±)-**3**/(±)-**4** is 2.8:6.8:1.0. In a *Newman*-type projection looking down the C_5 axis of the C_{70} core onto the two polar pentagons, the two addends in **2** adopt a twelve o'clock, those in (±)-**3** a two o'clock, and those in (±)-**4** a five o'clock geometrical relationship (*Fig. 2*). Similar addition patterns were also obtained in other bis-functionalization reactions, with the two o'clock geometric relationship being highly favored in each case [15–18]. This product distribution strongly deviates from the statistical 1:2:2 distribution. Since steric interactions between the addends are absent, electronic factors must be involved. Several theoretical investigations indeed support that the regioselectivity of multiple cyclopropanations of both C_{60} [19] and C_{70} [14] is governed by the frontier molecular orbitals of the fullerene core (see below).

The chemistry of even higher adducts of C_{70} is less well-developed [1][17][20]. Starting from twelve and five o'clock bis-adducts such as **2** and (±)-**3**, *Diederich* and co-workers prepared defined tris-, tetrakis-, and hexakis-adducts by sequential *Bingel* cyclopropanation [6][14]; in addition, they isolated pure heptakis- and octakis-adducts of yet unknown constitution.

Although the regioselectivity in sequential multiple functionalizations of C_{70} – with 6-6 bonds of different reactivity – generally is higher than in the corresponding reactions of C_{60}, isomeric mixtures are often obtained that are difficult to separate. In 1994, *Diederich* and co-workers introduced the tether-directed remote functionaliza-

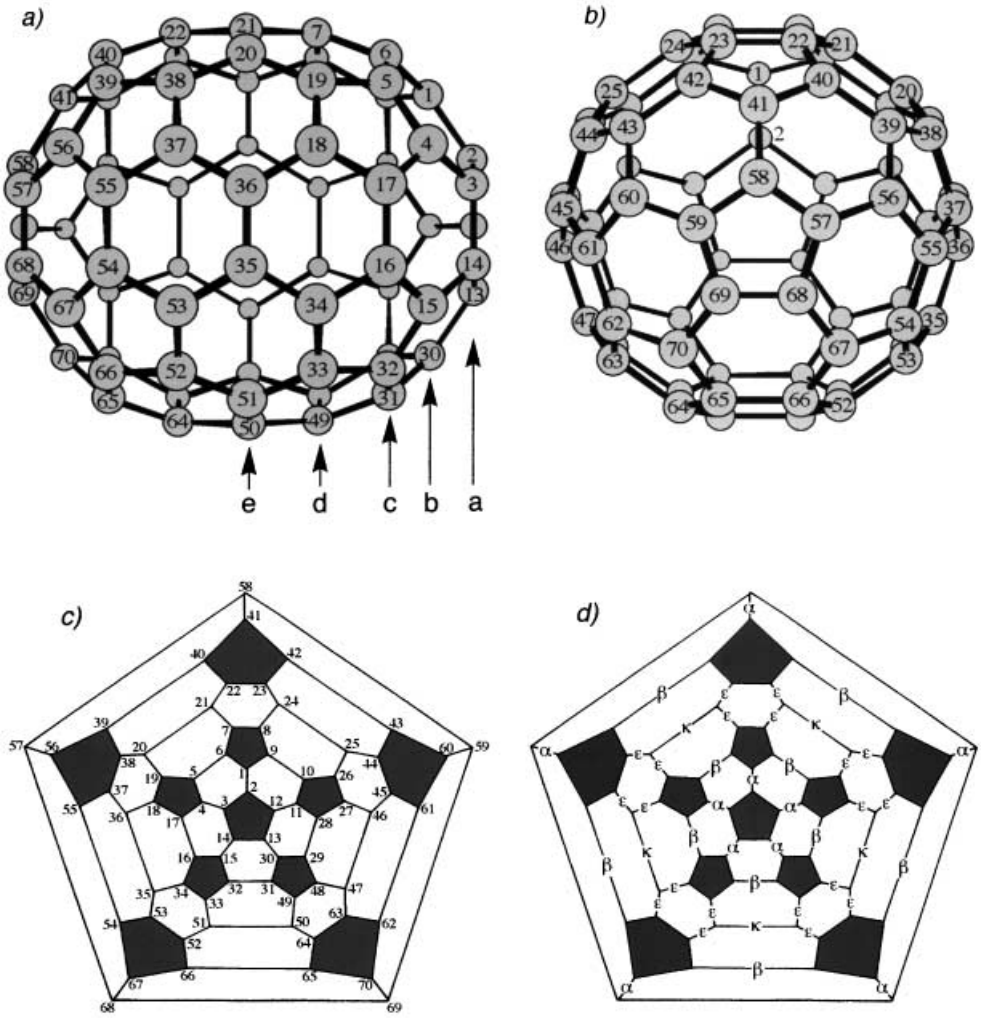

Fig. 1. *Views on* D_{5h}-C_{70} a) *perpendicular to* (indicating the five different types of C-atoms) *and* b) *along the* C_5-*symmetry axis, and* Schlegel *diagrams showing* c) *the numbering* (clockwise) *of the C-atoms and* d) *the four different types* $\alpha, \beta, \varepsilon,$ *and* $\varkappa$ *of 6-6 bonds.* The curvature and reactivity towards nucleophiles decreases from α- to $\varkappa$-type bonds.

tion technique as a general method to control regio- and stereoselectivity in covalent fullerene chemistry [21]. This strategy has proven to be a powerful tool in the multiple derivatization of C_{60} [22–26], but had not previously been applied to C_{70} or other higher fullerenes.

Here, we report the application of the tether-directed remote functionalization to prepare C_{70} bis- and tetrakis-adducts (for preliminary communications of parts of this work, see [27][28]). We show that crown ether tethered bis-malonates undergo highly regioselective macrocyclizations with the higher C-sphere, providing access to a new

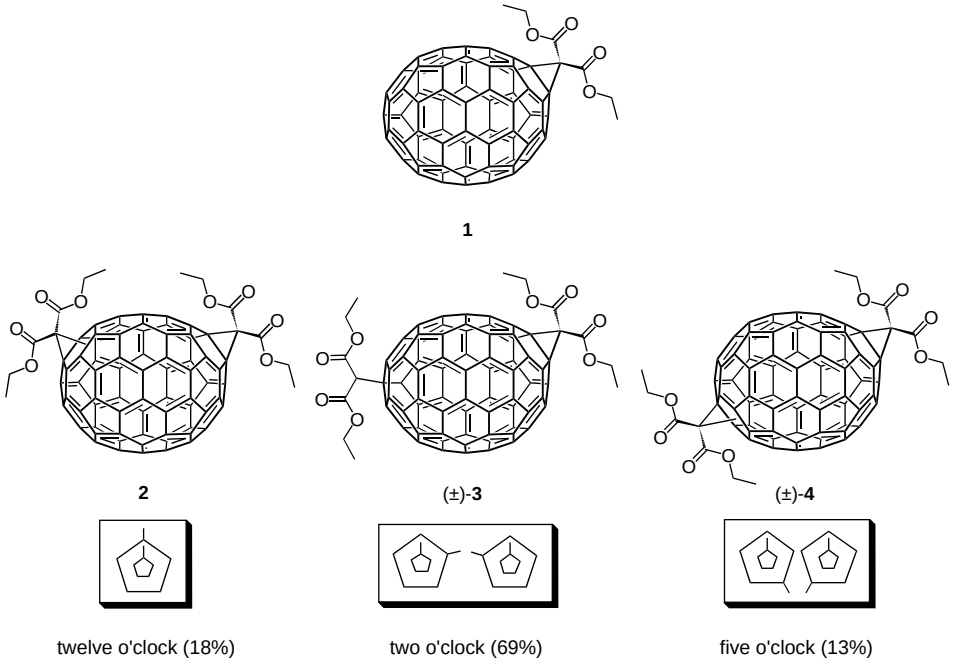

Fig. 2. *Mono-* (**1**) *and regioisomeric bis-adducts* (**2**, (±)-**3**, and (±)-**4**) *formed by* Bingel *cyclopropanation of* C_{70}. Also shown are *Newman*-type projections looking down the C_5-symmetry axis of the C_{70} core onto the two polar pentagons, which show the relative orientations of the addends.

series of mono- and bis-crown ether conjugates (for cyclophane-type crown ether conjugates of C_{60}, see [29][30]; for examples of other C_{60}-appended crown ethers, see [31]). Crown ether–fullerene conjugates attract substantial interest as advanced supramolecular materials [32] and have found application in sensing devices for cations [33]. We describe the X-ray crystallographic characterization of the new C_{70} crown ether derivatives and their ionophoric properties, as determined with ion-selective electrodes (ISEs). We also demonstrate in electrochemical studies that cation complexation strongly affects the redox potentials of the C_{70} core as a result of the close proximity of the ionophore-bound cation to the fullerene surface. In addition, we report exploratory studies on the formation of new higher adducts – up to a heptakis-adduct – starting from five o'clock bis-adduct (±)-**4**, which, for the first time, was obtained in larger amounts by tether-directed synthesis.

2. Results and Discussion. – 2.1. *Cyclophane-Type* C_{70} *Mono-Crown Ether Conjugates* – 2.1.1. *Tether Design and Computational Predictions.* For the first covalently templated functionalization of C_{70}, we chose bis-malonate **5** with an *anti*-substituted dibenzo[18]crown-6 (DB18C6) tether (*Fig. 3*). In previous work, *Bingel* macrocyclization of **5** with C_{60} in the presence of K^+ ions (to rigidify the template) had proceeded with complete regioselectivity, affording exclusively a *trans-1* C_{60} crown ether conjugate in which the template spans the entire fullerene sphere [29].

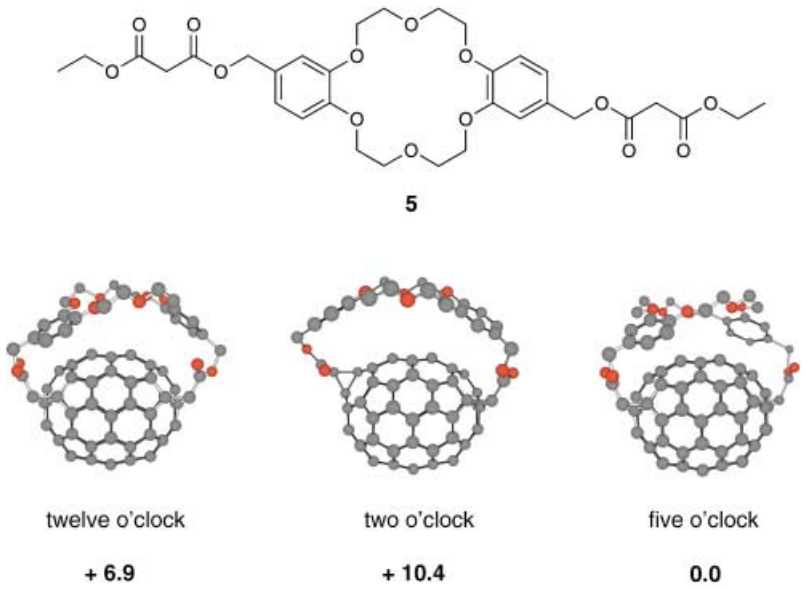

Fig. 3. *MM2 Calculations on the relative stabilities of three regioisomeric bis-adducts that can form in the macrocyclization of C_{70} with bis-malonate* **5** *featuring an* anti-*substituted DB18C6 unit.* Relative energies are given in kcal mol^{-1}. The EtOOC side chains at the methano bridge C-atoms are replaced by H-atoms in the calculations. All H-atoms have been omitted for clarity. Depicted are the lowest-energy conformers calculated for each regioisomer.

MM2 Calculations [34] were performed to investigate the relative stability of the regioisomeric bis-adducts expected to form in the bis-cyclopropanation of C_{70} with **5**. We had previously found that calculations of relative product stabilities provide a good prediction of the regioisomers that are formed preferentially [29]. Since two sequential *Bingel* additions to C_{70} occur exclusively at the α-type 6-6 bonds on opposite poles (*Fig. 2*), we considered only this mode of functionalization in the computations. To reduce the number of possible conformers, the EtOOC residues at the two methano bridge C-atoms were replaced by H-atoms.

Molecular-dynamics [35] and Monte Carlo [36] simulations suggest that [18]crown-6 (18C6) is highly flexible, spanning a large number of low-energy conformations. Free DB18C6 is less flexible as a result of the double benzanellation, and four preferred conformations were identified in the literature [37]. Among these, the conformation in which all $-O-C(sp^3)-C(sp^3)-O-$ rotamers are alternate $\pm$ *gauche*, leading to a C_{2v}-symmetric crown ether, is the most favorable one. In our calculations on the C_{70}-DB18C6 conjugates, we considered this conformation as well as a structure in which the $-O-C(sp^3)-C(sp^3)-O-$ rotamers are alternating *gauche* and *anti*. The latter, in which two O-atoms are pointing outward away from the crown ether cavity, is structurally similar to the calculated lowest-energy (C_i-symmetric) conformation of 18C6. For all three regioisomers (twelve, two, and five o'clock), it was found that the all-*gauche* conformation of the crown ether moiety, which is the preferred conformation upon cation complexation, is more stable than the *gauche-anti* conformation, in line with

previous force-field calculations [37d]. Differences in energy between the two conformations range from 0.3 kcal/mol in the two o'clock bis-adduct to 2.7 kcal/mol in the five o'clock bis-adduct. Furthermore, the calculations predicted the five o'clock regioisomer to be more stable than the twelve and two o'clock regioisomers by 6.9 and 10.4 kcal/mol, respectively (*Fig. 3*). Based on these computational results, we expected the macrocyclization of **5** with C_{70} to proceed with a high degree of selectivity. Additionally, it was calculated that the macrocyclization of **5** with C_{70} to afford the five o'clock adduct is more exothermic (by 1.6 kcal mol^{-1}) than the corresponding reaction [29] with C_{60}.

In principle, *in-in*, *in-out,* and *out-out* stereoisomerism, depending on how the two EtOOC residues (or the two H-atoms in the calculations) at the two methano bridge C-atoms are oriented, could generate a mixture of configurational diastereoisomers for each bis-addition pattern [38]. However, the calculations predicted only the *out-out* isomers to be feasible for each regioisomer, with the two other configurations being by several kcal mol^{-1} higher in energy. Finally, it should be noted that, as a result of the planar chirality of the crown ether tether, the two and five o'clock bis-adducts may be formed as pairs of diastereoisomers. The calculated energy difference is small (1.6 kcal/mol) in case of the five o'clock bis-adducts.

The structures of the three possible regioisomeric C_{70} bis-adducts formed by macrocyclization of C_{70} with bis-malonate **6**, featuring a *syn*-disubstituted DB18C6 tether, were also calculated (*Fig. 4*). It was found that the change from *anti* to *syn* substitution of DB18C6 dramatically alters the relative stability of the regioisomeric bis-adducts. In all cases, the lowest-energy conformation of the macrocyclic bridge was found to be the same (*out-out* configuration with all-*gauche* conformation of the crown-ether moiety), but the twelve o'clock regioisomer was now calculated to be the most stable, followed by the two o'clock (+0.1 kcal/mol) and the five o'clock (+5.0 kcal/mol) bis-adduct.

2.1.2. *Synthesis of C_{70} Mono-Crown Ether Conjugates Featuring a Five O'Clock Addition Pattern.* Macrocyclization of C_{70} with bis-malonate **5** under modified *Bingel* conditions (I_2, 1,8-diazabicyclo[5.4.0]undec-7-ene (DBU), PhMe) in the presence of KPF_6 (10 equiv.; added to rigidify the tether by complexation) afforded, after chromatographic separation (SiO_2-*H*; PhMe/AcOEt 1:1), compounds (±)-**7a** and (±)-**7b** in a 56:44 ratio and an overall yield of 41% (*Scheme 1*). Their identity as isomeric C_{70} bis-adducts was established by the matrix-assisted laser-desorption-ionization time-of-flight (MALDI-TOF) mass spectra, which depicted for each of the two compounds the Na^+ complex of the molecular ion as the parent peak at *m*/*z* 1507.1950 ($[M+Na]^+$, $C_{102}H_{36}NaO_{14}$; calc. 1507.1997). Transesterification of pure (±)-**7a** and (±)-**7b**, or a mixture of both (Cs_2CO_3, THF/EtOH 1:1) afforded, as single product, the C_2-symmetric five o'clock bis-adduct (±)-**4**, as revealed by spectral comparison (^{1}H- and ^{13}C-NMR) with an authentic sample obtained by sequential *Bingel* bis-cyclopropanation [5a][14]. As predicted by the computer modeling (*Sect. 2.1.1*), macrocyclization of C_{70} with **5** proceeds with complete regioselectivity to provide the regioisomer least favored in the kinetically controlled, sequential bis-cyclopropanation (*Fig. 2*). Furthermore, the transesterification results show that compounds (±)-**7a** and (±)-**7b** are two diastereoisomeric pairs of enantiomeric fullerene crown ether conjugates featuring the same addition pattern and differing only

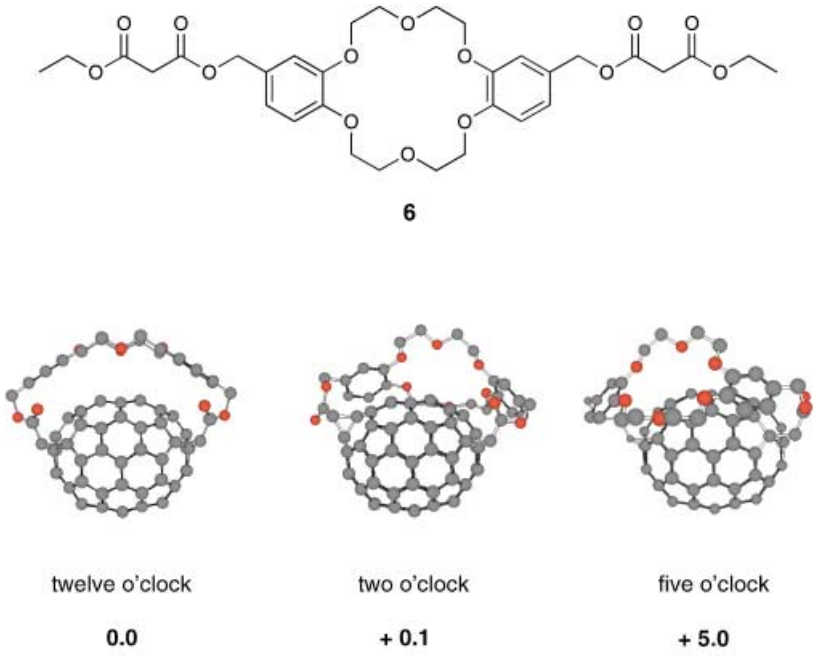

Fig. 4. *MM2 Calculations on the relative stabilities of three regioisomeric bis-adducts that can form in the macrocyclization of C_{70} with bis-malonate* **6** *featuring a* syn*-substituted DB18C6 unit.* Relative energies are given in kcal mol^{-1}. The EtOOC side chains at the methano bridge C-atoms are replaced by H-atoms in the calculations. All H-atoms have been omitted for clarity. Depicted are the lowest-energy conformers calculated for each regioisomer.

in the orientation of the DB18C6 tether (planar chirality). Although KPF_6 was added in the first *Bingel* macrocyclizations, it was later found that the absence of salt did not affect the regioselectivity at all; a result in contrast to observations made in the addition of **5** to C_{60} [29a,b]. However, the diastereoisomeric ratio changed slightly in the absence of salt, providing (±)-**7a** and (±)-**7b** in a ratio of 37:63 and a substantially enhanced yield of 68%. The increase in yield probably results from more-efficient extraction and purification in the absence of coordinating K^+ ions.

The ^{1}H- and ^{13}C-NMR spectra ($CDCl_3$) support the C_2 symmetry of the two conjugates (±)-**7a** and (±)-**7b**. For example, the ^{13}C-NMR spectrum of (±)-**7a** displayed two C=O resonances (163.29 and 162.00 ppm), 33 signals for fullerene C(sp^2)-atoms (156.17–111.64 ppm), two for the fullerene C(sp^3)-atoms (66.90 and 66.56 ppm), and one for the methano bridge C-atoms (36.68 ppm). Variable-temperature ^{1}H-NMR (VT-NMR) indicated that a considerable barrier exists for the rotation of the crown ether moiety around the arms linking it to the C-sphere. The spectrum of (±)-**7a** in $(CDCl_2)_2$ did not change significantly upon heating from 293 to 393 K. In particular, the *AB* system of the benzylic CH_2 protons (δ 5.77 and 4.88 ppm) did not show any signs of broadening due to exchange. Even after prolonged heating (10 h) of a sample of (±)-**7a** in $(CDCl_2)_2$ at 393 K, the spectrum did not indicate the presence of the typical *AB*

Scheme 1. *Synthesis of* (±)-**7a** *and* (±)-**7b**

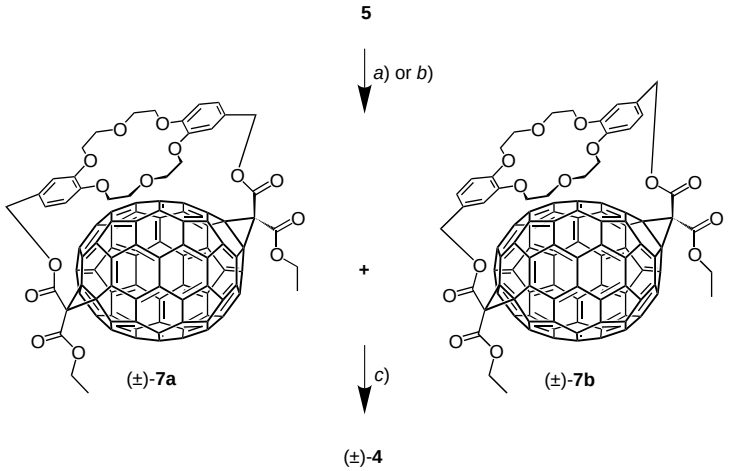

a) C_{70}, I_2, DBU, KPF_6 (10 equiv.), PhMe/MeCN, r.t.; 23% ((±)-**7a**), 18% ((±)-**7b**). *b*) C_{70}, I_2, DBU, PhMe/MeCN, r.t.; 25% ((±)-**7a**), 43% ((±)-**7b**). *c*) Cs_2CO_3, THF/EtOH 1:1, KPF_6, r.t.; 41%.

system (δ 5.44 and 5.38 ppm) for the benzylic CH_2 protons of (±)-**7b**. Hence, the two diastereoisomers do not interconvert.

Mono- and bis-cyclopropanations of C_{70} are accompanied by a significant color change from red (C_{70}) to red-brown (for the mono- and bis-adducts). However, the fullerene π-chromophore is only slightly perturbed, as evidenced by the close similarity between the UV/VIS spectra of (±)-**7a** and C_{70} [39]. Also, the differences between the UV/VIS spectra of (±)-**7a** and (±)-**7b** are negligibly small (*Fig. 5*). Both spectra show weak longest-wavelength absorption maxima around 691 and 689 nm, respectively, followed by characteristic bands around $\lambda_{max} = 470-464$, 444–443, 403–402, and 370–368 nm. In the UV region, strong absorptions with molar extinction coefficients ε approaching 100000 M^{-1} cm^{-1} are observed around 297 and 275 nm.

2.1.3. *X-Ray Crystal Structure of* (±)-**7a**. The presence of the inherently chiral five o'clock addition pattern and the *out-out* orientation of the EtOOC groups in (±)-**7a** were unequivocally established by X-ray crystallography (*Fig. 6*). The fullerene core in this first crystal structure of a cyclopropanated C_{70} derivative has a spheroidal shape with a distance of 8.03 Å along the principal axis. As a consequence of cyclopropanation, the C-atoms C(1), C(2), C(67), and C(68) are pulled out of the C_{70}-surface leading to a slightly longer distance along the main axis than observed for the complex [(η^2-C_{70})Ir(CO)Cl(PPh_3)$_2$] (7.90 Å) [40]. Distances from the C-atoms at the equator to the center of the sphere range from 3.52–3.56 Å with a mean value of 3.54 Å. The bond lengths between the bridgehead atoms C(1)–C(2) and C(67)–C(68) of 1.605(9) and 1.596(10) Å, respectively, are strongly elongated compared to the analogous bonds reported for several η^2-transition metal C_{70}-complexes (1.512–1.523 Å) [16][17][41]. However, they are similar to the lengths of the corresponding bonds reported for the *trans-1* bis-cyclopropanated C_{60} crown ether conjugate (1.606–1.610 Å) mentioned above [29b] and a *Diels-Alder* mono-adduct of C_{70} (1.603 Å) [42].

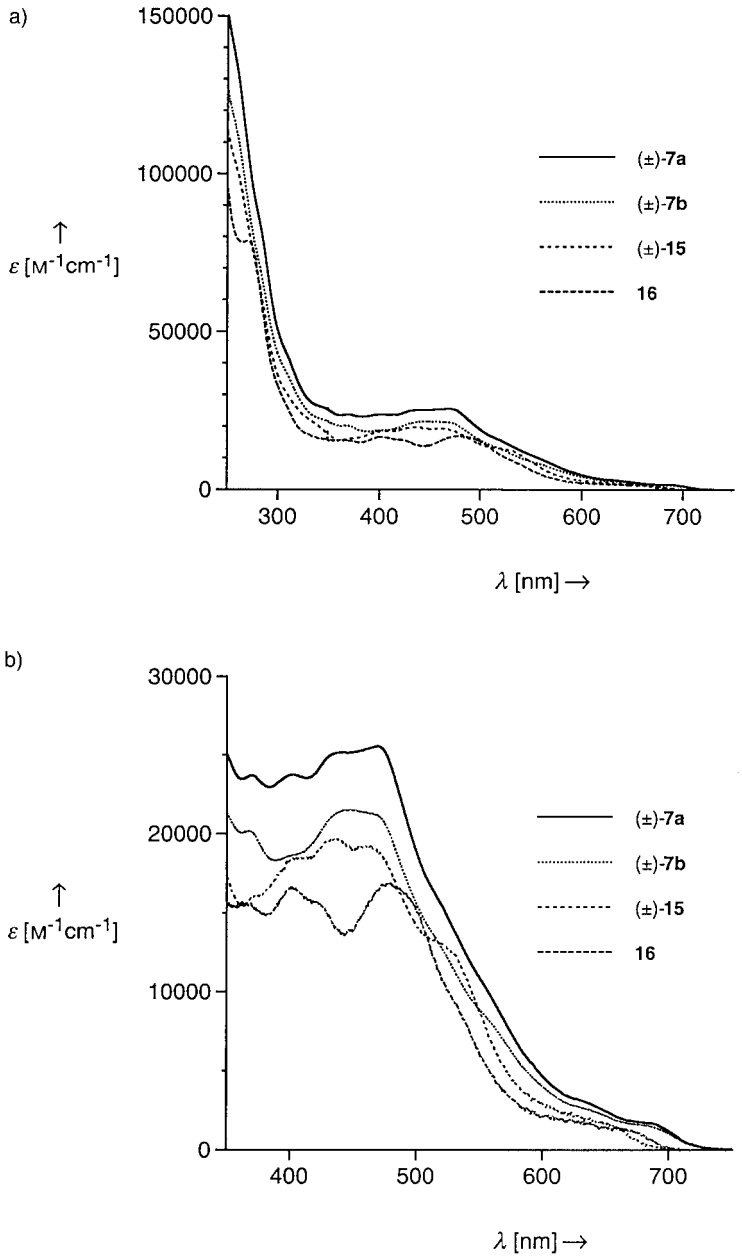

Fig. 5. *Comparison of the UV/VIS spectra* (CH_2Cl_2) *of* (±)-**7a**, (±)-**7b**, (±)-**15**, *and* **16**. *a*) Entire spectrum; *b*) expansion of the region between 400 and 700 nm.

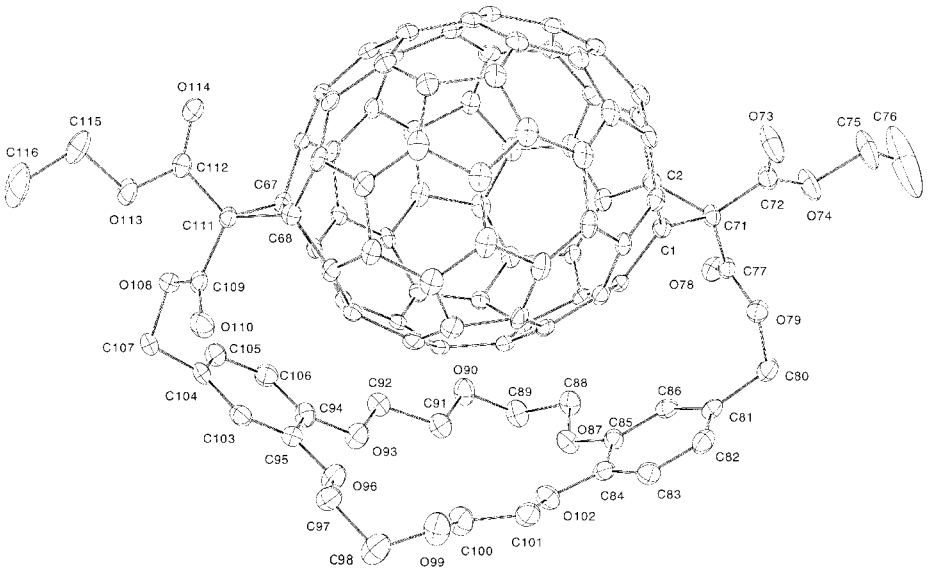

Fig. 6. *Crystal structure of* (±)-**7a**. Atomic displacement parameters obtained at 233 K are drawn at the 30% probability level.

Most geometrical features of (±)-**7a** are comparable to those of the latter *Diels-Alder* adduct. However, a significant difference is observed for the 6-5 bonds connected to the bridgehead atoms. In the case of (±)-**7a**, the lengths of these bonds are significantly shortened (1.480–1.500 Å *vs.* 1.523–1.531 Å in the *Diels-Alder* adduct). Note that the data of the *Diels-Alder* adduct, obtained at 193 K, are more accurate than the present data obtained at 233 K.

The crown ether moiety exists in a different conformation compared with those reported so far in the literature for uncomplexed DB18C6 [37]. To bridge the fullerene poles, it adopts an 'umbrella-shaped' geometry with a distorted C_2 symmetry. As a result, the two aromatic rings are slightly twisted against each other, as can be seen from the dihedral angles C(84)–C(85)–C(94)–C(95), C(83)–C(86)–C(106)–C(103), and C(81)–C(82)–C(104)–C(105), which are *ca.* 12°. The angle between the two mean aromatic ring planes is *ca.* 124°. This is comparable to the value reported for DB18C6 complexes (128–102°) [29b][37c,d], but considerably larger than for the uncomplexed C_{2v}-symmetric DB18C6 (98.8°) [37d]. Several close contacts between the DB18C6 tether and the fullerene surface are observed. One of the aromatic rings (C(94) to C(106)) is almost parallel to a fullerene hexagon with an interplanar distance of 3.97 Å. For the other aromatic ring, the closest contacts with the fullerene surface range from 3.38–3.97 Å, with a mean value of 3.61 Å.

2.1.4. *Synthesis of C_{70} Mono-Crown Ether Conjugates Featuring Twelve and Two O'Clock Addition Patterns.* Bis-malonate **6** with a *syn*-substituted DB18C6 tether was previously obtained only as an unseparable 1:1 mixture together with *anti*-isomer **5** [29a,b][43]. Synthesis of pure **6** started from 3,4-dihydroxybenzaldehyde **8**, which was regioselectively benzyl-protected to give **9** (*Scheme 2*) [43]. Minor amounts of the

other protected regioisomer and dibenzylated side product were removed by column chromatography. Alkylation of **9** with $(ClCH_2CH_2)_2O$ readily afforded **10** but subsequent cleavage of the benzyl ether moieties led to unforeseeable difficulties. Hydrogenolysis (H_2, Pd/C (10%)) in CH_2Cl_2 did not provide dicarbaldehyde **11**, but rather led in 93% yield to diphenol **12**, in which the aldehyde groups are reduced to Me groups. Similar observations were made by *Stoddart* and co-workers for the reduction of a closely related system [44]. Fortunately, the undesired aldehyde reduction could be suppressed by decreasing the solvent polarity, and, when the hydrogenolysis of **10** was performed in toluene, no **12** could be detected, and **11** was isolated in 77% yield. Subsequent *Williamson* macrocyclization with $(BrCH_2CH_2)_2O$ in the presence of KI afforded the DB18C6-dicarbaldehyde **13** in remarkable 92% yield (for a synthesis of an inseparable mixture of **13** and the corresponding *anti*-dicarbaldehyde, see [29a,b][45]). Reduction to **14** and esterification proceeded smoothly to provide the desired bis-malonate **6**.

Scheme 2. *Synthesis of* syn-*DB18C6-Tethered Bis-Malonate* **6**

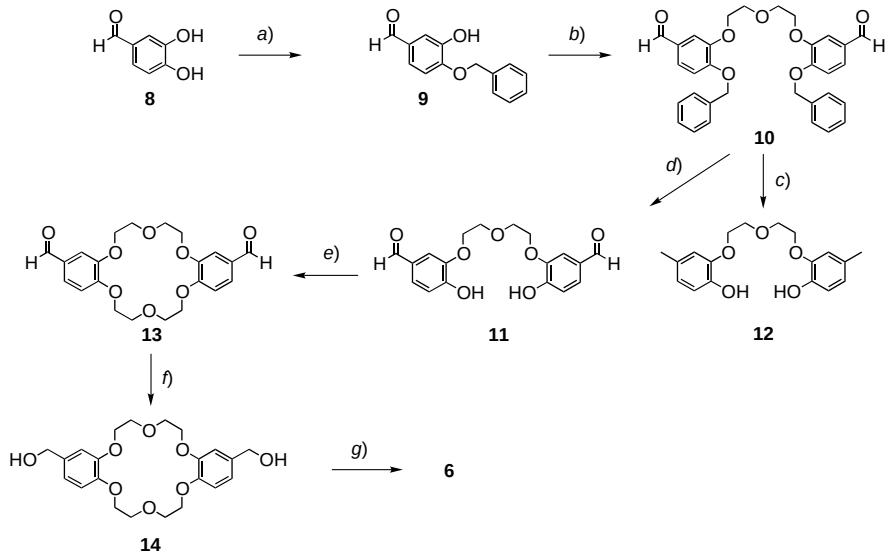

a) $PhCH_2Br$, K_2CO_3, DMF, 60°; 74%. *b*) $(ClCH_2CH_2)_2O$, K_2CO_3, DMF, 80°; 82%. *c*) H_2 (1 bar), Pd/C (10%), CH_2Cl_2, r.t.; 93%. *d*) H_2 (1 bar), Pd/C (10%), PhMe, r.t.; 77%. *e*) $(BrCH_2CH_2)_2O$, K_2CO_3, KI, DMF, 90°; 92%. *f*) $NaBH_4$, MeOH, r.t.; 98%. *g*) $ClOCCH_2CO_2Et$, pyridine, CH_2Cl_2, r.t.; 81%.

Bingel macrocyclization of **6** with C_{70} afforded the two regioisomeric bis-adducts (±)-**15** and **16** in yields of 26 and 32%, respectively, after chromatographic separation (*Scheme 3*). As in the case of (±)-**7a**/**b**, the identity of these compounds was unequivocally established by transesterification. The ^{1}H-NMR spectra obtained after transesterification were identical to those of the two o'clock ((±)-**3**) and twelve o'clock (**2**) bis-adducts obtained by sequential *Bingel* cyclopropanation [5a][14].

The structure assignments of (±)-**15** and **16** were also supported by the ^{1}H- and ^{13}C-NMR spectra. In the ^{1}H-NMR spectrum ($CDCl_3$) of (±)-**15**, the four benzylic

Scheme 3. *Synthesis of* (±)-**15** *and* **16**

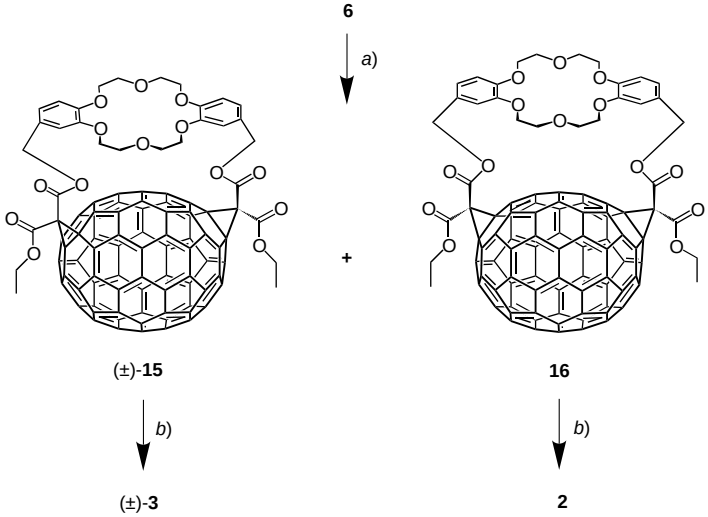

a) C_{70}, I_2, DBU, KPF_6, PhMe/MeCN, r.t.; 26% ((±)-**15**), 32% (**16**). *b*) Cs_2CO_3, THF/EtOH (1:1), KPF_6, r.t., 2 h.

protons appear as two *AB* systems, indicating C_1 symmetry. This symmetry is also inferred from the ^{13}C-NMR spectrum in which sixty-six fullerene C(sp^2)-atom resonances are observed. In contrast, the benzylic protons of **16** appear as a single *AB* system, indicating a higher degree of symmetry, either C_2 or C_s. The C_s symmetry of **16** could be deduced from the ^{13}C-NMR spectrum, which displayed thirty-eight fullerene C(sp^2)-atom resonances, ten of which exhibit half the intensity; in case of C_2 symmetry, one would expect to observe thirty-three signals of similar intensity.

The UV/VIS spectra of the two C_{70} crown ether conjugates are similar to those previously reported for C_{70} bis-adducts featuring two and twelve o'clock addition patterns (*Fig. 5*) [6][14]. Both (±)-**15** and **16** have their onset of absorption around 700 nm, and the lowest-energy absorption bands appear as shoulders centered at *ca.* 660 and 655 nm, respectively. Compared with (±)-**7a**, this corresponds to a small hypsochromic shift of *ca.* 30 nm. Overall, the spectra of (±)-**7a**, (±)-**15**, and **16** are very similar; however, there are some subtle differences that are characteristic for the different addition patterns. In the spectrum of (±)-**7a**, a band is present at λ_{max} 444 nm. This band is shifted to λ_{max} 434 nm in the case of (±)-**15** and to λ_{max} 423 nm for **16**. A unique characteristic of **16** is the short-wavelength band at λ_{max} 270 nm (*Fig. 5*,*a*).

2.1.5. *X-Ray Crystal Structure of* **16**. Evidence for the twelve o'clock addition pattern of **16** was provided by its X-ray crystal structure (*Fig. 7*). It clearly shows the tangential orientation of the ionophore moiety with the *out-out* geometry and linkage to the fullerene sphere through the methano bridges at C(1)–C(2) and C(41)–C(58). The structure is slightly distorted from C_2 symmetry as demonstrated by the different orientation of the EtOOC side chains.

An interesting feature of **16** is the inclusion of a H_2O molecule (O(200)); see *Fig. 8*) in the DB18C6 cavity. It is located close to the center and somewhat outside the crown

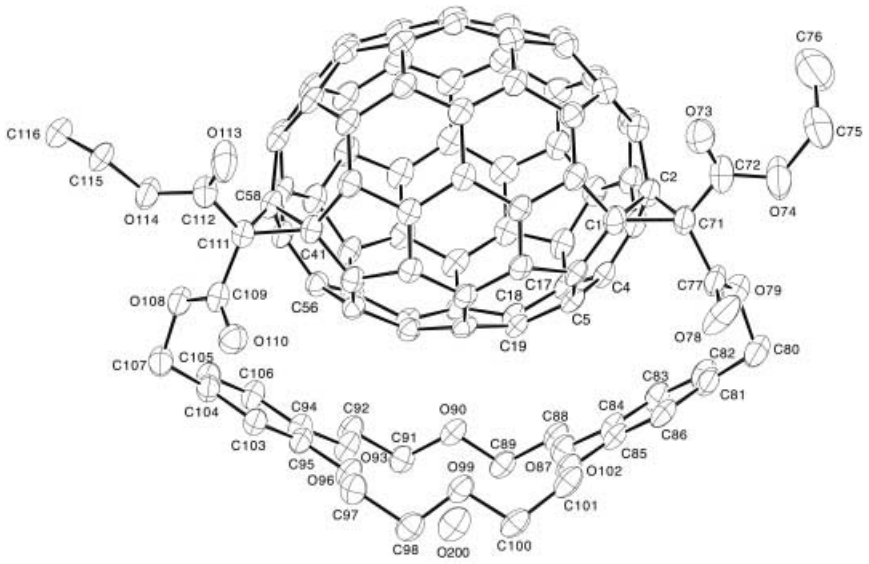

Fig. 7. *Crystal structure of* **16**. Atomic displacement parameters obtained at 208 K are drawn at the 30% probability level.

ether cavity. The distances between O(200) and the six crown ether O-atoms range from 3.08 to 3.25 Å, and the distance between O(200) and the mean plane of the corresponding O-atoms is *ca.* 1.5 Å. As a consequence of binding a H_2O molecule, all $-O-CH_2-CH_2-O-$ rotamers are in a pseudo-*gauche* conformation with angles ranging from 74–76° and the $-CH_2-CH_2-O-CH_2-$ rotamers adopt an *anti* conformation with angles between 172–178°. The crown ether moiety adopts an 'umbrella-shaped' structure, with an angle between the mean aromatic ring-planes of *ca.* 119°. A search in the *Cambridge Crystallographic Database* (*CCD*) for inclusion complexes of H_2O with crown ethers revealed that, in the majority of cases, the H_2O molecule residing in the cavity void is stabilized by additional H-bonds to neighboring molecules [46]. In some cases, this leads to large H-bonded networks [47]. Inclusion complexes in which the H_2O molecule is bound by a crown ether moiety only are rare [48]. The H_2O molecule typically forms two H-bonds and as a consequence, $O(H_2O)-O$(ether) bond distances fall into two categories, ranging from 2.8–3.1 Å for the H-bonded O(ether)-atoms and 3.4–4.0 Å for the nonbonded ones [46–48]. All these cases concern 18C6 complexes in which the crown ether adopts a pseudo-D_{3d} symmetry. In the present X-ray structure, O(200) shows one $C-H\cdots O$ contact to a CH_2Cl_2 molecule and one contact to C(83′) in the DB18C6 moiety of a neighboring fullerene conjugate, the $C\cdots O$ distances being 3.53 and 3.55 Å, respectively (*Fig. 8*).

Both benzene rings of the tether are in close stacking contact with the fullerene surface. The benzene ring C(81) to C(86) is nearly parallel to the neighboring fullerene pentagon C(5)–C(4)–C(17)–C(18)–C(19), the interplanar distance being 3.4 Å. The midpoint of a second benzene ring formed by C(94) to C(106) is positioned on top of C(56) with an atom-to-plane distance of 3.20 Å (*Fig. 8*).

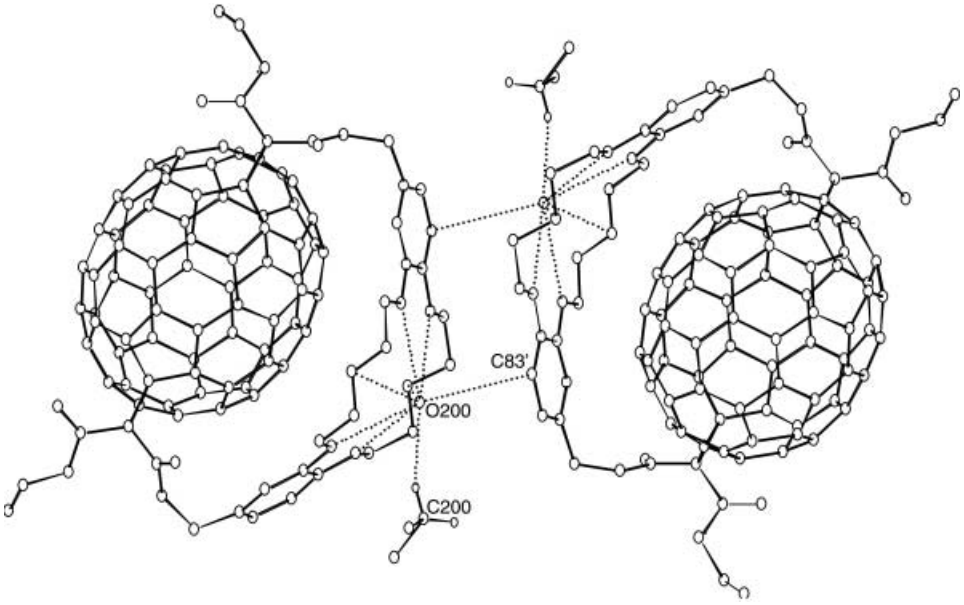

Fig. 8. *Two molecules of* **16** (related by an inversion center) *showing intermolecular contacts to the enclosed* H_2O *O-atom* (O(200)). The C···O distances in the contacts of O(200) to CH_2Cl_2 and to C(83′) in the DB18C6 moiety of a neighboring fullerene conjugate are 3.53 and 3.55 Å, respectively.

2.1.6. *Synthesis of a* C_{70} *Mono-Adduct with a DB18C6 Moiety Connected by a Single Flexible Linker.* In the cyclophane-type C_{70}-DB18C6 conjugates discussed so far, the flexibility of the crown ether moiety is substantially restrained. Furthermore, the close proximity of the fullerene sphere to the DB18C6 moiety inhibits complexation on the concave side of the crown ether. Since both factors may affect cation-binding affinities of the ionophoric site, it was desirable to compare the complexation properties of these compounds with those of a suitable reference conjugate containing a flexible crown ether (*vide infra*). For this purpose, we synthesized the C_{70} mono-adduct (±)-**22**, in which the crown ether moiety is covalently attached to the C-sphere by one arm only, thus retaining its full conformational flexibility (*Scheme 4*). Double alkylation of catechol (= benzene-1,2-diol, **17**) with $(ClCH_2CH_2)_2O$ afforded dichloride **18**, which was transformed into crown ether **19** [45][49] by macrocyclization with 3,4-dihydroxybenzaldehyde (**8**) [50]. Reduction (→ **20**), esterification (→ **21**), and *Bingel* addition provided the desired C_1-symmetric conjugate (±)-**22**, which was fully characterized.

2.2. *Formation of Higher Adducts of* C_{70}. 2.2.1. *Synthesis of Tris- and Tetrakis-Adducts Starting from Five O'Clock Bis-Adducts* (±)-**4** *and* (±)-**7a**. Transesterification of a mixture of (±)-**7a** and (±)-**7b** (*vide supra*) provided, for the first time, good access to the five o'clock bis-adduct (±)-**4** (*Scheme 1*), which was formed only in low yield by sequential double *Bingel* addition (*Fig. 2*) [5b][6][14]. This improved availability of (±)-**4** enabled us to investigate its reactivity in additional cyclopropanation reactions. When (±)-**4** was reacted with 1 equiv. of diethyl malonate (modified *Bingel* conditions: I_2, DBU, PhMe/Me_2SO 4:1), a single isolable new compound ((±)-**23**) was obtained in

Scheme 4. *Synthesis of* (±)-**22**

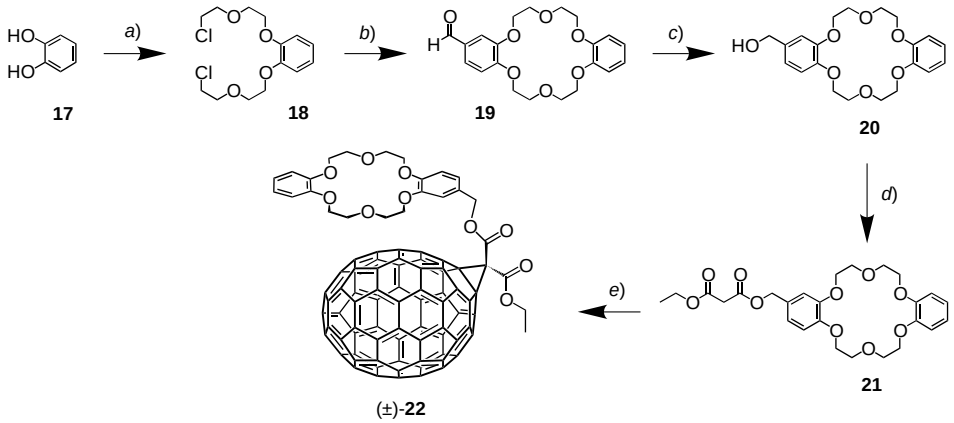

a) $(ClCH_2CH_2)_2O$, K_2CO_3, DMF, 85°; 35%. *b*) **8**, K_2CO_3, KI, DMF, 80°; 34%. *c*) $NaBH_4$, MeOH, r.t.; 95%. *d*) $ClOCCH_2CO_2Et$, pyridine, CH_2Cl_2, r.t.; 50%. *e*) C_{70} (0.8 equiv.), I_2 (0.8 equiv.), DBU (2.4 equiv.), PhMe, r.t.; 81%.

36% yield, together with unreacted starting material (30%; *Scheme 5*). The new C_{70} derivative was identified by MALDI-*Fourier*-transform-MS (MALDI-FT-MS) as a tris-adduct (*m*/*z* 1337.1623 ($[M+Na]^+$, $C_{91}H_{30}NaO_{12}$; calc. 1337.1629)).

Reaction of (±)-**4** with 2 equiv. of diethyl malonate afforded, besides (±)-**23** (18%), a single isolable product ((±)-**24**) in 54% yield, which was characterized by MALDI-TOF-MS as a C_{70} tetrakis-adduct. The most intense peak in the mass spectrum corresponds to the Na complex of the molecular ion at *m*/*z* 1495.2206 ($[M+Na]^+$, $C_{98}H_{40}NaO_{16}$; calc. 1495.2209). Reaction of (±)-**4** with 3 equiv. of diethyl malonate afforded tetrakis-adduct (±)-**24** as the sole product in 75% yield. The formation of even higher adducts was not observed under these conditions. No change in product distribution was observed when (±)-**4** was reacted with diethyl 2-bromomalonate under the original *Bingel* conditions.

Similarly, reaction of (±)-**7a** with 2 equiv. of diethyl malonate under modified *Bingel* conditions afforded a single new compound ((±)-**25**; 50%), which was fully characterized as a tetrakis-adduct featuring the same addition pattern as shown for (±)-**24** (*Scheme 6*). Apparently, the presence of the crown ether tether does not affect the regioselectivity for attachment of the third and fourth addends.

Tris- and tetrakis-cyclopropanation of (±)-**4** (*Scheme 5*) and the corresponding reaction of (±)-**7a** (*Scheme 6*) occur with remarkable degree of regioselectivity. In theory, addition to the different 6-6 bonds of (±)-**4** could result in 24 possible tris-adducts, whereas ten different C_2-symmetric tetrakis-adducts are possible starting from (±)-**23**, assuming that the additions occur only at 6-6 bonds. Nevertheless, only one unique tris-adduct and one unique tetrakis-adduct are formed.

Although the ^{1}H- and ^{13}C-NMR spectra are in full agreement with the proposed geometries of (±)-**23** (C_1 symmetry), (±)-**24** (C_2 symmetry), and (±)-**25** (C_1 symmetry), they do not allow an unambiguous structure assignment. The addition

Scheme 5. *Synthesis of Tris-Adduct* (±)-**23** *and Tetrakis-Adduct* (±)-**24**

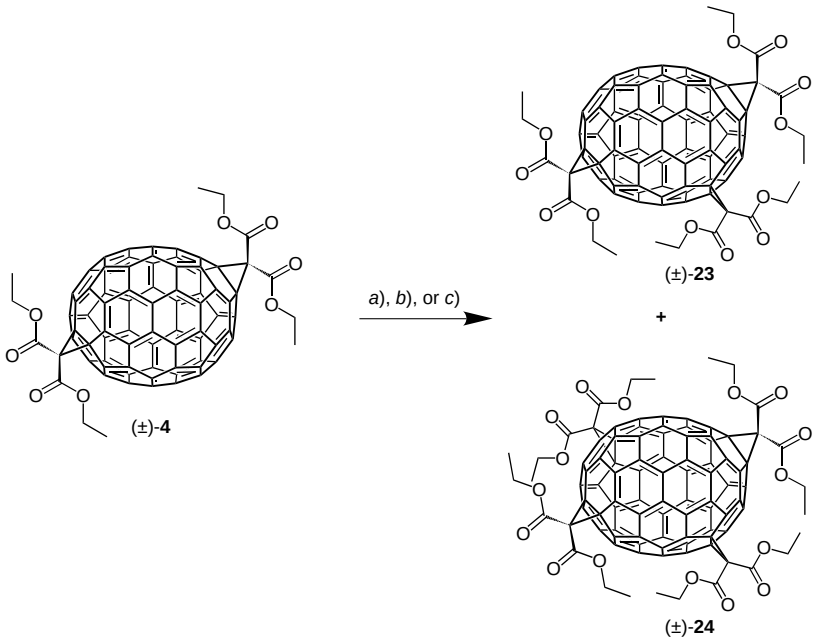

a) $(EtO_2C)_2CH_2$ (1 equiv.), I_2, DBU, PhMe/Me_2SO 4:1, r.t.; 30% ((±)-**4**), 36% ((±)-**23**). *b*) $(EtO_2C)_2CH_2$ (2 equiv.), I_2, DBU, PhMe/Me_2SO 4:1, r.t.; 18% ((±)-**23**), 54% ((±)-**24**). *c*) $(EtO_2C)_2CH_2$ (3 equiv.), I_2, DBU, PhMe/Me_2SO 4:1, r.t.; 75% ((±)-**24**).

Scheme 6. *Synthesis of Tetrakis-Adduct* (±)-**25**

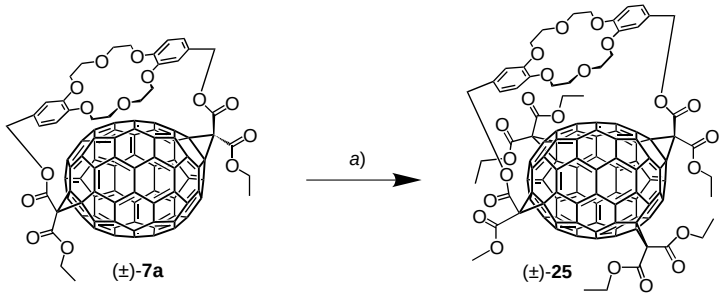

a) $(EtO_2C)_2CH_2$ (2.5 equiv.), DBU, PhMe/Me_2SO 4:1, r.t.; 50%.

patterns proposed are, however, strongly supported by earlier results from the cyclopropanation of **2** and (±)-**3** (*Fig. 2*) leading to tris- and tetrakis-adducts [6][14]. In these studies, it was found that the preferred pattern for bis-cyclopropanation within the same hemisphere of C_{70} is similar to that established for C_{60}. In the case of C_{60}, the second addition preferably occurs at a so-called equatorial (*e*) position (for positional notation, see: [51]). In the C_{70} bis-adduct (±)-**4**, a similar ('*e*-type') geometric

relationship exists between the bridged α-type bond C(1)–C(2) and the β-type bond C(31)–C(32) (and, correspondingly, between the bridged α-type bond C(67)–C(68) and the β-type bond C(42)–C(43) in the opposite hemisphere). For steric and electronic reasons (high LUMO coefficients [14]), the third and fourth kinetically controlled *Bingel* additions to give (±)-**23** and (±)-**24**, respectively, occur at these β-type bonds.

The UV/VIS spectrum of tris-adduct (±)-**23** exhibits a series of poorly resolved absorption bands with an end-absorption near 700 nm (*Fig. 9*). The only characteristic feature is an absorption maximum at λ_{max} 406 nm. It should also be noted that the molar extinction coefficients are strongly reduced when compared to those of the bis- (*Fig. 5*) and tetrakis-adducts. For the latter ((±)-**24** and (±)-**25**), the onset of absorption occurs near 660 nm. The first absorption band, which corresponds to the HOMO-LUMO transition, is visible as a shoulder at *ca.* 625 nm. A further characteristic feature of the tetrakis-adducts is the absorption maximum at λ_{max} 425–430 nm. The molar extinction coefficients are similar to those of the bis-adducts.

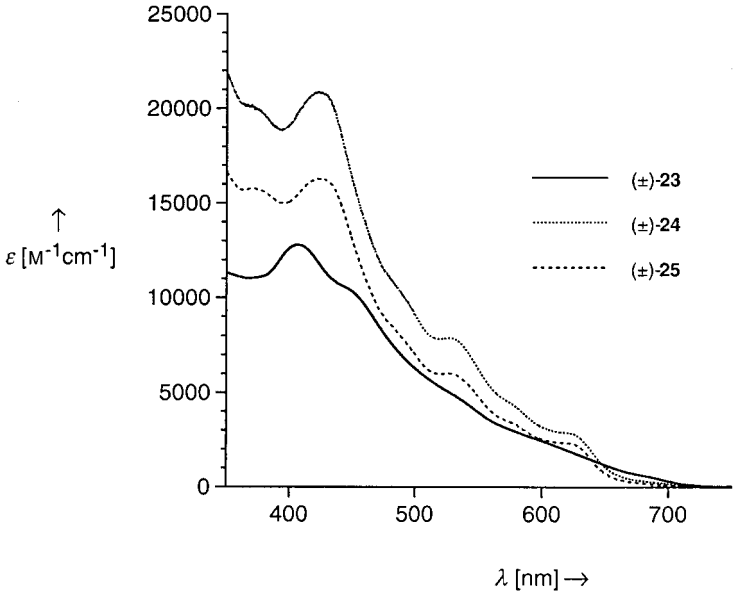

Fig. 9. *Comparison of the UV/VIS spectra* (CH_2Cl_2) *of* (±)-**23**, (±)-**24**, *and* (±)-**25**. Shown is only the VIS region between 400 and 700 nm; for the UV absorptions, see the *Exper. Part*.

2.2.2. *Synthesis of C_{70} Pentakis- to Heptakis-Adducts Starting From Five O'Clock Bis-Adduct* (±)-**4**. Previous investigations on the *Bingel* cyclopropanation of the twelve o'clock (**2**) and two o'clock ((±)-**3**) bis-adducts had shown that even higher adducts (beyond tetrakis-adducts) could be obtained, if more polar solvents such as pure Me_2SO [14] were used. In this environment, the nucleophilic addition reaction is greatly accelerated [52], whereas the selectivity is reduced. Similar findings were made in this study, starting from five o'clock bis-adduct (±)-**4**.

When (±)-**4** was reacted with diethyl 2-bromomalonate (6 equiv.) and DBU (9 equiv.) for 2 h in Me_2SO, four main product *Fractions I–IV* were obtained besides traces of tris-adduct (±)-**23** and tetrakis-adduct (±)-**24** (*Scheme 7*). The four fractions, which displayed distinct differences in color, were isolated by preparative TLC (SiO_2; CH_2Cl_2/AcOEt 98:2) and identified by MALDI-FT-MS as a pentakis-adduct *Fraction I* (*m*/*z* 1653.2779 ($[M+Na]^+$, $C_{105}H_{50}NaO_{20}$; calc. 1653.2788)), two hexakis-adducts *Fractions II* and *III* (*m*/*z* 1811.3363 ($[M+Na]^+$, $C_{112}H_{60}NaO_{24}$; calc. 1811.3367)), and a heptakis-adduct *Fraction IV* (*m*/*z* 1969.3949 ($[M+Na]^+$, $C_{119}H_{70}NaO_{28}$; calc. 1969.3951)).

Scheme 7. *Synthesis of C_{70} Pentakis- to Heptakis-Adducts Starting from* (±)-**4**

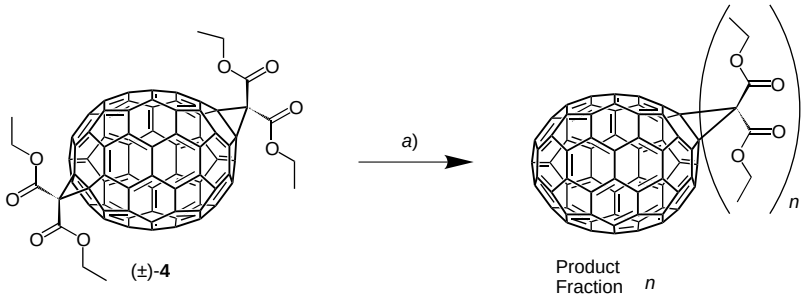

Product Fraction	*n*
I	5
II	6
III	6
IV	7

a) Diethyl 2-bromomalonate (6 equiv.), DBU (9 equiv.), Me_2SO, r.t.; 9.8% (pentakis-adduct *Fraction I*), 18.8% (hexakis-adduct *Fraction II*), 7.4% (hexakis-adduct *Fraction III*), 15.6% (heptakis-adduct *Fraction IV*).

In the absence of X-ray crystal-structure analyses, a conclusive structure assignment could not be made; however, from the NMR and UV/VIS data, some important conclusions could be drawn. The ^{13}C-NMR spectrum revealed that the dark-brown pentakis-adduct *Fraction I* contained two isomers in a ratio of *ca.* 1:1. The appearance of 120 resonances for the fullerene C(sp^2)-atoms is consistent with two C_1-symmetric pentakis-adducts (*Fig. 10*,*a*). Accordingly, the spectrum displays ten signals between 43 and 36 ppm, the region where the methano bridge C-atoms in cyclopropanated fullerenes resonate (*Fig. 10*,*b*). Thus, we can conclude that no methanofullerene substructures with bridged 6-5-open (or possibly 6-6-open) bonds had formed, in which the bridging C-atom resonance is shifted substantially downfield into the region at *ca.* 60 ppm [14]. The number of possible structures for the two compounds in *Fraction I* could be narrowed down further with the aid of density-functional-theory (DFT) calculations (*vide infra*).

The two bright-red and purple-red hexakis-adducts *Fractions II* and *III*, respectively, were characterized only by HR (high resolution)-MALDI-FT-MS and UV/VIS, since low quantities of material and the presence of impurities (including several minor isomers) largely prevented the recording of NMR spectra with a good signal-to-noise ratio. Meaningful ^{13}C-NMR spectral data were obtained only for *Fraction II*, indicating the presence of at least two hexakis-adducts in a ratio of *ca.* 4.5:1. All fullerene C(sp^2)-

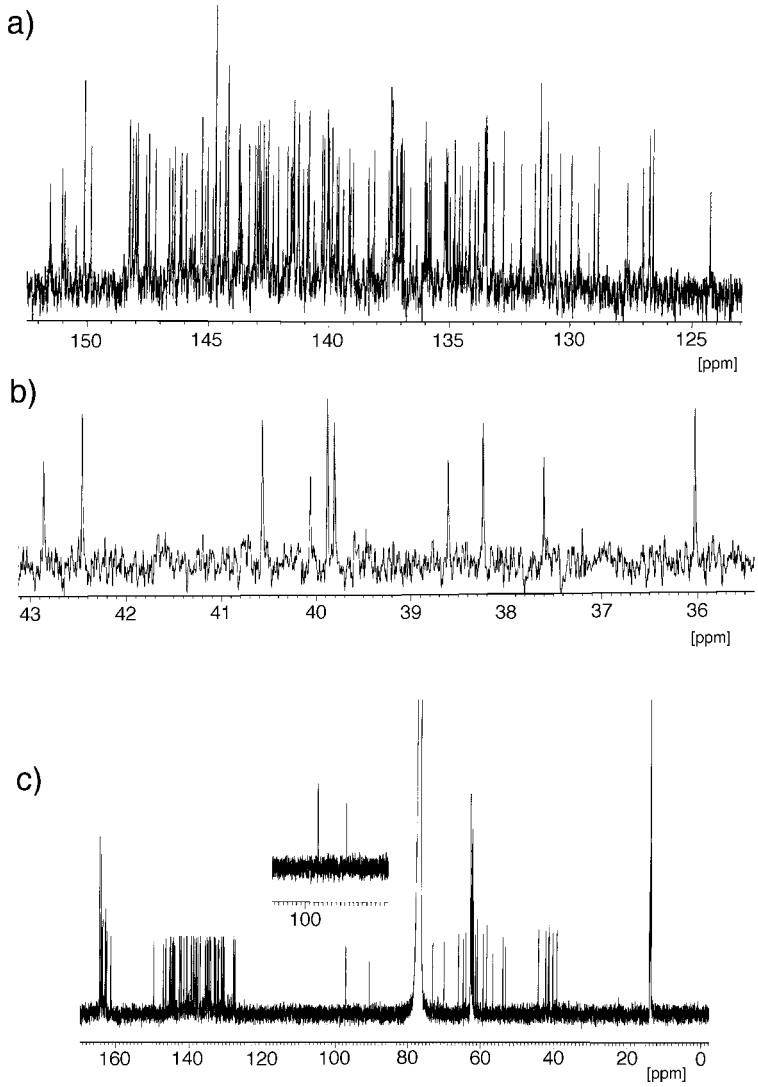

Fig. 10. *^{13}C-NMR Spectra* (125.8 MHz, $CDCl_3$) *of pentakis-adduct* Fraction I (*a*, *b*) *and heptakis-adduct* Fraction IV (*c*). Spectrum *a* shows the fullerene C(sp^2)-atom region and spectrum *b* the methano-C-atom region in the spectrum of *Fraction I*, which contains two C_1-symmetric pentakis-adducts. The inset in spectrum *c* shows two resonances at unusual chemical shift of the pure C_1-symmetric heptakis-adduct present in *Fraction IV*.

atoms were found to resonate between 150 – 126 ppm, which suggests that all additions led to the formation of cyclopropanated 6-6 bonds rather than methano-bridged 6-6-open or 6-5-open substructures. A methano-bridged 6-5-open substructure had previously been reported for a C_{70} hexakis-adduct prepared by *Bingel* additions to the two o'clock bis-adduct (±)-**3** [14] (for other examples of 6-5-open methanofuller-

enes, see [53]). The two major hexakis-adducts *IIa* and *IIb* in *Fraction II* could be separated by preparative TLC (SiO_2; CH_2Cl_2/AcOEt 39:1).

The orange-yellow heptakis-adduct fraction consists of one pure C_1-symmetric isomer according to ^{1}H- and ^{13}C-NMR spectroscopy. The ^{13}C-NMR spectrum (*Fig. 10,c*) comprises 56 resonances between 150 and 126 ppm corresponding to the fullerene C(sp^2)-atoms. Six (out of seven expected for an all-cyclopropanated derivative) signals are observed for the methano-bridge C-atoms in the region between 45 and 39 ppm, whereas 13 (out of 14 expected) resonances of the fullerene C(sp^3)-atoms appear in the region between 74 and 53 ppm. However, two additional signals with an anomalous shift appear at 97 and 91 ppm (*Fig. 10,c*). All these features are consistent with a structure in which one of the $(EtO_2C)_2C$ addends bridges a 6-6-open or a 6-5-open bond.

A comparison between the UV/VIS spectra (CH_2Cl_2) of *Fractions I–IV* also revealed some interesting details (*Fig. 11*). Whereas the onset of absorption of bis-adduct (±)-**4**, tris-adduct (±)-**23**, tetrakis-adduct (±)-**24**, pentakis-adduct *Fraction I*, and hexakis-adduct *Fraction II* occurs at $\geq$660 nm, a change to $\leq$600 nm is observed for the second hexakis- (*III*) and the heptakis- (*IV*) adduct fractions. This shift suggests a significant reduction of the remaining fullerene π-chromophore.

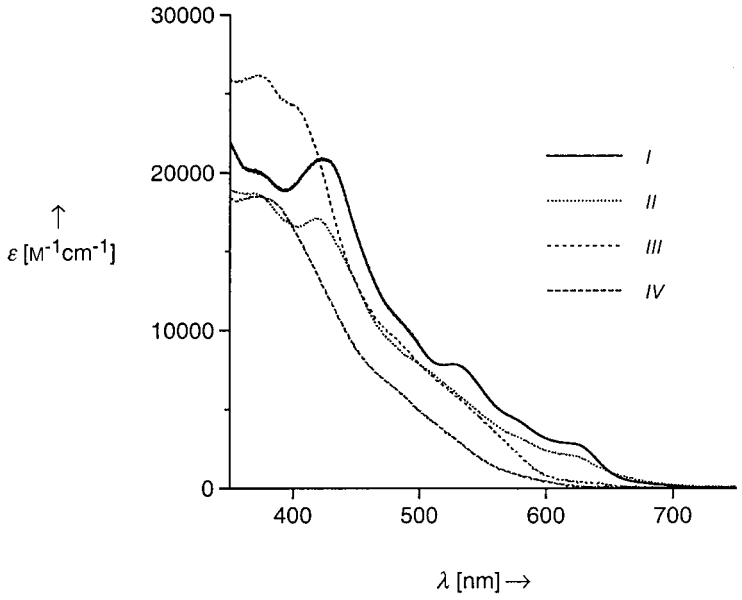

Fig. 11. *Comparison of the UV/VIS spectra* (CH_2Cl_2) *of higher-adduct* Fractions I–IV. Shown is only the VIS region between 400 and 700 nm; for the UV absorptions, see the *Exper. Part.*

2.2.3. *Regioselectivity of Multiple Cyclopropanations: A Density-Functional-Theory (DFT) Study.* Successful theoretical rationalizations of the experimentally observed regioselectivity in kinetically controlled nucleophilic *Bingel* cylopropanations of C_{60} [19] and C_{70} [14] are based on calculations of the coefficients of the *l*owest *u*noccupied *m*olecular *o*rbital (LUMO) according to semi-empirical or *ab initio* methods.

Additions occur preferentially at 6-6 bonds with large LUMO coefficients, providing the best interaction with the *h*ighest *o*ccupied *m*olecular *o*rbital (HOMO) of the nucleophile.

Here, we apply density-functional-theory (DFT) calculations [54] to optimize the structures of the fullerene adducts and calculate their frontier molecular orbitals. In the first step, the accuracy of the method was evaluated by comparing the results for C_{70}, mono-adduct **1** and the twelve (**2**) and two o'clock ((±)-**3**) bis-adducts with those obtained in previous *ab initio* studies [14]. In all calculations, the $(EtO_2C)_2C$ addends were replaced by CH_2 bridges (H_2C).

The LUMO and the LUMO + 1 of C_{70} are degenerate (*Fig. 12,a*), and both orbitals are mainly located at the poles, with large coefficients at the polar α-type bonds. The LUMO + 2, which is nearly isoenergetic ($\Delta E = 0.046$ eV), bears no coefficients at the pole. These findings are in agreement with the experimental results: mono-addition occurs exclusively at the α-type bonds as a result of favorable interactions between the HOMO of the nucleophile and the LUMO and LUMO + 1 of C_{70}. They differ, however, from a recent study at the RHF-PM3 (restricted *Hartree-Fock*-parametric method 3) level of theory, in which was reported a different order for the lowest unoccupied orbitals [8].

The DFT calculations revealed that the LUMO in mono-adduct **1*** (* indicates in the following that all $(EtO_2C)_2C$ are replaced by CH_2 in the calculations) has large orbital coefficients at the α-type bonds C(56)–C(57) and C(59)–C(60) on the opposite pole (*Fig. 12,b*). Addition to these bonds leads to formation of two o'clock bis-adduct (±)-**3***, which is, indeed, the main product in the *Bingel* bis-cyclopropanation of C_{70} (*Fig. 2*). Two other α-type bonds, C(67)–C(68) and C(69)–C(70), bear small LUMO coefficients. Addition to these bonds leads to five o'clock bis-adduct (±)-**4***, which is the least favored regioisomer in the sequential *Bingel* bis-cyclopropanation. The formation of the twelve o'clock adduct **2*** can be rationalized by the interaction of the HOMO of the nucleophile with the LUMO + 2 of the monoadduct. The LUMO + 2 is only by 0.156 eV higher in energy and bears very large coefficients at the α-type bond C(41)–C(58) at which attack occurs. These results are in good agreement with the previous *ab initio* RHF-SCF (self-consistent field) calculations with the 3-21G basis set [14].

The LUMO of the five o'clock bis-adduct (±)-**4*** has large coefficients at the β-type bonds C(16)–C(17), C(28)–C(29), C(31)–C(32), C(39)–C(40), C(42)–C(43), and C(61)–C(62) (*Fig. 12,c*). Additionally, the LUMO + 1, which is nearly isoenergetic ($\Delta E = 0.01$ eV), has substantial coefficients at the β-type bonds C(31)–C(32) and C(42)–C(43). Experimentally, it is observed that the third addition preferentially occurs at the two latter bonds. In the resulting C_1-symmetric tris-adduct (±)-**23***, the LUMO coefficients at C(42)–C(43) become even more pronounced (*Fig. 12,d*) and attack at that bond leads to the formation of C_2-symmetric tetrakis-adduct (±)-**24***.

The calculations also allow a tentative prediction of the structures for the two C_1-symmetric compounds in pentakis-adduct *Fraction I* (*Sect. 2.2.3*). The computed LUMO of tetrakis-adduct (±)-**24*** has large coefficients at the hexagon C(18)–C(19)–C(20)–C(38)–C(37)–C(36) through which the C_2-axis passes (*Fig. 13,a*). In particular, the coefficients at the 6-5 bonds C(18)–C(19) and C(37)–C(38) are large. Addition to these bonds, followed by valence isomerization

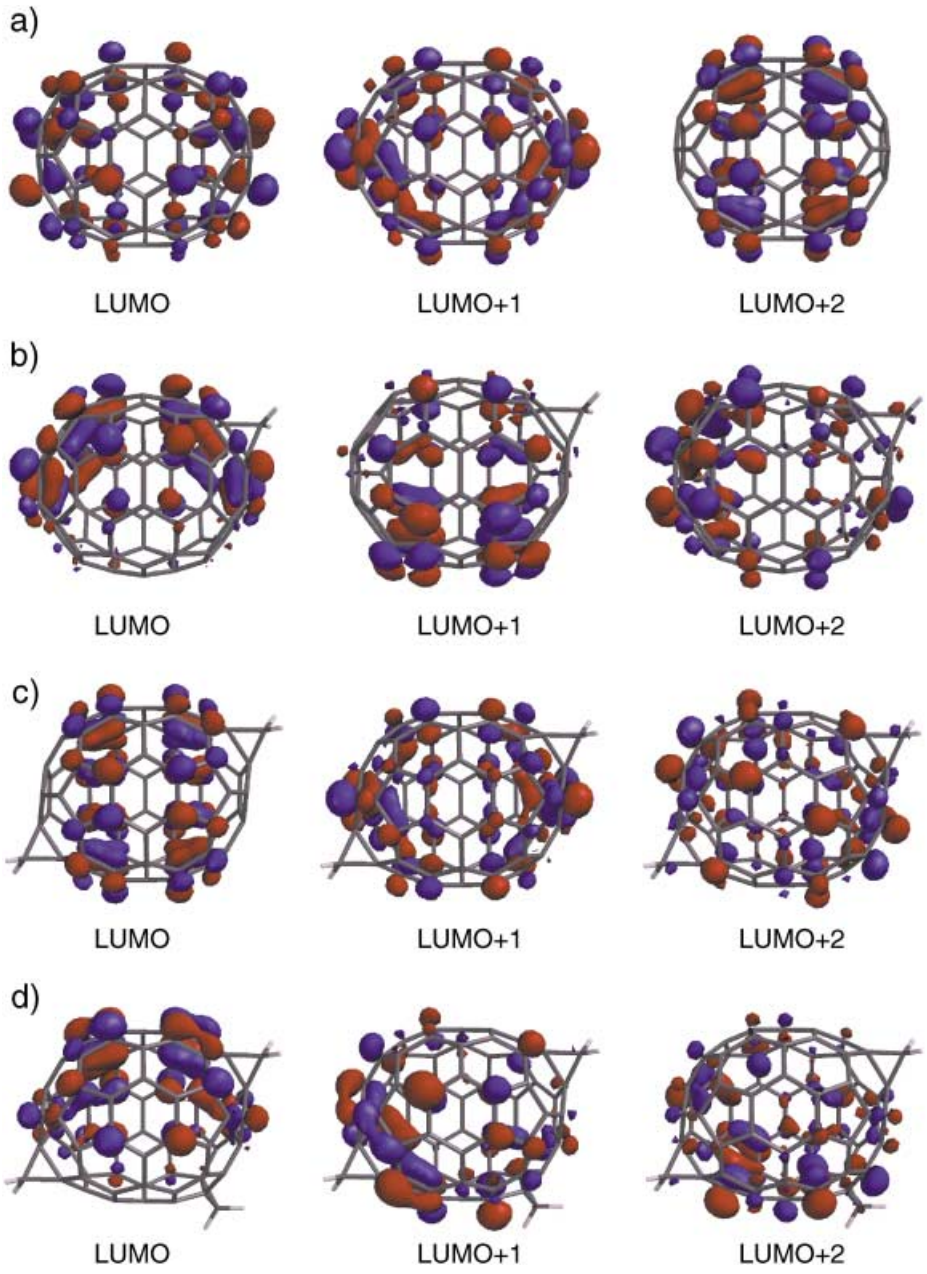

Fig. 12. *Calculated LUMO, LUMO + 1, and LUMO + 2 of* a) C_{70}, b) C_{70} mono-*adduct* **1***, c) C_{70} *bis-adduct* (±)-**4***, *and* d) C_{70} *tris-adduct* (±)-**23***. The star (*) indicates that the $(EtO_2C)_2C$ addends in the experimentally prepared products are replaced by CH_2 addends in the computational study. The DFT calculations were performed with the p*BP*/DN (perturbational *Becke-Perdew*/numerical split-valence basis set) model. Visualization was done with the SPARTAN (SGI V. 5.1.3) graphics module [54].

[14][53a], would lead to the formation of pentakis-adduct ((±)-**26a***, *Fig. 13,b*), in which the 6-5 bond is opened. Indeed, a geometry optimization of this regioisomer led to the 6-5 open structure, although the input structure possessed a 6-5 bond. The NMR data (*Fig. 10*), however, do not support formation of a 6-5-open methanofullerene. Smaller coefficients are present at the β-type bonds C(5)–C(6), C(54)–C(55), C(16)–C(17), and C(39)–C(40). Addition to the latter two bonds leads to the formation of pentakis-adduct (±)-**26b***.

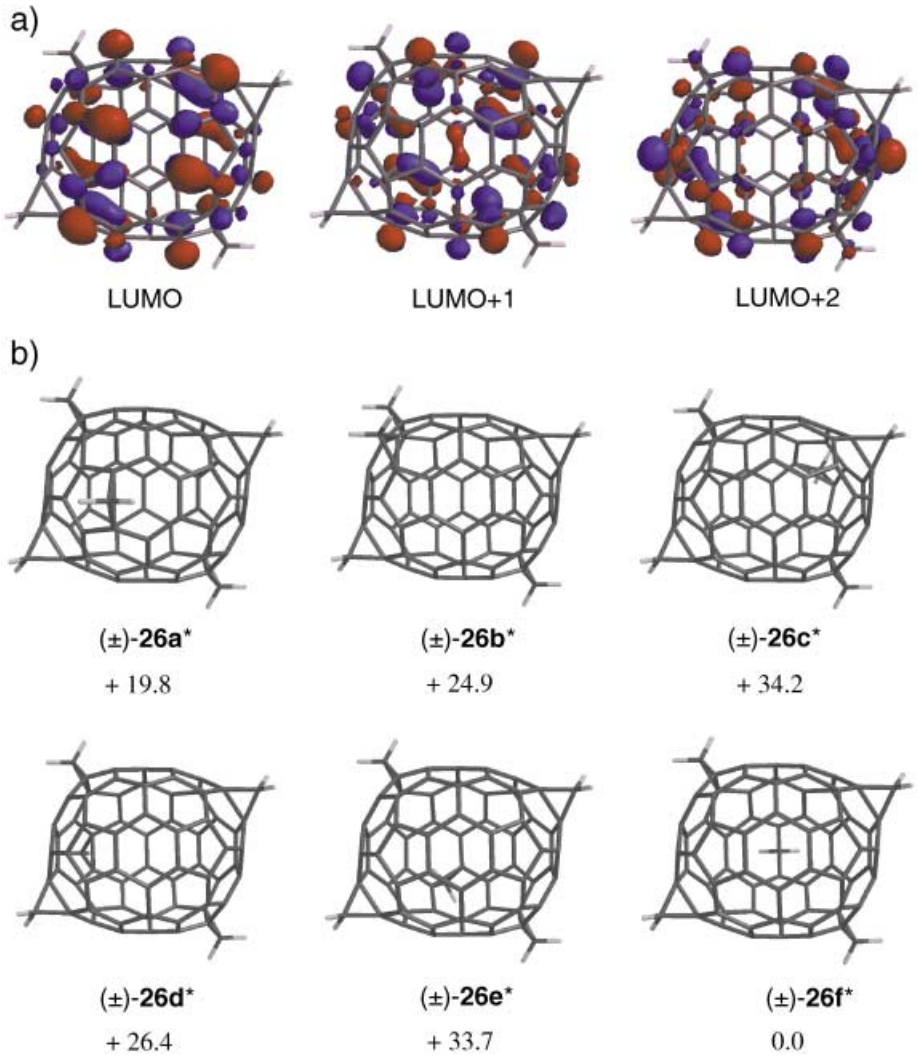

Fig. 13. a) *Calculated LUMO, LUMO+1, and LUMO+2 of C_{70} tetrakis-adduct* (±)-**24*** *and* b) *possible structures for the two products in pentakis-adduct* Fraction I. The star (*) indicates that the $(EtO_2C)_2C$ addends in the experimentally prepared products are replaced by CH_2 addends in the computational study. The DFT calculations were performed with the p*BP*/DB model and visualizations with the SPARTAN (SGI V. 5.1.3) graphics module [54].

The LUMO + 1 is mainly located at the opposite face, centered around the $\varkappa$-type bond C(46)–C(47), through which the C_2-symmetry axis passes. Large coefficients are present at the 6-5 bonds C(27)–C(28) and C(62)–C(63), the β-type 6-6 bonds C(28)–C(29) and C(61)–C(62), the ε-type 6-6 bonds C(27)–C(46) and C(47)–C(63), and the $\varkappa$-type 6-6-bond C(46)–C(47). Addition to these bonds may lead to the formation of pentakis-adducts (±)-**26c***, (±)-**26d***, (±)-**26e***, and (±)-**26f***, respectively (*Fig. 13*,*b*).

For a tentative structure proposal, we introduce, in addition to the experimental evidence for the absence of addition to 6-5 bonds, the following boundary conditions derived from the previous experience with nucleophilic multiple substitutions of C_{70}: *i*) additions do not occur at 6-6 bonds of a hexagon that already bears an addend, and *ii*) additions do not occur at 6-6 bonds on the equator. On this basis, only structures (±)-**26b***, (±)-**26d***, and (±)-**26e*** are feasible. Of these regioisomers, (±)-**26b*** and (±)-**26d*** are nearly isoenergetic and lower in energy than (±)-**26e***. Therefore, we propose structures (±)-**26b***/(±)-**26d*** for the two compounds present in approximately equal amounts in pentakis-adduct *Fraction I*.

2.3. *Synthesis of C_{70} Bis-Crown Ether Conjugates.* A model of (±)-**7a**/**b** showed that the distance between the two reactive β-type 6-6 bonds (which, in C_{60}, would be classified as *e*-type; see above) is similar to that between the two bonds already functionalized. Thus, it should be possible to bridge the C-sphere with a second crown ether by *Bingel* macrocyclization, allowing, for the first time, the study of the electrochemistry of a fullerene sandwiched between two crown-ether bound cations. MM2 Calculations [34] predicted that bis-malonate **5** with an *anti*-DB18C6 tether would have the right length to bridge the two β-type bonds in an almost strain-free fashion.

Reaction of (±)-**7a** with **5** under modified *Bingel* conditions afforded a mixture of four isomeric products (**27**, *Scheme 8*) in 69% yield. The formation of C_{70} bis-crown ether adducts was confirmed by HR-MALDI-FT-MS (*m*/*z* 2151.4120 ($[M+Na]^+$, $C_{134}H_{72}NaO_{28}$; calc. 2151.4102)). We had anticipated the formation of two diaster-

Scheme 8. *Macrocyclization of* (±)-**7a** *with Bis-Malonate* **5** *Afforded a Mixture of Four Major Isomers* (**27**)

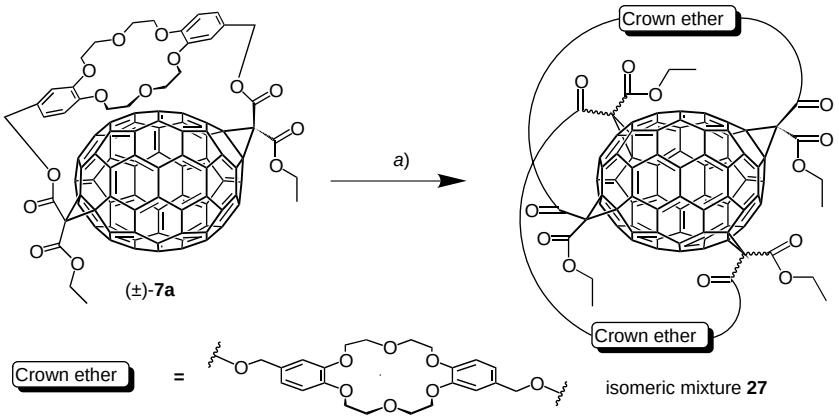

a) **5** (1 equiv.), I_2 (2 equiv.), DBU (6 equiv.), PhMe/Me_2SO 4 : 1, r.t.; 69%.

eoisomeric pairs of enantiomers, in analogy to the formation of (±)-**7a** and (±)-**7b**, and the isolation of additional isomers, which could result from configurational (*in-out*) isomerism at the methano-bridge C-atoms, was quite unexpected. Although partial product separation was achieved by TLC, we did not succeed in preparative separations by column chromatography. Also, attempted separation by HPLC proved to be unsatisfactory, since it was tedious and resulted in extensive decomposition of the products.

We subsequently changed to bis-malonate **6** with the *syn*-DB18C6 tether to achieve the second bridging, hoping that the reduced tether length would make *in-out* isomerism less likely. Furthermore, the *syn*-tether does not introduce additional planar chirality into the product. When (±)-**7a** was reacted with **6** under modified *Bingel* conditions, a single bis-crown ether conjugate, (±)-**28a**, was indeed formed regio- and stereoselectively in 31% yield (*Scheme 9*). Similarly, the reaction of (±)-**7b** with **6** led to tetrakis-adduct (±)-**28b** in 26% yield. The addition pattern in (±)-**28a**/**b** is C_2-symmetric and identical to that in (±)-**24** and (±)-**25**, but the overall symmetry is C_1, as inferred from the ^{1}H- and ^{13}C-NMR spectra, due to the two different types of DB18C6 tethers. Thus, the ^{1}H-NMR spectrum shows in the region between 5.9 and 4.6 ppm two sets of benzylic CH_2 resonances, belonging to the *anti*- and *syn*-substituted tether, respectively. The protons of each benzylic CH_2 group appear as one *AB* system resulting in a total of four well-resolved *AB* systems. The UV/VIS spectra of (±)-**24**, (±)-**25**, and (±)-**28a/b** expectedly are virtually identical, providing additional support for the correct structural assignment of the bis-crown ether conjugates.

2.4. *Ionophoric Properties.* The cation binding properties of all C_{70} crown ether conjugates were studied in the organic membrane phase of ion-selective electrodes (ISEs). The compound under study was dissolved in the ISE membrane bis(2-ethylhexyl) sebacate (=decanedioate) (DOS)/poly(vinyl chloride) (PVC) together with the cation exchanger sodium tetrakis[3,5-bis(trifluoromethyl)phenyl]borate (NaTFPB) that determines the total concentration of cations in the organic phase [55][56]. Close to Nernstian responses of 54 to 59 mV/decade proved the existence of a local equilibrium at the membrane/sample phase boundary in all cases. Therefore, the electromotive-force (EMF) values could be used for the determination of thermodynamic parameters [57].

The ionophoric properties of the crown ether conjugates are indicated by a significantly improved K^+-ion selectivity as compared to membranes containing only the ion exchanger (NaTFPB) but no ligand (*Table 1*, last entry). The selectivities of the five o'clock and twelve o'clock bis-adducts (±)-**7a/b** and **16** with respect to Na^+ and NH_4^+ ions do not differ significantly. The selectivity of the two o'clock derivative (±)-**15** for Na^+ ions, however, is by *ca.* one order of magnitude higher than that of the two other C_{70}-ionophore conjugates with regioisomeric addition patterns. Since the C_{70} bis-crown ether conjugates may also form 1:2 (ligand/ion) complexes, they were additionally investigated in membranes having a molar excess of ion exchanger. Membranes with an excess of C_{70} bis-crown ether conjugate (±)-**28a** or (±)-**28b** show a somewhat lower selectivity for Na^+ and a higher one for NH_4^+ ions than the C_{70} mono-crown ether conjugates. With a molar excess of ion exchanger, all selectivities are closer to those of the ionophore-free membrane. The membrane with reference compound (±)-**22**, in which the DB18C6 moiety has a higher conformational flexibility than in the

Scheme 9. *Synthesis of C_{70} Bis-Crown Ether Conjugates* (±)-**28a/b**

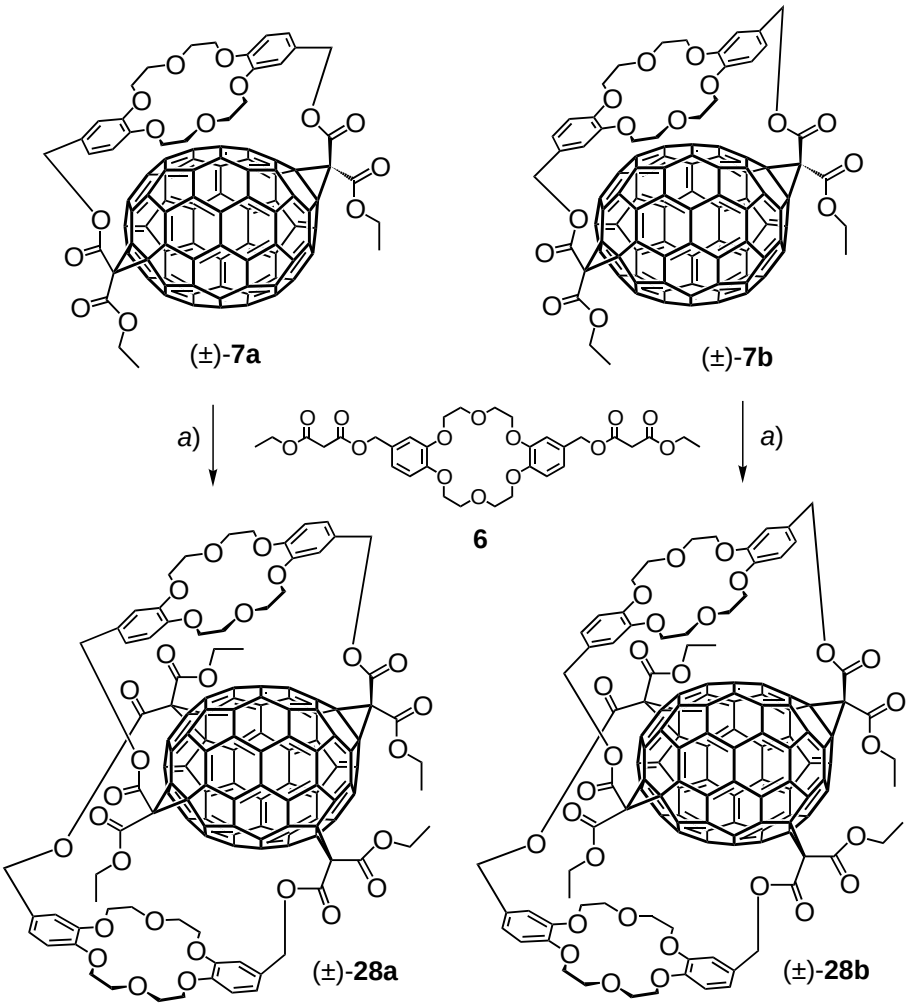

a), I_2, DBU, PhMe/Me_2SO 4:1, r.t.; 31% ((±)-**28a**), 26% ((±)-**28b**).

other crown ether conjugates shows a significantly weaker discrimination of Na^+ ions than the membranes with the other ionophores.

Effective complex-formation constants, β_{IL}^{eff} (I: alkali metal ion, L: ligand; see *Table 2*), with K^+ ions were determined by the sandwich-membrane method [58]. The potential of a double membrane with the same composition of both of its layers except that one contains an ionophore and the other not is a direct measure of the decrease of free-ion activities through complexation. Since the potential is defined by the activities of free ions, the formal complex-formation constants include effects of ion-pair formation [58]. The complex-formation constants with NH_4^+, Na^+, and H^+ ions were

Table 1. *Potentiometric Selectivity Coefficients, log K^{pot}_{KJ}, of ISEs Based on C_{70} Crown Ether Conjugates and Concentrations of Investigated Ligand and Ion Exchenger NaTFPB*[a]) *in the ISE Membranes*

Ligand	log K^{pot}_{KJ}			Ligand	NaTPFPB
	Na^+	NH_4^+	H^+	[mmol/l]	[mmol/l]
(±)-**7a**	-2.11 ± 0.01	-1.53 ± 0.01	-2.68 ± 0.02	4.95	2.53
(±)-**7b**	-2.29 ± 0.01	-1.50 ± 0.01	-1.84 ± 0.02	4.94	2.54
(±)-**15**	-3.64 ± 0.01	-1.45 ± 0.01	-1.84 ± 0.02	4.81	2.54
16	-2.28 ± 0.01	-1.47 ± 0.01	-1.85 ± 0.02	5.01	2.53
(±)-**22**	-1.19 ± 0.03	-1.63 ± 0.03	-2.97 ± 0.03	2.37	1.15
(±)-**25**	-2.38 ± 0.04	-2.06 ± 0.04	-1.39 ± 0.01	2.52	1.40
(±)-**28a**	-1.61 ± 0.01	-1.75 ± 0.01	-2.88 ± 0.03	0.92	0.25 (27.34 mol-%)
(±)-**28a**	-0.54 ± 0.02	-0.31 ± 0.01	-0.32 ± 0.03	0.92	1.65 (180 mol-%)
(±)-**28b**	-2.09 ± 0.01	-1.71 ± 0.02	-2.38 ± 0.03	1.11	0.44 (39.50 mol-%)
(±)-**28b**	-0.84 ± 0.03	-0.50 ± 0.01	-0.71 ± 0.02	1.11	1.91 (174.40 mol-%)
No ligand	-0.48 ± 0.03	-0.18 ± 0.02	0.14 ± 0.04		

[a]) Sodium tetrakis[3,5-bis(trifluoromethyl)phenyl]borate. Mol-% are given with respect to the ligand concentration.

Table 2. *Effective Complex Formation Constants of C_{70} Crown Ether Conjugates,* $\log \beta^{eff}_{IL}$, *Obtained for the Organic Membrane Phase with the Sandwich Membrane Method (*for K^+ ions*) and from the Potentiometric Selectivity Coefficients (*for the other ions)[a])

Ligand	Stoichiometry[b])	K^+	Na^+[c])	Na_4^+[c])	H^+[c])
(±)-**7a**	1 : 1	5.90 ± 0.05	4.28 ± 0.05	4.57 ± 0.05	3.12 ± 0.06
(±)-**7b**	1 : 1	5.90 ± 0.03	4.10 ± 0.03	4.60 ± 0.03	3.17 ± 0.04
(±)-**15**	1 : 1	6.03 ± 0.06	2.88 ± 0.06	4.79 ± 0.06	4.14 ± 0.07
16	1 : 1	6.06 ± 0.04	4.28 ± 0.04	4.79 ± 0.04	4.16 ± 0.05
(±)-**22**	1 : 1	6.34 ± 0.04	5.63 ± 0.05	4.91 ± 0.05	3.03 ± 0.06
(±)-**25**	1 : 1	6.04 ± 0.01	4.25 ± 0.05	4.82 ± 0.06	3.86 ± 0.06
(±)-**28a**	1 : 1	6.24 ± 0.05[d])	4.82 ± 0.04	4.39 ± 0.04	2.94 ± 0.06
(±)-**28a**	1 : 2	11.51 ± 0.07[d,e])			
(±)-**28b**	1 : 1	6.37 ± 0.07[d])	4.45 ± 0.09	4.53 ± 0.10	3.59 ± 0.10
(±)-**28b**	1 : 2	11.48 ± 0.09[d,e])			

[a]) Error bounds: standard deviations of five measurements. [b]) Assumed host-guest stoichiometries. The values for (±)-**28a** and (±)-**28b** were obtained from two measurements, with a molar excess of the ligand and the ion exchanger, respectively. [c]) The ISE membrane conditions do not allow a correct determination of the formation constant for the second complexation step. [d]) Calculated by iteration. [e]) $\log \beta^{eff}_{I_2L}$.

subsequently calculated from the ratio of the potentiometric selectivity coefficients obtained with membranes with and without ionophore, with K^+ as the reference ion [59] (see *Table 1* and *Exper. Part*).

As indicated by *Table 2*, the complex-formation constants with K^+ and NH_4^+ ions ($0.8 - 2.3 \times 10^6$ and $2.5 - 8.1 \times 10^4$ l mol^{-1}, resp.) are rather indifferent from the nature of the C_{70} mono- and bis-crown ether conjugates. On the other hand, more significant differences between the various ligands are observed in the complexation of Na^+ and

H^+ ions. The two o'clock conjugate (±)-**15** forms *ca.* 20 times weaker complexes with Na^+ ions than the other crown ether conjugates. Reference compound (±)-**22**, in which the crown ether is linked to C_{70} by one arm only, forms significantly stronger complexes with K^+ and Na^+ ions than the cyclophane-type crown ether conjugates. This demonstrates that the double bridging in the latter reduces the ability of the DB18C6 moiety to adopt the most favorable binding conformation. As a consequence, the binding affinity of the cyclophane-type conjugates toward K^+ and Na^+ ions decreases by *ca.* 0.5 and 1.2 logarithmic units in log β_{IL}^{eff}, respectively. The stronger decrease of the binding constant for Na^+ ions and the concomitant improvement of the K^+ ion selectivity of the cyclophane-type C_{70} mono-crown ether conjugates nicely reflects the fact that the cavity size of the doubly fixed crown ether nearly matches the diameter of a K^+ ion, while it is too large for a Na^+ ion [37c,d].

The C_{70} bis-crown ether conjugates may form complexes with both 1:1 and 1:2 host-guest stoichiometry. The respective complex formation constants with K^+ ions were obtained from two sandwich membrane measurements, one with an excess of ligand (30–40 mol-% cation exchanger) and one with an excess of cations (170–180 mol-% ion exchanger). As indicated by the values of β_{IL}^{eff} and $\beta_{I_2L}^{eff}$, the two binding sites of the bis-crown ether conjugates of C_{70} have similar affinity for K^+ ions. Unfortunately, the determination of 1:2 complex formation constants of interfering ions with C_{70} bis-crown ether conjugates was not possible, because their complexes are so weak that, at submillimolar concentrations, the 1:2 complexes exist at very low concentrations only. Under these conditions, the method is not applicable.

2.5. *Electrochemistry.* 2.5.1. *C_{70} Mono-Crown Ether Conjugates.* To determine the effects of cation complexation on the redox properties of the crown ether conjugates, cyclic voltammetric (CV) studies were performed in PhMe/MeCN 4:1 in the absence and presence of KPF_6, $NaBF_4$, $Ba(CF_3SO_3)_2$, and NH_4PF_6 (*Fig. 14* and *Table 3*). Based on the ΔE_{pp} values (separation between the potentials of the conjugated oxidation and reduction peaks), the first fullerene-centered reduction waves of these conjugates appear to be either reversible or quasi-reversible. However, with the exception of (±)-**16**, the second reductions are chemically irreversible as judged by the appearance of additional oxidation waves on the reverse scan. Consequently, cation-binding effects were monitored for only the first reductions.

Based on the ΔE_{pp} values and the cathodic/anodic current ratio, the first-reduction waves of (±)-**7a** and (±)-**7b** are both electrochemically and chemically reversible. It should be noted that the first-reduction potentials of (±)-**7a** and (±)-**7b** are slightly cathodically shifted as compared to those of the five o'clock bis-adduct (±)-**4** bearing diethyl malonate addends (−1.11 V) [60]. This indicates some electron donation from the benzocrown ether moiety to the C-sphere, presumably through π-π stacking of the DB18C6 benzene rings with the fullerene surface. This effect is even more pronounced for a fullerene with two appended crown ethers, as demonstrated by the differences in the first-reduction potentials (170 mV) of (±)-**28a** and (±)-**24** (*Table 4*). Similar to the behavior of the previously reported cyclophane-type C_{60}-DB18C6 conjugate [29a,b], addition of substoichiometric amounts of Na^+ ions to a solution of (±)-**7a** causes the appearance of a new, poorly resolved, yet clearly discernible redox wave, which is anodically shifted by 70 mV relative to that for the free compound. This new redox couple, assigned to the cation complex, grows at the expense of the one for the

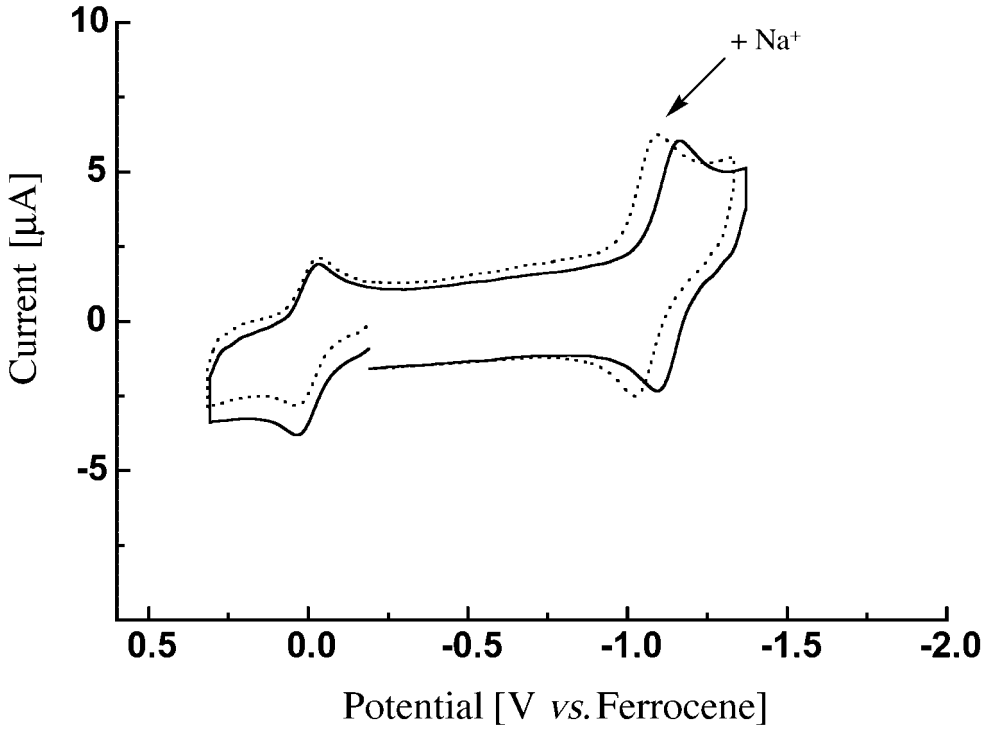

Fig. 14. *CV Response of* (±)-**7a** *in the absence* (——) *and presence* (·····) *of 1 equiv. of* $NaBF_4$ *at a scan rate of 100 mV* s^{-1}

Table 3. *Redox Potentials of* C_{70} *Crown Ether Conjugates* (*vs.* Ferrocene/ferricinium (Fc/Fc^+) couple) *in the Absence or Presence of Alkali Metal Cations.* Values in parenthesis are the ΔE_{pp} in mV[a]).

	E_1/V	E_2/V	$+KPF_6$ E_1/V	$+NaBF_4$ E_1/V	$+Ba(CF_3SO_3)_2$ E_1/V	$+NH_4PF_6$ E_1/V
(±)-**7a**	−1.13 (67)	−1.57[b])	−1.05 (65)[c])	−1.06 (68)[d])	−1.05 (83)[e])	−1.08 (68)[f])
(±)-**7b**	−1.14 (68)	−1.58[b])	−1.07 (68)[c])	−1.06 (67)[d])	−1.06 (82)[e])	−1.09 (68)[f])
(±)-**15**	−1.17 (75)	−1.56[b])	−1.09 (68)[c])	−1.09 (68)[d])	−1.06 (99)[e])	−1.10 (86)[f])
16	−1.09 (69)	−1.46 (73)	−1.07 (66)[c])	−1.04 (63)[d])	−0.98 (84)[e])	−1.09 (67)[f])
(±)-**22**	−1.04 (63)	−1.45[b])	−1.03 (68)			
(±)-**28a**	−1.47[b])	−1.72[b])	−1.31[b])[g])	−1.30[b])[h])	–	–
(±)-**28b**	−1.44 (83)	−1.74[b])	−1.27 (76)[g])	−1.27 (87)[h])	–	–
(±)-**25**	−1.43[b])	−1.71[b])	−1.33[b])[c])	−1.34[b])[d])	–	–

[a]) Measurements were performed under Ar in PhMe/MeCN 4 : 1 containing 0.1M Bu_4NPF_6 as the supporting electrolyte. Concentration of ionophores: 0.2 – 0.3 mM. Salts were dissolved in MeCN and added in μl amounts. Glassy carbon working electrode. Nonaqueous Ag/Ag^+ reference electrode. Pt wire counter electrode. Scan rate 100 mV s^{-1}. [b]) Cathodic peak potential. The reversibility of the first reduction of (±)-**28a** and (±)-**25** was difficult to ascertain due to the presence of a small, yet significant redox couple resulting from a minor fullerene impurity. [c]) +1.0 Equiv. of KPF_6. [d]) +1.0 Equiv. of $NaBF_4$. [e]) +1.0 Equiv. of $Ba(CF_3SO_3)_2$. [f]) +1.0 Equiv. of NH_4PF_6. [g]) +2.0 Equiv. of KPF_6. [h]) +2.0 Equiv. of $NaBF_4$.

uncomplexed species as the concentration of Na^+ ions increases. This was firmly established by the observation of isopotential points on both the forward and reverse scans. Addition of 1 equiv. of Na^+ ions causes the redox wave of the free compound to disappear completely, and further addition causes no further observable changes in the voltammetry. This behavior implies strong complexation between the crown ether conjugate and one Na^+ ion [61]. The anodic shift must be attributed to the electrostatic effect of the Na^+ ion that is bound to the DB18C6 ionophore in close proximity to the fullerene surface. The behavior with K^+ ions was very similar (*Table 3*), and the same was observed for (±)-**7b** and (±)-**15** with either cation. Similar electrostatic effects have been observed for fulleropyrrolidinium salts that are reduced at a potential which is 60 mV less negative with respect to C_{60} [62].

Table 4. *Redox Potentials of Higher C_{70} Adducts with Malonate Addends* (*vs.* Fc/Fc^+). Values in parenthesis are the ΔE_{pp} in mV[a]).

	E_1/V	E_2/V	E_3/V
C_{70}	0.97 (60)	– 1.37 (61)	– 1.82 (61)
29	– 1.05 (62)[b])	– 1.44 (67)[b])	– 1.84 (59)[b])
(±)-**30**	– 1.11 (66)[b])	– 1.47[b])	– 1.88[b])
(±)-**23**	– 1.16 (69)	– 1.61[c])	– 1.97[c])
(±)-**24**	– 1.30(78)	– 1.60[c])	
Pentakis-adduct *Fraction I*	– 1.40[c])	– 1.66[c])	
Hexakis-adduct *Fraction II*	– 1.49[c])	– 1.67[c])	
Heptakis-adduct *Fraction IV*	– 1.50[c])		

[a]) Measurements were performed under Ar in PhMe/MeCN 4 : 1 containing 0.1M Bu_4NPF_6 as the supporting electrolyte. Concentration of ionophores: 0.2 – 0.3 mM. Glassy carbon working electrode. Nonaqueous Ag/Ag^+ reference electrode. Pt wire counter electrode. Scan rate 100 mV s^{-1}. [b]) Taken from [60]. [c]) Cathodic peak potential.

Similar cation complexation-induced effects were also obtained with the twelve o'clock conjugate **16,** but with a much smaller anodic shift of the first reduction potential in the presence of K^+ ions (20 mV). The smaller shift can be attributed to a larger average distance between the cation and the fullerene core. This increase in distance results in a weaker electrostatic interaction. Na^+-Ion complexation by **16** induces an anodic shift of 50 mV (*Table 3*).

The addition of NH_4^+ ions results in comparable anodic shifts of the first reduction potential of compounds (±)-**7a**, (±)-**7b**, and (±)-**15**. On the other hand, the same ions cause no observable changes in the first reduction of **16**. Addition of Ba^{2+} ions induces a shift of 80 mV for compounds (±)-**7a** and (±)-**7b** and 110 mV for (±)-**15**. Interestingly, Ba^{2+}-ion complexation also shifts the first reduction of **16** by 110 mV. A shift of this magnitude was not anticipated given the behavior of **16** in the presence of monovalent cations. An argument could be made that the increased charge of a divalent cation induces larger shifts. However, the behavior of (±)-**7a** and (±)-**7b** as well as that previously reported for the C_{60}-DB18C6 conjugate [29b] indicates that K^+ and Ba^{2+} ions cause similar shifts despite the difference in charge density of the two cations. In the case of the C_{60}-DB18C6 conjugate, this behavior was attributed to the stronger solvation of the divalent cations, which inhibits their interaction with the crown ether

moiety. A possible explanation for the different behavior encountered for **16** could be (according to computer-model examinations) the added flexibility of the crown ether tether in this twelve o'clock bis-adduct, compared with the ionophores featuring the regioisomeric two and five o'clock addition patterns. As a result of this flexibility, the complexes of **16** with K^+ and Ba^{2+} ions could be structurally different and the orientation of the bound cation with respect to the surface of the C-sphere could change substantially.

The redox properties of mono-adduct (±)-**22** provide an interesting comparison. The first reduction is reversible and occurs at -1.04 V, a value virtually identical to that previously recorded for **29** (-1.05 V in CH_2Cl_2 [60]) (*Fig. 15*). Upon addition of 1 equiv. of KPF_6, a negligibly small anodic shift of 10 mV is recorded, which can be attributed to a change in solvent polarity. It, thus, appears as if, in solution, there is no interaction between the bound cation and the fullerene core. On the other hand, MM2 calculations [34] predict that, in the gas phase, the conformation in which the crown ether is positioned on top of the fullerene core is more stable by 14 kcal mol^{-1} than the alternative conformation with the crown ether rotated outwards. MM2 Calculations of the K^+-ion complex of (±)-**22** indicate that the cation prefers a location on top of the midpoint of a fullerene hexagon with a cation-midpoint distance (3.82 Å) similar to the distance calculated for the potassium complex of (±)-**7a** (3.85 Å). Since no anodic potential shift is recorded upon addition of K^+ ions, it is concluded that, in solution, the alternative conformations are more effectively stabilized, probably through enhanced solvation.

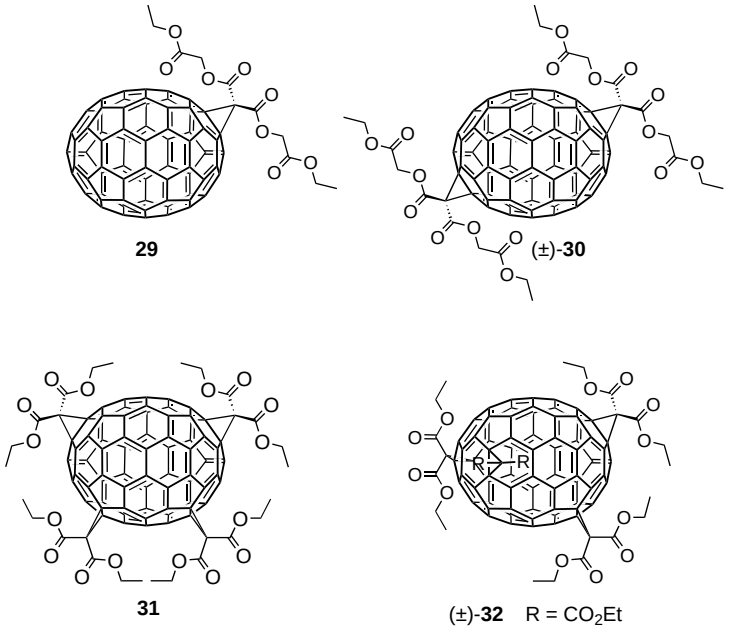

Fig. 15. *Structures of previously prepared mono-* (**29**), *five o'clock bis-* ((±)-**30**), *and tetrakis-* (**31** *and* (±)-**32**) *adducts of* C_{70} *used as controls in the electrochemical studies.* The latter two were obtained by bis-cyclopropanation of twelve o'clock and two o'clock bis-adducts, respectively [6][14].

2.5.2. *C_{70} Bis-Crown Ether Conjugates.* Much larger shifts are measured when the fullerene is sandwiched between two cations. Addition of 1 equiv. of K^+ ions to tetrakis-adducts (±)-**28a/b** led to the appearance of two new, poorly resolved redox couples that must correspond to the 1:1 and 1:2 host-guest complexes, respectively. Addition of 2 equiv. of K^+ ions resulted in only one redox couple, which is anodically shifted by 170 mV with respect to the corresponding wave in the absence of the salt (*Fig. 16*). The addition of more K^+ ions caused no further changes in the voltammetric response. This clearly establishes that the redox couple, shifted by 170 mV, corresponds to a complex with two K^+ ions. Similar anodic shifts were observed upon addition of $NaBF_4$.

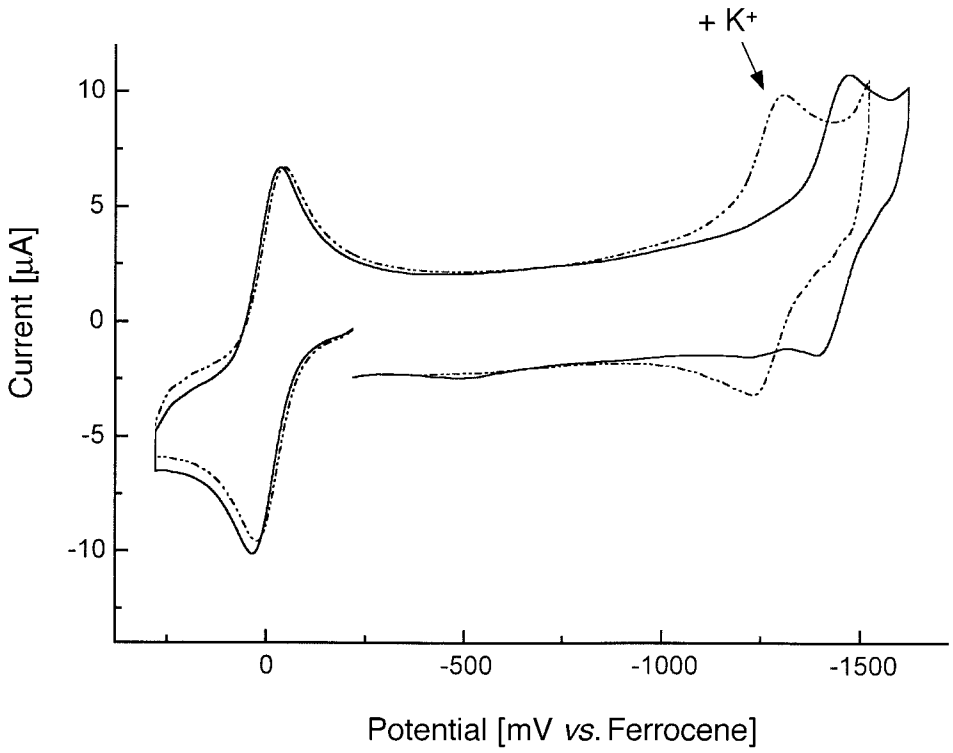

Fig. 16. *CV Response of* (±)-**28b** *in the absence* (——) *and presence* (– ··– ··–) *of 2 equiv. of KPF_6 at a scan rate of 100 mV s^{-1}*

The magnitude of the cation-induced redox shift in (±)-**28a/b** (170 mV) is *ca.* twice that measured for (±)-**7a/b**; accordingly, there is no cooperative effect between the two binding sites. MM2 Calculations indicate that the cation in the *anti*-DB18C6 site is located above the midpoint of a hexagon, whereas, in the *syn*-DB18C6 site, it sits above the midpoint of a pentagon. However, the redox effects resulting from cation binding at both sites are similar. This implies that the potential shifts only depend on the distance and not on the location of the cation with respect to the fullerene surface. Hence, it is concluded that the measured anodic shifts are caused purely by electrostatic effects, in

contrast to the π-interactions observed for sandwich complexes of C_{60} and C_{70} with zinc(II) porphyrins [63].

2.5.3. *Electrochemistry of C_{70} Bis- to Heptakis-Adducts with Malonate Addends.* For the complete series of C_{70} adducts, up to the heptakis-adduct, the redox characteristics were determined by cyclic voltammetry (*Table 4*), although the exact position of the addends on the fullerene surface is unknown for the pentakis- to the heptakis-adducts (for investigations of the changes in redox properties as a function of degree of addition in series of C_{60} derivatives, see [64]). For the purpose of comparison, the data previously recorded for C_{70} mono-adduct **29** and bis-adduct (±)-**30** (*Fig. 15*) featuring a five o'clock addition pattern were included [60]. Although the nature of the malonate addends varies slightly in the entire series, the resulting effect on the electrochemistry of the fullerene core should be negligible. Based on the ΔE_{pp} values, the first reduction step appears to be reversible for the tris- and tetrakis-adducts (±)-**23** and (±)-**24** and quasi-reversible for the compounds in the pentakis-, hexakis-, and heptakis-adducts, *Fractions I, II,* and *IV*, respectively (*Sect. 2.2.2*).

As a general trend, it is found that the first reduction becomes more difficult with an increasing degree of functionalization [64]. Upon changing from C_{70} to tetrakis-adduct (±)-**24**, the first-reduction potential shifts cathodically by 330 mV. Upon progressing to the hexakis-adduct *Fraction II*, a further cathodic shift of 190 mV occurs. No further shift in the first-reduction potential is observed upon moving to the heptakis-adduct *Fraction IV* (*Table 4*).

The reduction potentials are also remarkably dependent on the nature of the addition pattern. Thus, the first reduction of tris-adduct (±)-**23** is cathodically shifted by 30 mV compared to the tris-adduct derived by cyclopropanation of a twelve o'clock bis-adduct similar to (±)-**3** but with malonate addends as in (±)-**30** (*Fig. 15*) [60]. In the series of isomeric tetrakis-adducts **31**, (±)-**32**, and (±)-**24**, the latter possesses the lowest reduction potential, followed by (±)-**32** (+70 mV) and **31** (+110 mV). A plot of the DFT-calculated LUMO energies *vs.* the first-reduction potentials demonstrates a good correlation between these variables (*Fig. 17*). A similar correlation had been previously found for a series of C_{60} mono- to hexakis-adducts [64].

3. Conclusions. – In this study, we have expanded the scope of the tether-directed remote functionalization method from C_{60} to the higher fullerene C_{70}. *Bingel* macrocyclization of the C_{70} with a DB18C6-tethered bis-malonate provided with complete regioselectivity the cyclophane-type C_{70} crown ether conjugates (±)-**7a/b**, featuring the kinetically disfavored five o'clock addition pattern. The crown ether is a true template, since it can be readily removed by transesterification, giving a much improved access to the five o'clock bis-adduct (±)-**4**. Starting from (±)-**4**, novel tris- and tetrakis-adducts were prepared with complete regioselectivity without using a tether. This result supports previous studies [6] [14] that suggested that the formation of higher adducts of C_{70} proceeds with remarkable selectivity, despite the lower symmetry and the larger number of possible reactive bonds compared with C_{60}. Starting from the C_{70} crown ether conjugates (±)-**7a/b**, fullerene bis-crown ether conjugates ((±)-**28a/b**) were prepared for the first time. Cation-binding studies with ion-selective electrodes (ISEs) revealed that cyclophane-type C_{70} mono- and bis-crown ethers form stable complexes with Na^+ and K^+ ions. The comparison with reference compound

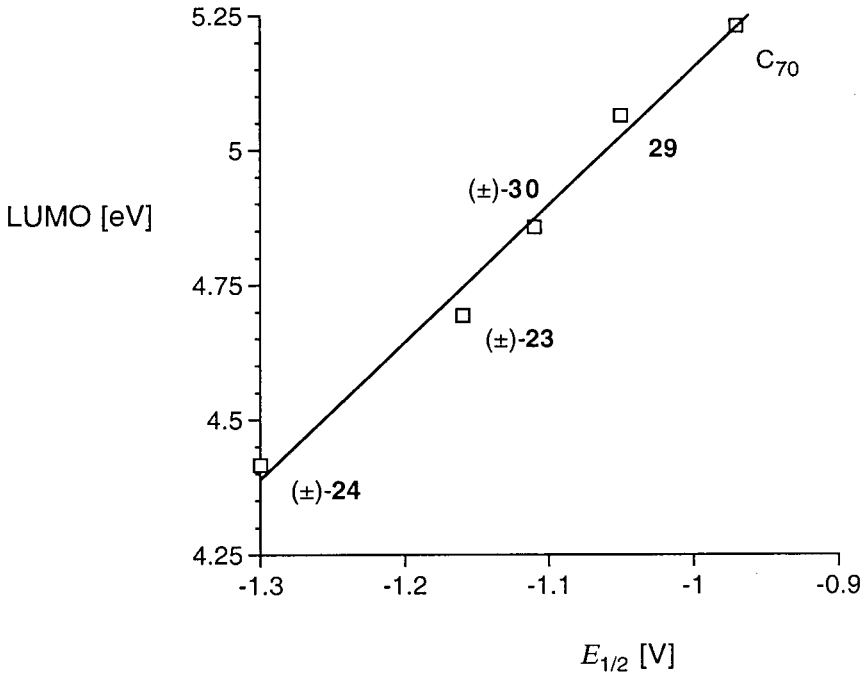

Fig. 17. *Plot of the first reduction potential* E*1/2* vs. *the DFT-calculated LUMO energy for a series of* C_{70} *adducts.* In all calculations, the $(RO_2C)_2$ addends were substituted by CH_2 addends.

(±)-**22**, which has a conformationally flexible crown ether moiety, showed that the cyclophane-type derivatives are less-efficient binders, presumably as a result of reduced conformational flexibility of the doubly bridged ionophoric site and the blocking of one of its faces by the C-sphere.

Electrochemical studies revealed that the binding of Na^+ and K^+ ions by the mono-crown ether conjugates (±)-**7a/b** shifts the first fullerene-centered reduction potential anodically by *ca.* 80 mV. This cation-complexation-induced shift is comparable to those previously reported for a C_{60} crown ether conjugate [29a,b]. For monovalent cations, the shift appears to correlate nicely with the distance of the cation to the fullerene surface. Negligible shifts were recorded for the C_{70} crown ether conjugate (±)-**22** in which the ionophoric DB18C6 moiety is attached to the C-sphere by one linker only and, therefore, possesses full conformational freedom. This demonstrates that a perturbation of the fullerene reduction potentials occurs only when the cation is tightly held close to the fullerene surface. This conclusion is of great importance for future developments of fullerene-based electrochemical ion sensors. For the C_{70} bis-crown ether conjugates (±)-**28a/b**, which form complexes with the C-sphere sandwiched between two ionophore-bound K^+ or Na^+ ions, record anodic shifts (up to 170 mV) of the fullerene-centered first-reduction potential were measured. The interaction between the fullerene core and the crown-ether-bound cations is of a purely electrostatic nature, and no cooperative effects are observed between the two ionophoric sites.

Experimental Part

General. C_{70} (99.5%, gold grade) was purchased from *Hoechst*. All other chemicals were purchased from *Aldrich* and *Fluka*, and used as received. CH_2Cl_2 was distilled from CaH_2 and PhMe from Na. All reactions were conducted in standard glassware under a protective atmosphere of Ar, applying a positive pressure of the protective gas. In the case of reactions of C_{70} derivatives, solvents were vigorously degassed with Ar under sonification for at least 15 min. Evaporation and concentration *in vacuo* were carried out under water aspirator pressure. Further drying of the residues was carried out at 0.1 Torr. Chromatography refers to flash chromatography (FC) on SiO_2 60 (230–400 mesh, 0.04–0.063 mm) or SiO_2–*H* (5–40 μm) from *Fluka*; solvents were of technical grade and distilled prior to use; head pressure of *ca.* 0.3 bar. TLC: *Alugram SIL G/UV*$_{254}$ SiO_2-coated plates from *Macherey-Nagel*; visualisation by UV light (254 nm). Prep. TLC: SiO_2 *60* F_{254} plates from *Merck*. M.p.: *Büchi 510* melting-point apparatus; uncorrected. UV/VIS (λ_{max} [nm], (ε [$M^{-1}cm^{-1}$])): *Varian-CARY 5 UV/VIS-NIR* spectrophotometer with a 1-cm cell at r.t. IR ([cm^{-1}], KBr): *Nicolet 600* FT-IR spectrometer. NMR (^1H, ^{13}C; δ [ppm], *J* [Hz]): *Varian Gemini 200*, *Varian Gemini 300*, or *Bruker 500* spectrometer at 298 K with residual solvent peaks as internal reference. MS (*m/z* (%)): EI mass spectra were recorded on a *VG-Tribid* instrument operating at 70 eV and FAB spectra on a *VG-ZAB-2SEQ* instrument (matrix: 3-nitrobenzyl alcohol); HR-MALDI spectra were measured on an *IonSpec Fourier Transform* (FT) Instrument, using a two-layer technique (tl), with 2,5-dihydroxybenzoic acid (DHB) in MeOH/H_2O as matrix, and the compound typically dissolved in CH_2Cl_2. Elemental analyses were performed by the *Mikrolabor* at the *Laboratorium für Organische Chemie* at *ETH Zürich*.

(±)-out,out-*71,72-Diethyl 71,72-[(6,7,9,10,17,18,20,21-Octahydrodibenzo[*b,k*][1,4,7,10,13,16]hexaoxacyclooctadecin-2,13-diyl)dimethylene]-1,2:67,68-bismethano[70]fullerene-71,71,72,72-tetracarboxylate* ((±)-**7a** and (±)-**7b**). A soln. of C_{70} (98 mg, 0.1167 mmol) in PhMe (190 ml) was sonicated and purged with Ar; then **5** (75.8 mg, 0.1167 mmol), I_2 (59.3 mg, 0.2333 mmol), and KPF_6 (214.7 mg, 1.167 mmol) in MeCN (8.8 ml) were added. Subsequently, DBU (106.6 mg, 0.700 mmol) in CH_2Cl_2 (1.8 ml) was added during 2 h, and the soln. was stirred overnight at r.t. The mixture was poured into H_2O (200 ml), the layers were separated, and the aq. layer was extracted with PhMe (3 × 100 ml). The combined org. layers were washed with H_2O (3 × 200 ml), dried ($MgSO_4$), and concentrated *in vacuo*. The residual black solid was purified by FC (SiO_2; PhMe/MeOH 9:1) followed by another FC (SiO_2-*H*; PhMe/AcOEt 1:1) to afford, in order of elution, (±)-**7a** (40.0 mg, 23.1%), and (±)-**7b** (31.4 mg, 18.1%).

Data of (±)-**7a**: Black solid. M.p. >250°. R_f (SiO_2; PhMe/MeOH 9:1) 0.47. UV/VIS (CH_2Cl_2): 274 (sh, 97100), 298 (sh, 53300), 370 (23700), 402 (23700), 444 (25200), 470 (25600), 505 (sh, 17400), 638 (sh, 2830), 691 (sh, 1510). IR (KBr): 2911*w*, 2856*w*, 1739*s*, 1511*m*, 1444*m*, 1422*m*, 1361*w*, 1272*s*, 1244*s*, 1211*s*, 1167*m*, 1139*s*, 1086*w*, 1042*w*, 856*w*, 794*w*, 744*w*, 667*w*, 578*w*, 533*w*, 456*w*. ^1H-NMR (500.1 MHz, $CDCl_3$): 6.93–6.91 (*m*, 4 H); 6.44 (*d*, *J* = 7.6, 2 H); 5.77 (*d, AB, J* = 11.0, 2 H); 4.88 (*d, AB, J* = 11.0, 2 H); 4.58–4.47 (*m*, 4 H); 4.19–4.02 (*m*, 6 H); 3.94–3.85 (*m*, 6 H); 3.75–3.71 (*m*, 2 H); 3.45 (*q, J* = 7.4, 2 H); 1.50 (*t, J* = 7.1, 6 H). ^{13}C-NMR (125.8 MHz, $CDCl_3$): 163.29; 162.00; 156.17; 155.19; 151.82; 150.84; 150.20; 150.14; 148.83; 148.63; 148.44; 148.21; 148.14; 147.98; 147.46; 147.25; 146.64; 146.55; 144.16; 143.88; 143.39; 143.15; 141.98; 141.82; 141.04; 140.85; 140.59; 138; 97; 138.80; 138.43; 137.19; 135.89; 133.62; 132.54; 132.44; 131.53; 130.46; 127.28; 123.78; 115.15; 111.64; 70.07; 69.79; 69.46; 68.90; 67.13; 66.90 (fullerene C(sp^3)); 66.56 (fullerene C(sp^3)); 63.56 (CH_2); 36.68 (methano bridge); 14.28 (CH_3). MALDI-FT-MS (DHB): 1523.2 (12, $[M+K]^+$), 1507.2 (87, $[M+Na]^+$). HR-MALDI-FT-MS (DHB): 1507.1950 ($[M+Na]^+$, $C_{102}H_{36}NaO_{14}^+$; calc. 1507.1997).

Data of (±)-**7b**: Black solid. M.p. >250°. R_f (SiO_2; PhMe/MeOH 9:1) 0.42. UV/VIS (CH_2Cl_2): 275 (sh, 80600), 296 (sh, 46100), 368 (20200), 403 (sh, 18700), 443 (21500), 464 (sh, 21300), 504 (sh, 14900), 545 (sh, 9400), 641 (sh, 2470), 689 (sh, 1410). IR (KBr): 2922*w*, 2856*w*, 1739*s*, 1511*m*, 1444*m*, 1422*m*, 1361*w*, 1267*s*, 1239*s*, 1222*s*, 1167*m*, 1133*m*, 1089*w*, 1044*w*, 856*w*, 800*w*, 744*w*, 667*w*, 572*w*, 533*w*, 456*w*. ^1H-NMR (500.1 MHz, $CDCl_3$): 7.18 (*dd*, *J* = 8.2, 1.9, 2 H); 6.84 (*d*, *J* = 1.8, 2 H); 6.77 (*d*, *J* = 8.2, 2 H); 5.44 (*d*, *AB*, *J* = 11.0, 2 H); 5.38 (*d*, *AB*, *J* = 11.0, 2 H); 4.52–4.46 (*m*, 4 H); 4.08–3.71 (*m*, 16 H); 1.47 (*t*, *J* = 7.1, 6 H). ^{13}C-NMR (125.8 MHz, $CDCl_3$): 163.67; 163.05; 156.38; 154.88; 151.88; 151.07; 150.22; 150.05; 149.26; 148.98; 148.16; 148.09; 148.01; 147.90; 147.74; 147.22; 146.71; 146.57; 144.45; 143.85; 143.26; 142.94; 142.31; 141.99; 141.56; 140.92; 140.49; 140.12; 138.48; 137.36 (2C); 136.30; 133.45; 132.81; 132.43; 132.09; 130.56; 127.62; 124.54; 114.88; 111.72; 69.88; 69.81; 69.18; 68.41; 68.07; 67.33 (fullerene C(sp^3)); 66.71 (fullerene C(sp^3)); 63.55 (CH_2); 36.35 (methano bridge); 14.24 (CH_3). MALDI-FT-MS (DHB): 1523.2 (12, $[M+K]^+$), 1507.2 (87, $[M+Na]^+$). HR-MALDI-FT-MS (DHB): 1507.1950 ($[M+Na]^+$, $C_{102}H_{36}NaO_{14}^+$; calc. 1507.1997).

*Transesterification of (±)-***7a** *and (±)-***7b**. To a 1:1 mixture of (±)-**7a** and (±)-**7b** (200 mg, 0.1346 mmol) in THF (100 ml) and EtOH (100 ml), KPF_6 (198 mg, 1.077 mmol) and Cs_2CO_3 (1.79 g, 4.04 mmol) were added

under Ar. After stirring for 3 h at r.t., the mixture was partitioned between H_2O (400 ml, acidified to pH 1 with CF_3CO_2H) and PhMe (200 ml). The layers were separated, and the aq. layer was extracted with PhMe (2 × 200 ml). The combined org. layers were washed with H_2O (5 × 200 ml), dried ($MgSO_4$), and concentrated *in vacuo*. The residual black solid was purified by FC (SiO_2; CH_2Cl_2/hexanes 1:1) to afford (±)-**4** (64 mg, 41%). All anal. and spectroscopic data were found to be in accord with those previously reported [5a][14].

4-Benzyloxy-3-hydroxybenzaldehyde (**9**). A mixture of **8** (35.0 g, 253 mmol) and K_2CO_3 (32.0 g, 232 mmol) in DMF (300 ml) was stirred under Ar at 60° for 4 h. $PhCH_2Br$ (33.1 ml, 47.7 g, 279 mmol) was added and the mixture stirred at r.t. for 12 h. After evaporation *in vacuo*, the residue was partitioned between AcOEt (500 ml) and H_2O (500 ml). The org. layer was washed successively with sat. aq. NH_4Cl soln. (3 × 200 ml), H_2O (2 × 200 ml), and sat. aq. NaCl soln. (2 × 200 ml), dried (Na_2SO_4), and concentrated *in vacuo*. FC (SiO_2; hexanes/AcOEt 7:3 → 1:1) followed by crystallization (hexane/CH_2Cl_2) afforded **9** (39.1 g, 74%). White needles. M.p. 121–123°. R_f (SiO_2; hexanes/AcOEt 1:1) 0.48. ^{1}H-NMR (300 MHz, $CDCl_3$): 9.85 (*s*, 1 H); 7.48–7.39 (*m*, 7 H); 7.05 (*d*, *J* = 8.2, 1 H); 5.83 (*s*, 1 H); 5.22 (*s*, 2 H). ^{13}C-NMR (75 MHz, $CDCl_3$): 191.4; 151.3; 146.7; 135.5; 131.1; 129.2; 129.0 (2×); 128.1 (2×); 124.6; 114.7; 111.8; 71.4. EI-MS (70 eV): 228 (7, M^+), 137 (2, [$M - C_7H_7$]$^+$), 91 (100, [C_7H_7]$^+$). Anal. calc. for $C_{14}H_{12}O_3$ (228.25): C 73.67, H 5.30; found: C 73.83, H 5.47.

4,4′-Bis(benzyloxy)-3,3′-oxybis(ethyleneoxy)dibenzaldehyde (**10**). To **9** (20.0 g, 87.6 mmol) and K_2CO_3 (24.2 g, 175.2 mmol) in DMF (300 ml), $(ClCH_2CH_2)_2O$ (5.1 ml, 6.24 g, 43.8 mmol) was added. The mixture was stirred under Ar at 80° for 42 h. After evaporation *in vacuo*, the residue was subjected to FC (SiO_2; hexanes/AcOEt 4:1 → 3:2) to yield a white solid that was recrystallized (hexane/CH_2Cl_2) to afford **10** (18.9 g, 82%). White needles. M.p. 127–129°. R_f (SiO_2; hexanes/AcOEt 1:1) 0.42. ^{1}H-NMR (200 MHz, $CDCl_3$): 9.84 (*s*, 2 H); 7.45–7.29 (*m*, 14 H); 7.02 (*d*, *J* = 8.8, 2 H); 5.20 (*s*, 4 H); 4.25–4.20 (*m*, 4 H); 4.03–3.99 (*m*, 4 H). ^{13}C-NMR (50 MHz, $CDCl_3$): 191.0; 154.2; 149.5; 136.3; 130.4; 128.7 (2×); 128.1; 127.3 (2×); 126.6; 113.1; 112.0; 70.8; 69.8; 69.0. HR-MALDI-FT-MS (DHB): 549.1879 ([M + Na]$^+$, $C_{32}H_{30}NaO_7^+$; calc. 549.1889). Anal. calc. for $C_{32}H_{30}O_7$ (526.58): C 72.99, H 5.74; found: C 72.97, H 5.82.

4,4′-Bis(hydroxy)-3,3′-oxybis(ethyleneoxy)dibenzaldehyde (**11**). To **10** (5.80 g, 11.0 mmol) in PhMe (300 ml), Pd/C (10%; 0.60 g, 0.56 mmol) was added, and the mixture was stirred vigorously under H_2 (1 atm) for 2.5 h. Upon complete conversion (TLC), the catalyst was removed by filtration through a *Celite* pad, and the filtrate was concentrated *in vacuo*. FC (SiO_2; CH_2Cl_2/AcOEt 9:1 → 7:3) yielded **11** (2.96 g, 77%). White solid. M.p. 131–133°. R_f (SiO_2; CH_2Cl_2/AcOEt) 0.24. ^{1}H-NMR (300 MHz, $CDCl_3$): 9.83 (*s*, 2 H); 8.12 (br. *s*, 2 H); 7.53–7.49 (*m*, 4 H); 7.10 (*d*, *J* = 8.4, 2 H); 4.31–4.28 (*m*, 4 H); 3.94–3.91 (*m*, 4 H). ^{13}C-NMR (50 MHz, $CDCl_3$): 190.2; 153.0; 146.0; 129.5; 128.2; 115.7; 114.3; 69.5; 69.0. EI-MS: 346 (89, M^+), 137 (100, [$C_7H_5O_3$]$^+$). Anal. calc. for $C_{18}H_{18}O_7$ (346.34): C 62.42, H 5.24; found: C 62.24, H 5.42.

*6,7,9,10,17,18,20,21-Octahydrodibenzo[*b,k*][1,4,7,10,13,16]hexaoxacyclooctadecin-2,14-dicarbaldehyde* (**13**). A mixture of **11** (1.00 g, 2.89 mmol), K_2CO_3 (2.39 g, 17.3 mmol), and KI (1.92 g, 11.5 mmol) in DMF (100 ml) was stirred under Ar for 1.5 h at 80°. Then, $(BrCH_2CH_2)_2O$ (0.40 ml, 0.69 g, 3.18 mmol) was added, and the mixture was stirred under Ar at 80° for 42 h. Evaporation *in vacuo* provided crude product that was partitioned between $CHCl_3$ (100 ml) and H_2O (100 ml). The aq. layer was extracted with $CHCl_3$ (3 × 50 ml), and the combined org. layers were washed with H_2O (3 × 50 ml), dried ($MgSO_4$), and concentrated *in vacuo*. FC (SiO_2; CH_2Cl_2/AcOEt 9:1 → 7:3) afforded **13** (1.11 g, 92%). White solid. M.p. 210–212°. R_f (SiO_2; CH_2Cl_2/AcOEt 1:1) 0.12. ^{1}H-NMR (300 MHz, $CDCl_3$): 9.83 (*s*, 2 H); 7.43 (*dd*, *J* = 8.4, 1.8, 2 H); 7.38 (*d*, *J* = 1.8, 2 H); 6.94 (*d*, *J* = 8.4, 2 H); 4.26–4.21 (*m*, 8 H); 4.07–4.01 (*m*, 8 H). ^{13}C-NMR (50 MHz, $CDCl_3$): 191.2; 154.4; 149.4; 130.5; 127.0; 111.9; 110.7; 77.4; 69.7; 68.7; 68.6. EI-MS: 416 (1, M^+). Anal. calc. for $C_{22}H_{24}O_8$ (416.43): C 63.44, H 5.81; found: C 63.65, H 5.97.

*6,7,9,10,17,18,20,21-Octahydrodibenzo[*b,k*][1,4,7,10,13,16]hexaoxacyclooctadecin-2,14-dimethanol* (**14**). To a stirred suspension of **13** (200 mg, 0.480 mmol) in MeOH (50 ml), $NaBH_4$ (55 mg, 1.44 mmol) was added at 0°. After 20 min, the now clear soln. was warmed to r.t., and stirring was continued for 1 h. The mixture was neutralized by adding a few drops of 0.3M CF_3CO_2H. The residue obtained by evaporation *in vacuo* was partitioned between $CHCl_3$ (50 ml) and H_2O (50 ml). The aq. layer was extracted with $CHCl_3$ (8 × 20 ml). The combined org. layers were dried ($MgSO_4$) and evaporated *in vacuo* to give **14** (198 mg, 98%). White solid. M.p. 162–164°. ^{1}H-NMR (300 MHz, $(CD_3)_2SO$): 6.92–6.80 (*m*, 4 H); 6.55 (br. *s*, 2 H); 5.08 (*t*, *J* = 5.4, 2 H); 4.43 (*d*, *J* = 5.4, 4 H); 4.14–4.02 (*m*, 8 H); 3.92–3.80 (*m*, 8 H). ^{13}C-NMR (75 MHz, $(CD_3)_2SO$): 147.9; 146.9; 135.2; 118.7; 112.3; 111.3; 69.0 (2×); 67.8; 67.6; 62.8. HR-MALDI-FT-MS (DHB): 443.1665 ([M + Na]$^+$, $C_{22}H_{28}NaO_8^+$; calc. 443.1682). Anal. calc. for $C_{22}H_{28}NaO_8$ (420.46): C 62.85, H 6.71; found: C 62.53, H 6.35.

*1,1′-Diethyl 3,3′-[(6,7,9,10,17,18,20,21-Octahydrodibenzo[*b,k*][1,4,7,10,13,16]hexaoxacyclooctadecin-2,14-diyl)dimethylene]bis(malonate)* (**6**). To a suspension of **14** (90.0 mg, 0.203 mmol) and pyridine (32.7 µl, 32.1 mg, 0.406 mmol) in dry CH_2Cl_2 (25 ml), $ClOCCH_2CO_2Et$ (76.7 µl, 91.7 mg, 0.609 mmol) was slowly added

at 0° under Ar. After 30 min, an additional equiv. of pyridine (16.3 µl, 16.1 mg, 0.203 mmol) was added, and the mixture was stirred at r.t. for 1 h. The mixture was poured into H_2O (50 ml), the layers were separated, and the aq. layer was extracted with CH_2Cl_2 (2 × 50 ml). The combined org. layers were washed with H_2O (3 × 50 ml), dried ($MgSO_4$), and evaporated *in vacuo* to afford a white solid, which was further purified by FC (SiO_2; CH_2Cl_2/MeOH 99:1) to give **6** (112 mg, 81%). White solid. M.p. 110–112°. R_f (SiO_2; CH_2Cl_2/MeOH 19:1) 0.20. UV/VIS (CH_2Cl_2): 233 (8840), 281 (3230), 286 (sh, 2780). IR (KBr): 2989*w*, 2933*w*, 1750*s*, 1733*s*, 1719*s*, 1517*s*, 1433*w*, 1333*s*, 1261*s*, 1141*s*, 1060*m*, 978*w*, 806*w*. ^{1}H-NMR (300 MHz, $CDCl_3$): 6.96–6.83 (*m*, 6 H); 5.12 (*s*, 4 H); 4.22–4.15 (*m*, 12 H); 4.06–4.02 (*m*, 8 H); 3.41 (*s*, 4 H); 1.27 (*t*, *J* = 7.2, 6 H). ^{13}C-NMR (75 MHz, $CDCl_3$): 166.83; 166.78; 149.36; 149.15; 128.60; 122.05; 114.51; 113.78; 70.06 (2×); 69.17 (2×); 67.33; 61.67; 41.72; 14.06. HR-MALDI-FT-MS (DHB): 671.2312 ($[M+Na]^+$, $C_{32}H_{40}NaO_{14}^+$; calc. 671.2316). Anal. calc. for $C_{32}H_{40}NaO_{14}^+$ (648.66): C 59.25, H 6.22; found: C 59.19, H 6.18.

(±)-out,out-*71,72-Diethyl 71,72-[(6,7,9,10,17,18,20,21-Octahydrodibenzo[*b,k*][1,4,7,10,13,16]hexaoxacyclooctadecin-2,14-diyl)dimethylene]-1,2:56,57-dimethano[70]fullerene-71,71,72,72-tetracarboxylate* ((±)-**15**) *and* out,out-*71,72-Diethyl 71,72-[(6,7,9,10,17,18,20,21-Octahydrodibenzo[*b,k*][1,4,7,10,13,16]hexaoxacyclooctadecin-2,14-diyl)dimethylene]-1,2:41,58-dimethano[70]fullerene-71,71,72,72-tetracarboxylate* (**16**). To a degassed soln. of C_{70} (33 mg, 0.0385 mmol) in dry PhMe (70 ml), **6** (25 mg, 0.0385 mmol), I_2 (20 mg, 0.0771 mmol), and KPF_6 (71 mg, 0.385 mmol) in MeCN (2 ml) were added sequentially. Subsequently, DBU (0.035 ml, 32.2 mg, 0.2312 mmol) in CH_2Cl_2 (1 ml) was added during 35 min, and the soln. was stirred for 2 h at r.t. The mixture was partitioned between PhMe and H_2O, the layers were separated, and the aq. layer was extracted with CH_2Cl_2 (2 × 50 ml). The PhMe layer and the combined CH_2Cl_2 layers were washed separately with H_2O (3 × 50 ml), combined, dried ($MgSO_4$), and concentrated *in vacuo*. TLC (SiO_2; PhMe/MeOH 9:1) of the residual black solid showed the formation of two compounds that were separated by FC (SiO_2-*H*, PhMe/AcOEt 7:3 → 1:1) to afford (±)-**15** (15 mg, 26%), and **16** (18 mg, 32%).

Data of (±)-**15**: Black solid. M.p. > 250°. R_f (SiO_2; PhMe/MeOH 9:1) 0.31. UV/VIS (CH_2Cl_2): 260 (sh, 100700), 284 (sh, 60900), 335 (21200), 404 (17700), 434 (20800), 462 (20200), 527 (sh, 13400), 655 (sh, 2020). IR (KBr): 2946*w*, 2922*w*, 2867*w*, 2368*m*, 2356*m*, 2342*m*, 1745*s*, 1633*w*, 1517*w*, 1428*w*, 1384*w*, 1285*m*, 1250*m*, 1233*s*, 1172*w*, 1139*m*, 1089*w*, 1050*w*. ^{1}H-NMR (500.1 MHz, $CDCl_3$): 7.28 (*dd*, *J* = 7.3, 1.8, 1 H); 7.01 (*d*, *J* = 1.9, 1 H); 6.89–6.83 (*m*, 3 H); 6.41 (*d*, *J* = 7.7, 1 H); 5.94 (*d*, *J* = 11.0, 1 H); 5.78 (*d*, *J* = 11.2, 1 H); 5.04 (*d*, *J* = 11.0, 1 H); 4.92 (*d*, *J* = 11.2, 1 H); 4.60–4.45 (*m*, 4 H); 4.21–3.71 (*m*, 16 H); 1.55 (*t*, *J* = 7.2, 3 H); 1.48 (*t*, *J* = 7.1, 3 H). ^{13}C-NMR (125.8 MHz, $CDCl_3$): 163.73; 163.41; 162.96; 161.70; 155.56; 155.40; 154.93; 154.87; 152.72; 152.45; 152.19; 152.01; 151.59; 151.50; 150.83; 150.59; 150.42 (2×); 149.88; 149.31; 148.94; 148.82; 148.72; 148.31; 148.26; 148.07; 147.48; 147.08; 146.75; 146.37; 146.27; 146.19; 146.15; 145.70; 145.56; 144.85; 144.80; 144.41; 144.35; 144.26 (2×); 144.25; 143.62; 143.58; 143.18; 143.07; 142.40; 142.21; 142.13; 141.85; 141.28; 141.18; 141.04; 140.94; 140.70; 140.35; 140.11; 139.90; 139.17; 138.49; 138.11; 137.02; 136.87; 136.20; 135.62; 135.43; 133.15; 132.82; 132.72; 132.70; 131.35; 131.05; 130.82; 130.68; 127.85; 127.78; 124.44; 122.90; 115.13; 113.29; 112.28; 111.07; 70.30; 70.25; 69.82; 69.66; 69.37; 69.08; 68.51; 68.42; 67.73; 67.47; 66.82 (fullerene C(sp^3)); 66.64 (fullerene C(sp^3)); 66.32 (fullerene C(sp^3)); 66.62 (fullerene C(sp^3)); 63.59 (CH_2); 63.54 (CH_2); 38.29 (methano bridge); 38.01 (methano bridge); 14.37 (Me); 14.29 (Me). HR-MALDI-FT-MS (DHB): 1507.2008 ($[M+Na]^+$, $C_{102}H_{36}NaO_{14}^+$; calc. 1507.1997).

Data of **16**: R_f (SiO_2; PhMe/MeOH 9:1) 0.26. UV/VIS (CH_2Cl_2): 270 (78600), 363 (17400), 401 (18100), 423 (sh, 17000), 477 (18000), 537 (sh, 9180), 660 (sh, 1670). IR (KBr): 2940*m*, 2922*m*, 2867*m*, 2355*m*, 2331*m*, 1744*m*, 1638*m*, 1517*w*, 1428*w*, 1383*w*, 1267*s*, 1228*s*, 1172*s*, 1139*s*, 1089*s*, 794*w*. ^{1}H-NMR (500.1 MHz, $CDCl_3$): 7.09 (*dd*, *J* = 8.2, 2.0, 2 H); 6.98 (*d*, *J* = 2.0, 2 H); 6.79 (*d*, *J* = 8.2, 2 H); 5.60 (*d*, *J* = 10.9, 2 H); 5.33 (*d*, *J* = 10.9, 2 H); 4.532 (*q*, *J* = 7.2, 2 H); 4.529 (*q*, *J* = 7.1, 2 H); 4.12–4.09 (*m*, 2 H); 4.00–3.97 (*m*, 2 H); 3.95–3.89 (*m*, 4 H); 3.82–3.77 (*m*, 4 H); 3.71–3.64 (*m*, 4 H); 1.50 (*t*, *J* = 7.1, 6 H). ^{13}C-NMR (125.8 MHz, $CDCl_3$): 164.18 (2×); 163.69 (2×); 154.60 (2×); 153.87 (2×); 152.54 (2×); 152.40 (2×); 151.40 (2×); 151.33 (2×); 149.85 (2×); 149.28 (2×); 149.24 (2×); 149.07 (2×); 148.77 (2×); 148.69 (2×); 148.25 (2×); 147.96 (2×); 147.39 (2×); 147.30 (2×); 143.42 (2×); 143.00 (2×); 142.60 (2×); 142.55 (2×); 142.22 (2×); 141.52 (2×); 141.45 (2×); 141.39 (6×); 141.27 (2×); 140.32 (2×); 137.21 (2×); 136.88 (2×); 136.51; 136.36; 135.28; 135.18; 131.62; 131.31; 131.21; 130.99; 130.59; 130.42; 127.75 (2×); 124.36 (2×); 115.82 (2×); 112.46 (2×); 69.75 (2×); 69.66 (2×); 69.07 (2×); 68.55 (2×); 68.17 (2×); 66.11 (2×) (fullerene C(sp^3)); 66.07 (2×) (fullerene C(sp^3)); 63.66 (2×) (CH_2); 36.16 (2×) (methano bridge) ; 14.28 (2×) (Me). HR-MALDI-FT-MS (DHB): 1507.1990 ($[M+Na]^+$, $C_{102}H_{36}NaO_{14}^+$; calc. 1507.1997).

Transesterification of (±)-**15** *and* **16**. To (±)-**15** (8.9 mg, 0.0060 mmol) in dry EtOH/THF 1:1 (8.0 ml), KPF_6 (9.0 mg, 0.0489 mmol) and Cs_2CO_3 (79.9 mg, 0.245 mmol) were added under Ar. After stirring for 3 h, the mixture was partitioned between PhMe (50 ml) and H_2O (50 ml) and acidified to pH 1 with CF_3CO_2H. The

layers were separated, and the aq. layer was extracted with PhMe (2 × 25 ml). The combined org. layers were washed with H_2O (3 × 50 ml), dried ($MgSO_4$), and concentrated *in vacuo*. TLC (SiO_2; PhMe) showed one major compound (R_f 0.31). Comparison with an authentic sample, prepared by sequential *Bingel* bis-cyclopropanation of C_{70}, identified this compound as the two o'clock bis-adduct ((±)-**3**). However, some five o'clock adduct (±)-**4** could be detected too, indicating that (±)-**15** was contaminated with *ca.* 10% of the corresponding crown ether conjugate with a five o'clock addition pattern. The same procedure was carried out with **16**. After transesterification, a single compound was obtained (R_f (SiO_2; PhMe) 0.26), which was identified as the twelve o'clock bis-adduct **2**. All anal. and spectroscopic data of (±)-**3** and **2** were found to be in accord with those previously reported [5a][14].

1,2-Bis[2-(2-chloroethoxy)ethoxy]benzene (**18**). To **17** (11.0 g, 100 mmol) in anh. DMF (150 ml), purged with Ar for 15 min, K_2CO_3 (34.6 g, 250 mmol) was added. After stirring for 1 h at r.t., $(ClCH_2CH_2)_2O$ (85.8 g, 600 mmol) was added, and the mixture was stirred under Ar at 85° for 24 h. After cooling to r.t., the mixture was poured into H_2O (1 l) and extracted with CH_2Cl_2 (3 × 200 ml). The combined org. layers were washed successively with 2M NaOH (2 × 200 ml), 0.5M HCl (2 × 200 ml), and H_2O (2 × 200 ml). Drying ($MgSO_4$) and evaporation *in vacuo* yielded a yellow oil, which was purified by FC (SiO_2; CH_2Cl_2) to yield **18** (11.29 g, 35%). Pale yellow oil. R_f (SiO_2; CH_2Cl_2) 0.29. ^{1}H-NMR (300 MHz, $CDCl_3$): 6.93 (*s*, 4 H); 4.18 (*t*, *J* = 4.8, 4 H); 3.90 (*t*, *J* = 4.8, 4 H); 3.86 (*t*, *J* = 5.9, 4 H); 3.66 (*t*, *J* = 5.9, 4 H). ^{13}C-NMR (75 MHz, $CDCl_3$): 148.9; 121.8; 114.9; 71.6; 69.9; 68.9; 42.9. HR-MALDI-FT-MS (DHB): 345.0630 ($[M+Na]^+$, $C_{14}H_{20}Cl_2NaO_4^+$; calc. 345.0631). Anal. calc. for $C_{14}H_{20}Cl_2O_4$ (323.22): C 52.03, H 6.24, O 19.8; found: C 51.98, H 6.43, O 19.96.

*6,7,9,10,17,18,20,21-Octahydrodibenzo[*b,k*][1,4,7,10,13,16]hexaoxacyclooctadecin-2-carbaldehyde* (**19**). A mixture of **8** (1.1 g, 8.8 mmol), KI (5.31 g, 32.0 mmol), and K_2CO_3 (6.63 g, 48 mmol) in anh. DMF (400 ml) was purged with Ar for 15 min, then stirred under Ar at 80° for 1 h. Subsequently, **18** (2.58 g, 8.0 mmol) was added, and the mixture was stirred under Ar at 80° for 40 h. After evaporation *in vacuo*, the residue was partitioned between CH_2Cl_2 (100 ml) and H_2O (500 ml). The layers were separated, and the aq. layer was extracted with CH_2Cl_2 (4 × 100 ml). The combined org. layers were washed with H_2O (2 × 100 ml), dried ($MgSO_4$), and concentrated *in vacuo* to afford a brown solid. FC (SiO_2; $CHCl_3 \rightarrow CHCl_3$/MeOH 98:2), followed by precipitation from hexane/CH_2Cl_2, afforded **19** (1.07 g, 34%). White solid. R_f (SiO_2; $CHCl_3$/MeOH 5:1) 0.16. M.p. 184–185°. ^{1}H-NMR (300 MHz, $CDCl_3$): 9.83 (*s*, 1 H); 7.43 (*d*, *J* = 8.1, 1 H); 7.38 (*s*, 1 H); 6.94 (*d*, *J* = 8.1, 1 H); 6.89 (*s*, 4 H); 4.26–4.22 (*m*, 4 H); 4.19–4.15 (*m*, 4 H); 4.08–4.01 (*m*, 8 H). ^{13}C-NMR (75 MHz, $CDCl_3$): 191.0; 154.2; 149.2; 148.9; 148.8; 130.2; 126.9; 121.5; 121.3; 113.9; 113.7; 111.7; 110.6; 70.2; 70.1; 69.6; 69.5; 68.9 (2×); 68.8; 68.5. HR-MALDI-FT-MS (DHB): 411.1411 ($[M+Na]^+$, $C_{21}H_{24}NaO_7^+$; calc. 411.1414).

*6,7,9,10,17,18,20,21-Octahydrodibenzo[*b,k*][1,4,7,10,13,16]hexaoxacyclooctadecin-2-methanol* (**20**). To a stirred suspension of **19** (776 mg, 2.0 mmol) in MeOH (200 ml), $NaBH_4$ (303 mg, 8.0 mmol) was added at 0°. After 30 min, the now clear soln. was warmed to r.t. and stirred for 1 h. The mixture was neutralized with 0.3M CF_3CO_2H. The solvent was evaporated *in vacuo*, and the residue was partitioned between $CHCl_3$ (100 ml) and H_2O (200 ml). The layers were separated, and the aq. layer was extracted with $CHCl_3$ (4 × 100 ml). The combined org. layers were dried ($MgSO_4$) and evaporated *in vacuo* to give **20** (738 mg, 95%). White solid. M.p. 170–171°. R_f (SiO_2; $CHCl_3$/MeOH 5:1) 0.15. ^{1}H-NMR (300 MHz, $(CD_3)_2SO$): 6.95–6.78 (*m*, 7 H); 5.07 (br. *s*, 1 H); 4.40 (*s*, 2 H); 4.04 (br. *s*, 8 H); 3.83 (br. *s*, 8 H). ^{13}C-NMR (75 MHz, $(CD_3)_2SO$): 147.9 (2×); 147.6; 146.6; 134.9; 120.6 (2×); 118.4; 112.4 (2×); 112.0; 110.9; 68.8 (4×); 67.6; 67.5 (3×); 62.7. HR-MALDI-FT-MS (DHB): 413.1566 ($[M+Na]^+$, $C_{21}H_{26}NaO_7^+$; calc. 413.1571).

*1-Ethyl 3-[(6,7,9,10,17,18,20,21-Octahydrodibenzo[*b,k*][1,4,7,10,13,16]hexaoxacyclooctadecin-2-yl)methylene]malonate* (**21**). To a suspension of **20** (559 mg, 1.43 mmol) in dry CH_2Cl_2 (50 ml), $ClOCCH_2CO_2Et$ (541 µl, 647 mg, 4.30 mmol) was added at 0° under Ar, followed by slow addition of pyridine (230 µl, 227 mg, 2.87 mmol). After 1 h, the mixture was warmed to r.t., an additional equiv. of pyridine (115 µl, 114 mg, 1.43 mmol) was added, and stirring was continued at r.t. for 2 h. The mixture was poured into H_2O (100 ml), the layers were separated, and the aq. layer was extracted with CH_2Cl_2 (3 × 50 ml). The combined org. layers were washed with 1M HCl (1 × 50 ml), H_2O (3 × 100 ml), dried ($MgSO_4$), and evaporated *in vacuo* to afford a white solid, which was purified by FC (SiO_2; CH_2Cl_2/AcOEt 2:1) to give **21** (358 mg, 50%). White solid. M.p. 118–120°. R_f (SiO_2; $CHCl_3$/MeOH 5:1) 0.38. UV/VIS (CH_2Cl_2): 230 (30100), 278 (11400). IR (KBr): 2936*m*, 2873*w*, 1732*s*, 1591*m*, 1519*s*, 1506*s*, 1454*m*, 1431*w*, 1413*w*, 1370*w*, 1331*m*, 1254*s*, 1125*s*, 1060*m*, 1032*m*, 993*w*, 956*m*, 935*w*, 857*w*, 798*w*, 780*w*, 753*w*. ^{1}H-NMR (300 MHz, $CDCl_3$): 6.92–6.82 (*m*, 7 H); 5.09 (*s*, 2 H); 4.22–4.14 (*m*, 10 H); 4.05–4.00 (*m*, 8 H); 3.39 (*s*, 2 H); 1.24 (*t*, *J* = 7.2, 3 H). ^{13}C-NMR (75 MHz, $CDCl_3$): 166.54; 166.49; 149.10; 148.89 (2×); 148.84; 128.28; 121.84; 121.45; 121.42; 114.27; 113.98 (2×); 113.47; 70.08 (2×); 69.94 (2×); 69.08;

69.05; 69.00; 68.92; 67.23; 61.57; 41.66; 14.07. HR-MALDI-FT-MS (DHB): 527.1882 ($[M+Na]^+$, $C_{26}H_{32}NaO_{10}^+$; calc. 527.1888). Anal. calc. for $C_{26}H_{32}O_{10}$ (504.53): C 61.90, H 6.39; found: C 62.16, H 6.66.

*71-Ethyl 71-[(6,7,9,10,17,18,20,21-Octahydrodibenzo[*b,k*][1,4,7,10,13,16]hexaoxacyclooctadecin-2-yl)methylene]-1,2-methano[70]fullerene-71,71-dicarboxylate* ((±)-**22**). To C_{70} (210 mg, 0.25 mmol) in dry PhMe (400 ml), **21** (101 mg, 0.20 mmol) in dry MeCN (16 ml) and I_2 (50.8 mg, 0.20 mmol) were added sequentially, and the resulting mixture was purged with Ar under sonication for 30 min. DBU (99 µl, 91 mg, 0.60 mmol) in CH_2Cl_2 (2 ml) was added during 30 min, and the soln. was stirred overnight at r.t. The mixture was poured into H_2O (500 ml), the layers were separated, and the org. layer was washed with H_2O (3 × 200 ml). After drying ($MgSO_4$) and concentration *in vacuo*, a brown solid remained, which was purified by FC (SiO_2; PhMe/MeOH 98:2) to afford (±)-**22** (217 mg, 81%). Black solid. M.p. >250°. R_f (SiO_2, PhMe/MeOH 9:1) 0.26. UV/VIS (CH_2Cl_2): 234 (141100), 277 (sh, 75900), 308 (sh, 30200), 326 (sh, 24300), 353 (21900), 370 (20900), 402 (17700), 459 (19100), 537 (sh, 9290), 609 (sh, 3070), 663 (sh, 1360). IR (KBr): 2922*w*, 2867*w*, 1742*s*, 1590*w*, 1503*s*, 1450*m*, 1427*s*, 1252*s*, 1224*s*, 1133*s*, 736*m*. ^{1}H-NMR (500.1 MHz, $CDCl_3$): 7.04 (*dd*, *J* = 8.1, 1.9, 1 H); 6.98 (*d*, *J* = 1.9, 1 H); 6.90–6.78 (*m*, 5 H); 5.42 (*d*, *AB*, *J* = 11.5, 1 H); 5.37 (*d*, *AB*, *J* = 11.5, 1 H)); 4.48–4.43 (*m*, 2 H); 4.18–3.94 (*m*, 16 H); 1.39 (*t*, *J* = 7.1, 3 H). ^{13}C-NMR (125.8 MHz, $CDCl_3$): 163.43; 163.24; 155.14; 154.84; 151.26 (3×); 151.14; 150.93; 150.64; 150.62; 150.54; 150.44; 149.32; 149.27; 149.23; 149.20; 149.03; 149.01 (2×); 148.64 (3×); 148.57; 148.53; 148.47; 148.45; 148.40; 148.37; 148.35; 148.25; 147.48 (3×); 147.29; 147.22; 147.14; 146.97; 146.81; 146.35; 145.87 (2×); 145.77; 145.75; 144.93; 144.61; 143.87; 143.79; 143.76; 143.72; 143.46; 143.32; 142.79 (2×); 142.63; 142.61; 142.47; 141.58; 141.49; 141.41; 141.19; 140.05; 136.82; 136.61; 133.51; 133.42; 132.75; 132.72; 130.88; 130.85; 130.72; 130.70; 130.65 (2×); 127.50; 123.03; 121.34; 121.25; 114.55; 113.30; 113.19; 112.82; 70.01; 69.98; 69.79 (2×); 69.11; 68.80; 68.72; 68.58; 68.46; 66.80 (fullerene C(sp^3)); 66.17 (fullerene C(sp^3)); 63.56 (CH_2); 37.07 (methano bridge); 14.17 (Me). HR-MALDI-FT-MS (DHB): 1365.1737 ($[M+Na]^+$, $C_{96}H_{30}NaO_{10}^+$; calc. 1365.1737).

(±)-*Hexaethyl 1,2:31,32:67,68-Trimethano[70]fullerene-71,71,72,72,73,73-hexacarboxylate* ((±)-**23**). A soln. of (±)-**4** (13.45 mg, 0.01162 mmol) in PhMe (40 ml) was sonicated and purged with Ar; then, $(EtO_2C)_2CH_2$ (1.86 mg, 0.01162 mmol) and I_2 (2.95 mg, 0.01162 mmol) were added. Subsequently, MeCN (2.0 ml) was added, followed by slow addition (30 min) of DBU (5.31 mg, 0.03487 mmol) in PhMe (2.0 ml). The mixture was stirred for 2 h at r.t.; then Me_2SO (8.0 ml) was added over a period of 2 h. After stirring overnight at r.t., the mixture was partitioned between PhMe (50 ml) and H_2O (50 ml), and the aq. layer was extracted with PhMe (3 × 20 ml). The combined org. layers were washed with H_2O (3 × 50 ml), dried ($MgSO_4$), and concentrated *in vacuo*. FC (SiO_2; CH_2Cl_2) afforded (±)-**23** (5.48 mg, 36%), and starting material (±)-**4** (4.08 mg, 30%).

Data of (±)-**23**: Black solid. M.p. >250°. R_f (SiO_2; PhMe) 0.21. UV/VIS (CH_2Cl_2): 250 (65900), 271 (sh, 50000), 312 (sh, 18000), 406 (12800), 451 (sh, 10300), 537 (sh, 4620), 607 (sh, 2280), 687 (sh, 520). IR (KBr): 2974*w*, 2923*m*, 2852*w*, 2364*w*, 2341*w*, 1744*s*, 1442*w*, 1294*w*, 1231*s*, 1172*w*, 1091*m*, 1016*w*. ^{1}H-NMR (500.1 MHz, $CDCl_3$): 4.60-4.44 (*m*, 10 H); 4.22 (*q*, *J* = 7.0, 2 H); 1.52–1.42 (*m*, 15 H); 1.21 (*q*, *J* = 7.1, 3 H). ^{13}C-NMR (125.8 MHz, $CDCl_3$): 164.50; 163.82; 163.67; 163.62; 163.52; 163.37; 155.54; 154.60; 153.20; 151.78; 151.72; 151.11; 150.93; 150.50; 150.36; 150.30; 149.15; 148.18; 147.99; 147.90; 147.76; 147.72; 147.59; 147.30; 146.10; 144.73; 144.64; 144.54; 144.24; 144.15; 143.63; 143.55; 143.19; 142.78; 142.70; 142.53; 142.47; 142.11; 141.87; 141.61; 141.57; 141.01; 140.81; 140.73; 140.70; 140.45; 140.39; 140.29; 140.04; 139.39; 139.36; 138.40; 137.95; 137.53; 137.27; 137.08; 134.85; 134.46; 134.28; 134.23; 133.87; 133.68; 133.57; 133.37; 133.21; 132.91; 131.39; 129.62; 128.62; 128.19; 68.99 (fullerene C(sp^3)); 68.94 (fullerene C(sp^3)); 68.74 (fullerene C(sp^3)); 67.92 (fullerene C(sp^3)); 63.72 (fullerene C(sp^3)); 63.66 (fullerene C(sp^3)); 63.40 (2×) (CH_2); 63.36 (CH_2); 63.28 (CH_2); 63.25 (CH_2); 62.85 (CH_2); 38.05 (methano bridge); 37.99 (methano bridge); 37.65 (methano bridge); 14.25 (Me); 14.21 (4×) (Me); 13.96 (Me). MALDI-FT-MS (DHB): 1337.2 (40, $[M+Na]^+$), 1314.2 (44, M^+). HR-MALDI-FT-MS (DHB): 1337.1623 ($[M+Na]^+$, $C_{91}H_{30}NaO_{12}^+$; calc. 1337.1629), 1314.1756 (M^+, $C_{91}H_{30}O_{12}^+$; calc. 1314.1737).

(±)-*Octaethyl 1,2:31,32:39,40:69,70-Tetramethano[70]fullerene-71,71,72,72,73,73,74,74-octacarboxylate* ((±)-**24**). A soln. of (±)-**4** (16.4 mg, 0.01417 mmol) in PhMe (40 ml) was sonicated and purged with Ar; then $(EtO_2C)_2CH_2$ (4.54 mg, 0.02834 mmol) and I_2 (7.20 mg, 0.02834 mmol) were added. Subsequently, MeCN (2.0 ml) was added, followed by slow addition (30 min) of DBU (12.95 mg, 0.08502 mmol) in PhMe (2.0 ml). The mixture was stirred for 2 h at r.t.; then, Me_2SO (8.0 ml) was added over a period of 2 h. After stirring overnight at r.t., the mixture was partitioned between PhMe (50 ml), and H_2O (50 ml) and the aq. layer was extracted with PhMe (3 × 20 ml). The combined org. layers were washed with H_2O (3 × 50 ml), dried ($MgSO_4$), and concentrated *in vacuo*. FC (SiO_2; CH_2Cl_2) afforded (±)-**23** (3.35 mg, 18.0%), and (±)-**24** (11.27 mg, 54.0%).

Data of (±)-**24**: Black solid. M.p. >250°. R_f (SiO_2; PhMe) 0.06. UV/VIS (CH_2Cl_2): 252 (116800), 314 (sh, 35400), 350 (sh, 21900), 374 (sh, 20000), 423 (20900), 527 (7860), 579 (sh, 4260), 623 (sh, 2830). IR (KBr):

2978*w*, 2922*w*, 2361*s*, 2340*s*, 1744*s*, 1288*w*, 1235*s*, 1171*w*, 1089*w*, 1017*w*. ^{1}H-NMR (500.1 MHz, $CDCl_3$, 25°): 4.58 (*q*, *J* = 7.2, 4 H); 4.51 – 4.45 (*m*, 8 H); 4.29 – 4.24 (*m*, 4 H); 1.50 (*t*, *J* = 7.2, 6 H); 1.45 (*t*, *J* = 7.1, 6 H); 1.44 (*t*, *J* = 7.1, 6 H); 1.24 (*t*, *J* = 7.1, 6 H). ^{13}C-NMR (125.8 MHz, $CDCl_3$): 164.47; 163.95; 163.61 (2×); 151.77; 150.89; 150.78; 148.48; 147.97; 147.90; 147.37; 145.81; 144.49; 144.20; 143.80; 142.77; 142.53; 141.74 (2×); 141.61; 141.13; 141.01; 140.79; 140.77; 140.38; 137.91; 137.45; 134.88 (2×); 134.69; 134.24; 133.93; 133.09; 131.29; 128.74; 70.81 (fullerene C(sp^3)); 69.16 (fullerene C(sp^3)); 64.20 (fullerene C(sp^3)); 64.03 (fullerene C(sp^3)); 63.32 (CH_2); 63.24 (2×) (CH_2); 62.85 (CH_2); 40.49 (methano bridge); 39.21 (methano bridge); 14.21 (3×) (Me); 14.00 (Me). MALDI-FT-MS (DHB): 1495.2 (78, $[M + Na]^+$), 1472.2 (43, M^+). HR-MALDI-FT-MS (DHB): 1495.2206 ($[M + Na]^+$, $C_{98}H_{40}NaO_{16}^+$; calc. 1495.2209), 1472.2290 (M^+, $C_{98}H_{40}O_{16}^+$; calc. 1472.2316).

(±)-out,out-*71,72,72,73,73,74-Hexaethyl 71,74-[(6,7,9,10,17,18,20,21-Octahydrodibenzo[*b,k*][1,4,7,10,13,16]-hexaoxacyclooctadecin-2,13-diyl)dimethylene]-1,2:31,32:39,40:69,70-tetramethano[70]fullerene-71,71,72,72,73,73,74,74-octacarboxylate* ((±)-**25**). To a degassed soln. of (±)-**7a** (21.06 mg, 0.0142 mmol) in dry PhMe (40 ml) $(EtO_2C)_2CH_2$ (6.81 mg, 0.0425 mmol) in PhMe (0.9 ml) and I_2 (10.8 mg, 0.0425 mmol) were added sequentially. Subsequently, DBU (21.6 mg, 0.142 mmol) in PhMe (1 ml) was added during 1 h. After stirring for 2 h at r.t., Me_2SO (10 ml) was slowly added during 1 h. After stirring overnight at r.t., the soln. was partitioned between PhMe (50 ml) and H_2O (100 ml). The layers were separated, and the aq. layer was extracted with CH_2Cl_2 (3 × 50 ml). The PhMe and combined CH_2Cl_2 layers were washed separately with H_2O (3 × 50 ml), combined, dried ($MgSO_4$), and concentrated *in vacuo*. FC (SiO_2-*H*; PhMe/AcOEt 1:1) afforded (±)-**25** (19.59 mg, 50%). Red-brown solid. M.p. > 250°. R_f (SiO_2; PhMe/MeOH 9:1) 0.24. UV/VIS (CH_2Cl_2): 261 (sh, 78300), 314 (sh, 25600), 371 (15800), 424 (16300), 489 (sh, 7920), 524 (6020), 577 (sh, 3380), 625 (sh, 2270). IR (KBr): 2976*w*, 2929*w*, 2871*w*, 1744*s*, 1514*w*, 1240*s*, 1172*w*, 1141*w*, 1092*w*. ^{1}H-NMR (500.1 MHz, $CDCl_3$): 6.88 – 6.86 (*m*, 4 H); 6.42 (*d*, *J* = 8.0, 2 H); 5.75 (*d*, *J* = 11.0, 2 H); 4.87 (*d*, *J* = 11.0, 2 H); 4.56 (*q*, *J* = 7.0, 4 H); 4.54 – 4.45 (*m*, 4 H); 4.24 (*q*, *J* = 7.0, 4 H); 4.15 – 4.11 (*m*, 2 H); 4.08 – 4.00 (*m*, 4 H); 3.91 – 3.83 (*m*, 6 H); 3.75 – 3.69 (*m*, 2 H); 3.53 – 3.47 (*m*, 2 H); 1.50 (*t*, *J* = 7.1, 6 H); 1.49 (*t*, *J* = 7.1, 6 H); 1.23 (*t*, *J* = 7.1, 6 H). ^{13}C-NMR (125.8 MHz, $CDCl_3$): 164.39; 163.87; 163.54; 162.23; 151.13; 151.12; 150.52; 148.70; 148.32; 147.73; 147.72; 147.47; 147.03; 145.82. 144.97; 144.26; 143.44; 141.78; 141.71; 141.60; 141.58; 141.13; 140.99; 140.54; 140.12; 139.03; 138.48; 138.04; 137.36; 134.86; 134.78; 134.74; 134.25; 133.32; 131.87; 131.19; 128.47; 127.35; 123.70; 115.15; 111.70; 70.53 (fullerene C(sp^3)); 70.14; 69.91; 69.48; 68.77 (fullerene C(sp^3)); 68.77; 66.92; 64.16 (fullerene C(sp^3)); 63.88 (fullerene C(sp^3)); 63.44; 63.27; 62.76; 40.52 (methano bridge); 39.34 (methano bridge); 14.27 (Me); 14.24 (Me); 14.02 (Me). MALDI-FT-MS (DHB): 1839.3 (8, $[M + K]^+$), 1823.3 (75, $[M + Na]^+$), 1800.3 (5, M^+). HR-MALDI-FT-MS (DHB): 1823.3148 ($[M + Na]^+$, $C_{116}H_{56}NaO_{22}^+$; calc. 1823.3155).

Formation of Higher Adducts of C_{70} Starting From Bis-Adduct (±)-**4**. A soln. of (±)-**4** (27.53 mg, 0.02379 mmol) in dry PhMe (1.0 ml) was added to dry Me_2SO (25.0 ml), and the resulting suspension was sonicated and purged with Ar for 15 min. Subsequently, diethyl 2-bromomalonate (34.12 mg, 0.14275 mmol) in PhMe (0.86 ml) was added, followed by slow addition of DBU (32.61 mg, 0.21417 mmol) in PhMe (0.69 ml) during 30 min. After 1.5 h, TLC confirmed complete conversion of the starting material, and the mixture was worked up by partitioning between PhMe (100 ml) and H_2O (100 ml). The layers were separated, the aq. layer was extracted with PhMe (50 ml), and the combined org. layers were washed with H_2O (5 × 100 ml). Drying ($MgSO_4$) and concentration *in vacuo* afforded a brown film, which, according to TLC, contained four higher-adduct fractions as well as traces of tris- and tetrakis-adducts. Prep. TLC (SiO_2; CH_2Cl_2/AcOEt 98:2) afforded, in the order of elution, pentakis-adduct *Fraction I* (3.80 mg, 9.8%) as a mixture of two diastereoisomers, hexakis-adduct *Fraction II* containing a mixture of two major isomers, hexakis-adduct *Fraction III* (3.17 mg, 7.4%), and *Fraction IV* containing a single heptakis-adduct (7.24 mg, 15.6%). Separation of the two hexakis-adducts in *Fraction II* was achieved by prep. TLC (SiO_2; CH_2Cl_2/AcOEt 39:1) to afford adducts *IIa* (6.57 mg, 15.4%) and *IIb* (1.40 mg, 3.3%).

Fraction I: Decaethyl Pentamethano[70]fullerene-71,71,72,72,73,73,74,74,75,75-decacarboxylate. Brown-black solid. M.p. > 250°. R_f (SiO_2; CH_2Cl_2/AcOEt 79:1) 0.61. UV/VIS (CH_2Cl_2): 251 (sh, 97400), 276 (sh, 68800), 319 (sh, 27600), 372 (sh, 18400), 418 (16800), 509 (sh, 7250), 626 (sh, 1940). ^{1}H-NMR (500.1 MHz, $CDCl_3$): 4.58 – 4.31 (*m*, 14 H); 4.31 – 4.09 (*m*, 6 H); 1.52 – 1.36 (*m*, 21 H); 1.28 – 1.14 (*m*, 9 H). ^{13}C-NMR (125.8 MHz, $CDCl_3$): 164.40; 164.35; 164.29 (2×); 164.24 (2×); 164.13; 164.02; 163.88; 163.83; 163.81; 163.77; 163.76 (2×); 163.65; 163.60; 163.15; 163.09; 162.88; 162.79; 151.76; 151.25; 151.16; 150.35 (2×); 150.07; 148.50 (2×); 148.36; 148.25; 148.17 (2×); 147.82; 147.71; 147.43; 146.87; 146.74; 146.64; 146.42; 146.36; 146.17; 145.79; 145.52; 145.38; 145.28; 145.07; 144.96 (2×); 144.80; 144.56; 144.44 (2×); 143.98; 143.97; 143.89; 143.58; 143.31; 143.24; 143.15; 143.14; 143.11; 143.07; 142.99; 142.87; 142.78 (2×); 142.56; 142.36; 141.98; 141.83; 141.77; 141.71; 141.70; 141.52 (2×); 141.31; 141.15; 141.09; 140.87; 140.54; 140.46; 140.29 (2×); 140.26; 140.13; 139.93; 139.85; 139.67; 139.41; 139.34; 139.25; 138.59; 138.25; 137.75; 137.68; 137.65; 137.61; 137.44; 137.43; 137.36; 137.27; 137.22;

137.13; 136.85; 136.25; 136.19; 136.08; 136.00; 135.43; 135.37; 135.32; 135.20; 135.01; 134.81; 134.70; 134.38; 134.17; 134.04; 133.79; 133.72; 133.70; 133.69; 133.41; 132.99; 132.27; 131.68; 131.48 (2×); 131.16; 131.01; 130.66; 130.19; 129.90; 129.25; 129.07; 127.89; 127.25; 126.99; 126.83; 124.49; 73.82 (fullerene C(sp^3)); 73.38 (fullerene C(sp^3)); 72.24 (fullerene C(sp^3)); 71.65 (fullerene C(sp^3)); 71.12 (fullerene C(sp^3)); 70.55 (fullerene C(sp^3)); 70.13 (fullerene C(sp^3)); 69.30 (fullerene C(sp^3)); 65.13 (fullerene C(sp^3)); 64.77 (2×) (fullerene C(sp^3)); 64.43 (fullerene C(sp^3)); 63.21–62.47 (40×); 62.15 (fullerene C(sp^3)); 62.13 (fullerene C(sp^3)); 61.48 (fullerene C(sp^3)); 61.24 (fullerene C(sp^3)); 61.05 (fullerene C(sp^3)); 59.75 (fullerene C(sp^3)); 59.29 (fullerene C(sp^3)); 58.94 (fullerene C(sp^3)); 43.10 (methano bridge); 42.70 (methano bridge); 40.84 (methano bridge); 40.34 (methano bridge); 40.13 (methano bridge); 40.05 (methano bridge); 38.85 (methano bridge); 38.48 (methano bridge); 37.85 (methano bridge); 36.28 (methano bridge); 14.21–13.85 (20×) (Me). MALDI-FT-MS (DHB): 1669.3 (18.8, $[M+K]^+$), 1653.3 (87.0, $[M+Na]^+$), 1630.3 (6, M^+), 1495.2 (41, $[M+Na-C_7H_{10}O_4]^+$), 1472.2 (19, $[M-C_7H_{10}O_4]^+$), 1337.2 (44, $[M+Na-2\,(C_7H_{10}O_4)]^+$), 1314.2 (53, $[M-2\,(C_7H_{10}O_4)]^+$), 1156.1 (57, $[M-3\,(C_7H_{10}O_4)]^+$), 998.1 (46, $[M-4\,(C_7H_{10}O_4)]^+$), 840.0 (54, C_{70}^+). HR-MALDI-FT-MS (DHB): 1653.2779 ($[M+Na]^+$, $C_{105}H_{50}NaO_{20}^+$; calc. 1653.2788).

Fraction II: Dodecaethyl Hexamethano[70]fullerene-71,71,72,72,73,73,74,74,75,75,76,76-dodecacarboxylate. Isomer IIa: Red-brown solid. M.p. >250°. R_f (SiO_2; CH_2Cl_2/AcOEt 79:1) 0.32. UV/VIS (CH_2Cl_2): 261 (sh, 78300), 314 (sh, 25600), 371 (15800), 424 (16300), 489 (sh, 7920), 524 (6020), 577 (sh, 3380), 625 (sh, 2270). MALDI-FT-MS (DHB): 1827.3 (16, $[M+K]^+$), 1811.3 (76, $[M+Na]^+$), 1788.3 (45, M^+), 1743.3 (34, $[M-C_2H_5O]^+$), 1653.3 (23, $[M+Na-C_7H_{10}O_4]^+$), 1630.3 (12, $[M-C_7H_{10}O_4]^+$), 1472.2 (28, $[M-2\,(C_7H_{10}O_4)]^+$). HR-MALDI-FT-MS (DHB): 1811.3363 ($[M+Na]^+$, $C_{112}H_{60}NaO_{24}^+$; calc. 1811.3367). *Isomer IIb:* Red-brown solid. M.p. >250°. R_f (SiO_2; CH_2Cl_2/AcOEt 79:1) 0.17. UV/VIS (CH_2Cl_2): 252 (sh, 102400), 275 (sh, 79200), 316 (sh, 33500), 372 (20000), 425 (18600), 505 (sh, 7340), 600 (sh, 1840), 674 (sh, 240). MALDI-FT-MS (DHB): 1827.3 (16, $[M+K]^+$), 1811.3 (76, $[M+Na]^+$), 1788.3 (45, M^+), 1743.3 (34, $[M-C_2H_5O]^+$), 1653.3 (23, $[M+Na-C_7H_{10}O_4]^+$), 1630.3 (12, $[M-C_7H_{10}O_4]^+$), 1472.2 (28, $[M-2\,(C_7H_{10}O_4)]^+$). HR-MALDI-FT-MS (DHB): 1811.3363 ($[M+Na]^+$, $C_{112}H_{60}NaO_{24}^+$; calc. 1811.3367).

Fraction III: Dodecaethyl Hexamethano[70]fullerene-71,71,72,72,73,73,74,74,75,75,76,76-dodecacarboxylate: Red solid. M.p. >250°. R_f (SiO_2; CH_2Cl_2/AcOEt 79:1) 0.20. UV/VIS (CH_2Cl_2): 247 (sh, 89500), 275 (sh, 61900), 314 (sh, 31100), 374 (16700), 416 (sh, 14200), 482 (sh, 6310), 526 (sh, 4280), 567 (sh, 2310), 597 (sh, 960). MALDI-FT-MS (DHB): 1811.3 (96, $[M+Na]^+$), 1789.3 (38, M^+), 1743.3 (33, $[M-C_2H_5O]^+$), 1654.3 (34, $[M+Na-C_7H_{10}O_4]^+$), 1473.2 (54, $[M-2\,(C_2H_5O)]^+$). HR-MALDI-FT-MS (DHB): 1811.3387 ($[M+Na]^+$, $C_{112}H_{60}NaO_{24}^+$; calc. 1811.3367).

Fraction IV: Tetradecaethyl Heptamethano[70]fullerene-71,71,72,72,73,73,74,74,75,75,76,76,77,77-tetradecacarboxylate: Orange-red solid. M.p. >250°. R_f (SiO_2; CH_2Cl_2/AcOEt 79:1) 0.08. UV/VIS (CH_2Cl_2): 247 (sh, 81200), 271 (sh, 61700), 324 (sh, 27100), 372 (18500), 482 (sh, 6230), 530 (sh, 3050). ^{1}H-NMR (500.1 MHz, $CDCl_3$): 4.52–4.07 (*m*, 28 H); 1.60–1.12 (*m*, 42 H). ^{13}C-NMR (125.8 MHz, $CDCl_3$): 164.52 (2×); 164.16 (2×); 164.03; 163.75; 163.67; 163.61; 162.95; 162.87; 162.80; 162.74; 162.52; 161.37; 149.75; 147.26; 146.53; 145.43; 145.15; 145.13; 144.79; 144.59; 144.31; 144.10; 143.92; 142.75; 142.73; 142.29; 141.50; 140.93; 140.89; 140.82; 139.63; 139.47; 139.40; 139.05; 138.96; 138.93; 138.59; 138.20; 138.05; 137.68; 137.63; 137.17; 137.07; 135.73; 135.67; 135.51; 135.29; 135.00; 134.83; 134.52; 134.44; 134.17; 133.27 (2×); 133.18; 133.01; 132.77; 132.27; 132.05; 131.36; 131.21; 130.95; 130.83; 130.69; 130.57; 127.98; 127.90; 127.59; 97.16; 90.61; 73.14 (fullerene C(sp^3)); 70.13 (fullerene C(sp^3)); 66.07 (fullerene C(sp^3)); 64.80 (fullerene C(sp^3)); 64.03 (fullerene C(sp^3)); 62.83 (2×); 62.73 (2×); 62.60; 62.55; 62.43 (2×); 62.39 (2×); 62.31; 62.28; 62.19; 61.97; 61.43 (fullerene C(sp^3)); 61.02 (fullerene C(sp^3)); 60.95 (fullerene C(sp^3)); 59.33 (fullerene C(sp^3)); 58.39 (fullerene C(sp^3)); 56.66 (fullerene C(sp^3)); 54.01 (fullerene C(sp^3)); 53.20 (fullerene C(sp^3)); 44.25 (methano bridge); 42.18 (methano bridge); 41.53 (methano bridge); 41.24 (methano bridge); 40.26 (methano bridge); 39.14 (methano bridge); 13.98–13.57 (14×) (Me). MALDI-FT-MS (DHB): 1985.4 (15, $[M+K]^+$), 1969.4 (78, $[M+Na]^+$), 1946.4 (21, M^+), 1901.4 (32, $[M-C_2H_5O]^+$), 1811.3 (28, $[M+Na-C_7H_{10}O_4]^+$), 1788.3 (10, $[M-C_7H_{10}O_4]^+$), 1653.3 (14, $[M+Na-2\,(C_7H_{10}O_4)]^+$), 1630.3 (56, $[M-2\,(C_7H_{10}O_4)]^+$), 1472.2 (23, $[M-3\,(C_7H_{10}O_4)]^+$). HR-MALDI-FT-MS (DHB): 1969.3949 ($[M+Na]^+$, $C_{119}H_{70}NaO_{28}^+$; calc. 1969.3951).

(±)-out,out:out,out-*71,72,73,74-Tetraethyl 71,74-[(6,7,9,10,17,18,20,21-Octahydrodibenzo[*b,k*][1,4,7,10,13,16]-hexaoxacyclooctadecin-2,13-diyl)dimethylene]-72,73-[(6,7,9,10,17,18,20,21octahydrodibenzo[*b,k*][1,4,7,10,13,16]-hexaoxacylooctadecin-2,14-diyl)dimethylene]-1,2:31,32:39,40:69,70-tetramethano[70]fullerene-71,71,72,72,73,73,74,74-octacarboxylate* ((±)-**28a**). To a degassed soln. of (±)-**7a** (20.0 mg, 0.0135 mmol) in dry PhMe (30 ml), **6** (17.5 mg, 0.0269 mmol) in MeCN (2 ml) and I_2 (14.0 mg, 0.0552 mmol) were added sequentially. Subsequently, DBU (20.1 µl, 20.5 mg, 0.135 mmol) in MeCN (1 ml) was added during 35 min, followed by slow addition of Me_2SO (10 ml) over a period of 1 h. After stirring for 2 h, the soln. was partitioned between PhMe (50 ml) and

H_2O (100 ml). The layers were separated, and the aq. layer was extracted with CH_2Cl_2 (3 × 50 ml). The PhMe and combined CH_2Cl_2 layers were washed separately with H_2O (3 × 50 ml), combined, dried ($MgSO_4$), and concentrated *in vacuo*. The residual brown solid was purified by FC (SiO_2-*H*; PhMe/MeOH 19:1) to afford (±)-**28a** (9.0 mg, 31%). Red-brown solid. M.p. >250°. R_f (SiO_2; PhMe/MeOH 9:1) 0.08. UV/VIS (CH_2Cl_2): 269 (sh, 87900), 314 (sh, 32200), 375 (sh, 17300), 422 (18500), 490 (sh, 9720), 533 (sh, 7340), 579 (sh, 3700), 625 (sh, 2360). IR (KBr): 2956*w*, 2922*w*, 2878*w*, 2367*m*, 2344*m*, 1744*s*, 1633*m*, 1517*w*, 1456*w*, 1428*w*, 1383*w*, 1250*s*, 1172*w*, 1139*m*, 1094*w*, 1067*w*. ^{1}H-NMR (500.1 MHz, $CDCl_3$): 7.09 (*d*, *J* = 7.9, 1 H); 6.93 (*s*, 1 H); 6.86–6.80 (*m*, 5 H); 6.71 (*d*, *J* = 7.9, 1 H); 6.56 (*d*, *J* = 8.0, 1 H); 6.39 (*d*, *J* = 8.5, 1 H); 6.33 (*d*, *J* = 8.3, 1 H); 6.21 (*d*, *J* = 1.1, 1 H); 5.79 (*d*, *J* = 11.6, 1 H); 5.73 (*d*, *J* = 11.0, 1 H); 5.68 (*d*, *J* = 11.0, 1 H); 5.54 (*d*, *J* = 11.0, 1 H); 4.99 (*d*, *J* = 11.6, 1 H); 4.88 (*d*, *J* = 11.0, 1 H); 4.82 (*d*, *J* = 11.0, 1 H), 4.68 (*d*, *J* = 11.0, 1 H); 4.61–3.61 (*m*, 40 H); 1.54 (*t*, *J* = 7.1, 3 H); 1.53 (*t*, *J* = 7.1, 3 H); 1.49 (*t*, *J* = 7.1, 3 H); 1.30 (*t*, *J* = 7.1, 3 H). ^{13}C-NMR (125.8 MHz, $CDCl_3$): 164.62; 163.71; 163.61; 162.96; 162.47; 162.32; 162.08; 162.03; 151.65; 151.49; 151.01; 150.94; 149.42; 149.16; 149.12; 148.87. 148.85; 148.79; 148.66; 148.52; 148.26; 147.99; 147.71; 147.64; 147.48; 147.41 (2×); 147.30; 147.28; 147.06; 146.00; 145.00; 144.40; 144.35; 143.95; 143.90; 143.07; 142.34; 141.68; 141.64; 141.59; 141.51; 141.47; 141.27; 141.16; 141.15; 140.97; 140.96; 140.72; 140.68; 140.35; 139.16; 139.02; 138.98; 138.85 (2×); 138.51; 138.27; 138.06; 137.36; 137.00; 136.75; 135.11; 135.04; 134.79; 134.52; 134.20; 134.00; 133.95; 133.40; 133.24; 133.21; 132.35; 131.85; 131.62; 130.24; 129.27; 128.62; 127.32; 127.23; 126.87; 126.04; 123.64; 123.59; 123.43; 122.09; 115.17; 115.08; 114.20; 112.15; 112.10; 112.97 111.63 (2×); 70.68; 70.58 (2×); 70.40; 70.21; 70.05; 69.97; 69.92; 69.75; 69.65; 69.44 (2×); 69.38; 69.01; 68.80; 68.73; 68.66; 68.46; 68.10; 67.95; 67.72; 67.67; 66.97; 66.87; 64.07 (fullerene C(sp^3)); 64.05 (fullerene C(sp^3)); 63.40 (2×); 63.30 (fullerene C(sp^3)); 63.28 (fullerene C(sp^3)); 63.23; 62.98; 40.24 (methano bridge); 40.07 (methano bridge); 39.46 (methano bridge); 39.11 (methano bridge); 14.39 (Me); 14.33 (Me); 14.12 (Me); 14.09 (Me). MALDI-FT-MS (DHB): 2167.4 (9, $[M+K]^+$), 2151.4 (66, $[M+Na]^+$), 2107.4 (46, $[M-C_2H_5O]^+$), 2063.4 (28, $[M-2\,(C_2H_5O)]^+$), 840.0 (6, C_{70}^+). HR-MALDI-FT-MS (DHB): 2151.4130 ($[M+Na]^+$, $C_{134}H_{72}NaO_{28}^+$; calc. 2151.4102).

(±)-out,out:out,out-*71,72,73,74-Tetraethyl 71,74-[(6,7,9,10,17,18,20,21-Octahydrodibenzo[*b,k*][1,4,7,10,13,16]-hexaoxacyclooctadecin-2,13-diyl)dimethylene]-72,73-[(6,7,9,10,17,18,20,21octahydrodibenzo[*b,k*][1,4,7,10,13,16]-hexaoxacyclooctadecin-2,14-diyl)dimethylene]-1,2:31,32:39,40:69,70-tetramethano[70]fullerene-71,71,72,72,73,73,74,74-octacarboxylate* ((±)-**28b**). To a degassed soln. of (±)-**7b** (35.0 mg, 0.0236 mmol) in dry PhMe (35 ml), **6** (30.6 mg, 0.0471 mmol) in MeCN (2 ml) and I_2 (23.9 mg, 0.0942 mmol) were added sequentially. Subsequently, DBU (35.2 µl, 35.9 mg, 0.236 mmol) in MeCN (1 ml) was added during 35 min, followed by slow addition of Me_2SO (10 ml) over a period of 1 h. After stirring for 2 h, the soln. was partitioned between PhMe (50 ml) and H_2O (100 ml). The layers were separated, and the aq. layer was extracted with CH_2Cl_2 (3 × 50 ml). The PhMe and combined CH_2Cl_2 layers were washed separately with H_2O (3 × 50 ml), combined, dried ($MgSO_4$), and concentrated *in vacuo*. The residual brown solid was purified by FC (SiO_2-*H*; PhMe/MeOH 19:1) to afford (±)-**28b** (13.0 mg, 26%). Red-brown solid. M.p. >250°. R_f (SiO_2; PhMe/MeOH 9:1) 0.07. UV/VIS (CH_2Cl_2): 264 (sh, 91300), 314 (sh, 31800), 376 (sh, 17800), 422 (19300), 490 (sh, 8950), 533 (7130), 581 (sh, 3610), 630 (sh, 2300). IR (KBr): 2956*w*, 2922*m*, 2867*w*, 2367*m*, 2360*m*, 2345*m*, 1744*s*, 1633*m*, 1517*m*, 1461*w*, 1428*w*, 1383*w*, 1239*s*, 1172*m*, 1139*m*, 1094*w*, 1072*w*. ^{1}H-NMR (500.1 MHz, $CDCl_3$): 7.11 (*d*, *J* = 8.1, 1 H); 7.043 (*d*, *J* = 8.2, 1 H); 7.040 (*d*, *J* = 8.2, 1 H); 6.94 (*d*, *J* = 1.7, 1 H); 6.89 (*d*, *J* = 8.1, 1 H); 6.79 (*d*, *J* = 1.7, 1 H); 6.69–6.64 (*m*, 4 H); 6.48 (*d*, *J* = 8.0, 1 H); 6.21 (*d*, *J* = 1.7, 1 H); 5.83 (*d*, *J* = 11.7, 1 H); 5.54 (*d*, *J* = 11.2, 1 H); 5.45 (*d*, *J* = 11.0, 1 H); 5.41 (*d*, *J* = 11.0, 1 H); 5.30 (*d*, *J* = 11.0, 1 H); 5.22 (*d*, *J* = 11.0, 1 H); 5.01 (*d*, *J* = 11.7, 1 H); 4.68 (*d*, *J* = 11.2, 1 H); 4.64–4.55 (*m*, 6 H); 4.51–4.44 (*m*, 2 H); 4.38–3.63 (*m*, 32 H); 1.56 (*t*, *J* = 7.2, 3 H); 1.50 (*t*, *J* = 7.1, 3 H); 1.46 (*t*, *J* = 7.2, 3 H); 1.31 (*t*, *J* = 7.1, 3 H). ^{13}C-NMR (125.8 MHz, $CDCl_3$): 164.69; 163.94; 163.87; 163.49; 163.47; 163.09; 162.66; 162.16; 151.68; 151.20; 150.87; 150.65; 149.16 (2×); 149.12 (2×); 148.92; 148.87; 148.69; 148.59; 148.30; 147.97; 147.92 (2×); 147.70; 147.53; 147.42; 147.40; 147.30; 146.99; 145.89; 145.16; 144.58; 144.30; 144.08; 144.01; 143.12; 142.20; 142.07; 141.74; 141.68; 141.53; 141.31; 141.09; 140.78 (2×); 140.73; 140.51; 140.44; 140.37; 140.31; 139.93; 139.25; 139.06 (2×); 139.00; 138.62; 138.06; 137.42; 136.94; 136.64; 135.00; 134.98; 134.33 (2×); 134.26; 133.82; 133.67; 133.62; 133.45; 133.05; 132.50; 132.32 (2×); 130.28; 129.58; 128.13; 127.59; 127.44; 127.01; 126.12; 124.53; 124.42; 123.34; 121.86; 114.98; 114.53; 113.10; 112.39; 112.11 (2×); 112.00; 111.89 (2×); 70.79; 70.69; 70.45; 70.20; 70.16; 69.85 (2×); 69.77; 69.73; 69.65; 69.15; 69.08; 69.02; 68.97; 68.93; 68.86; 68.49 (2×); 68.37; 68.19 (2×); 68.03; 67.70; 67.56; 64.04 (2×) (fullerene C(sp^3)); 63.40; 63.36 (fullerene C(sp^3)); 63.34 (fullerene C(sp^3)); 63.32; 63.21; 63.04; 39.86 (methano bridge); 39.81 (methano bridge); 39.03 (methano bridge); 38.87 (methano bridge); 14.41 (Me); 14.36 (Me); 14.24 (Me); 14.09 (Me). MALDI-FT-MS (DHB): 2167.4 (8, $[M+K]^+$), 2151.4 (66, $[M+Na]^+$), 2107.4 (32, $[M-C_2H_5O]^+$), 2063.4 (19, $[M-2\,(C_2H_5O)]^+$), 840.0 (4, C_{70}^+). HR-MALDI-FT-MS (DHB): 2151.4120 ($[M+Na]^+$, $C_{134}H_{72}NaO_{28}^+$; calc. 2151.4102).

Ion-Selective Electrode (ISE) Membranes. Reagents. The salts and the membrane components sodium tetrakis[3,5-bis(trifluoromethyl)phenyl]borate (NaTFPB), bis(2-ethylhexyl) sebacate (DOS), and poly(vinyl chloride) (PVC) of high molecular weight were purchased from *Fluka*. THF was purchased from *Merck*. Aq. solns. were prepared by dissolving the appropriate salts in deionized water (*NANOpure*^{TM}, *Barnstead*, CH-4009 Basel, specific resistance: 18.0M Ω cm).

Membrane Preparation and EMF Measurements. Master membranes of 5.9-cm diameter were prepared as described in [29a,b] with a total of *ca.* 590 mg DOS/PVC 2:1 and a concentration of the ligands and NaTFPB as given in *Table 1*. One half of each membrane was used to prepare ISEs and the other one for the sandwich membrane experiment. Disks of 5-mm diameter were punched from the master membranes and glued with a THF/PVC slurry to a plasticized PVC tubing (i.d. 4 mm). Three ISEs were prepared for each membrane composition. The internal filling soln. and the conditioning soln. (overnight conditioning) were 10^{-3} M aq. LiCl solns. for all ISEs. All EMF measurements were carried out at r.t. (*ca.* 21°) in stirred solns. with the cell of the type Ag | AgCl | 3M KCl | 1M NH_4NO_3 | sample || membrane || inner filling soln. | AgCl | Ag. Potentials were measured with a 16-channel *Precision Electrochemistry EMF Interface* (*Lawson Labs Inc.*, Malvern, PA). Activity coefficients were calculated according to the *Debye-Hückel* approximation [65].

For all investigated cases, a close to Nernstian response was obtained in the respective chloride solns. in the concentration range of $10^{-1} - 10^{-3}$ M. Selectivity coefficients, $K^{pot}_{K,J}$, were obtained by the separate solutions method (SSM) [57][66] according to the procedure described in [67], which allows the determination of unbiased selectivity coefficients.

Effective complex formation constants with K^+ ions were determined with the sandwich membrane method [58] in 0.1M aq. KCl soln. Those for NH_4^+, Na^+, and H^+ ions were obtained from the selectivity coefficients of the membranes with and without ionophore ($K^{pot}_{K,J}$(L) and $K^{pot}_{K,J}$(IE), resp.) [55][59]:

$$\beta^{eff}_{JL} = \frac{K^{pot}_{K,J}(L)}{K^{pot}_{K,J}(IE)}\beta^{eff}_{KL}$$

The standard deviations for K^+ were calculated from the results obtained with five ISEs from the same membrane.

For the C_{70} bis-crowns ether conjugates (±)-**28a** and (±)-**28b**, effective complex formation constants, β^{eff}_{IL} and $\beta^{eff}_{I_2L}$, with K^+ ions were determined with the sandwich membrane method [58] in 0.1M aq. KCl solns. This requires the application of electroneutrality, the mass balances for the ligand and the anionic sites, and the formalism given in [58] for sandwich membranes. The constants were calculated by least-squares fitting. The standard deviations of the constants were calculated by developing the sum of squares into a *Taylor* series, omitting second- and higher-order terms.

X-Ray Crystal Structure of (±)-**7a**. X-Ray crystal data at 233 K for $C_{102}H_{36}O_{14}\cdot 6\,(CHCl_3)$ (M_r 2201.52): monoclinic space group $P2_1/n$ (No. 14), $D_c = 1.67$ g cm^{-3}, $Z = 4$, $a = 14.395(4)$, $b = 33.405(9)$, $c = 19.277(6)$ Å, $\beta = 108.67(2)°$, $V = 8782(4)$ Å^3. *Nonius CAD4* diffractometer, CuK_α radiation, $\lambda = 1.5418$ Å. Single crystals were obtained by diffusion of hexane into a $CHCl_3$ soln. A crystal with linear dimensions of *ca.* $0.3 \times 0.3 \times 0.25$ mm was mounted at low temp. to prevent evaporation of enclosed solvents. A semi-empirical absorption correction, based on psi-scans was applied to the data ($T(max) = 0.99$, $T(min) = 0.78$). The structure was solved by direct methods (SIR92) [68] and refined by full-matrix least-squares analysis (SHELXL-97) [69], with an isotropic extinction correction, and $w = 1/[\sigma^2(F_0^2) + (0.115P)^2 + 43.34P]$, where $P = (F_0^2 + F_c^2)/3$. It consists of one ordered molecule of (±)-**7a** and six slightly disordered $CHCl_3$ molecules. All heavy atoms were refined anisotropically (H-atoms isotropically, whereby H-positions are based on stereochemical considerations). Final $R(F) = 0.077$, $wR(F^2) = 0.205$ for 1262 parameters and 7220 reflections with $I > 2\sigma(I)$ and $2.6 < \theta < 53.0°$ (corresponding R values based on all 9732 reflections are 0.105 and 0.234, respectively). *Cambridge Crystallographic Data Centre* Deposition No. CCDC-182/1756.

X-Ray Crystal Structure of **16**. X-Ray crystal data at 208 K for $C_{102}H_{36}O_{14}\cdot H_2O\cdot CH_2Cl_2$ (Mr 1588.25): triclinic space group P_1 (No. 2), $D_c = 1.44$ g cm^{-3}, $Z = 2$, $a = 14.734(3)$, $b = 15.818(5)$, $c = 18.361(7)$ Å, $\alpha = 80.92(2)°$, $\beta = 66.51(2)°$, $\gamma = 68.65(2)°$, $V = 3655(2)$ Å^3. *Nonius CAD4* diffractometer, CuK_α radiation, $\lambda = 1.5418$ Å. Single crystals were obtained by diffusion of hexane into a CH_2Cl_2 soln. A crystal with linear dimensions of *ca.* $0.25 \times 0.15 \times 0.15$ mm was mounted at low temp. to prevent evaporation of enclosed solvents. The structure was solved by direct methods (SHELXS-97) [70] and refined by full-matrix least-squares analysis (SHELXL-97) [69], with an isotropic extinction correction, and $w = 1/[\sigma^2\ (F_0^2 + (0.173P)^2 + 4.149P]$, where

$P=(F_0^2+2F_c^2)/3$. It consists of one ordered molecule of **16**, one H_2O, and two disordered CH_2Cl_2 with population parameters of *ca.* 0.7 and 0.3, resp. All heavy atoms were refined anisotropically (H-atoms isotropically, whereby H-positions are based on stereochemical considerations). Final $R(F)=0.077$, $wR(F2)=0.219$ for 1109 parameters and 5225 reflections with $I>2\sigma(I)$ and $2.62\theta<49.94°$ (corresponding R values based on all 7360 reflections are 0.107 and 0.259, resp.). *Cambridge Crystallographic Data Centre* Deposition No. CCDC-179572.

Crystallographic data (excluding structure factors) for the structures reported in this paper have been deposited with the *Cambridge Crystallographic Data Centre*. Copies of the data can be obtained, free of charge, on application to the CCDC, 12 Union Road, Cambridge CB2 1EZ UK (fax: +44(1223)336033; e-mail: deposit@ccdc.cam.ac.uk).

Electrochemical Experiments. MeCN (*Aldrich*, ACS grade) was distilled over CaH_2. Toluene (*Aldrich*, HPLC grade) was kept under N_2 and used without further purification. Bu_4NPF_6 (*Fluka*) was recrystallized from EtOH, dried under vacuum at 80°, and stored in a dessicator. All other reagents were purchased from *Aldrich*. All salts were dried under vacuum at 80° and stored in a dessicator until used. The measurements were performed under Ar in degassed PhMe/MeCN 4:1 containing 0.1M Bu_4NPF_6 as the supporting electrolyte, using a three-electrode cell. The typical concentration of the fullerene–crown ether conjugates ranged from 0.2 mM to 0.3 mM. For (±)-**28a** and (±)-**28b**, a concentration of 0.5 mM was employed. The concentration of C_{70} was 0.7 mM. The electrochemical cell was kept under Ar, and the latter was saturated with vapors from both solvents. To saturate the atmosphere with these vapors, the Ar was bubbled through a separate chamber containing the solvent mixture. The saturation of the Ar flow with solvent helps to minimize evaporation (and thus concentration) effects. Salts were dissolved in MeCN and added in µl amounts. A *Bioanalytical Systems* (*BAS*) model 100 W potentiostat was used for all measurements. A glassy carbon electrode (3 mm diameter) from *BAS* was used as the working electrode and a nonaqueous Ag/Ag^+ electrode from *BAS* was the reference electrode. Ferrocene (0.5 mM) was added to the cell as an internal reference. A Pt wire served as the counter electrode. The scan rate was 100 mV s^{-1}, and soln. resistance compensation was applied at all times.

Computational Methods. All calculations were performed with SPARTAN 5.1.3 [54]. Input structures for the density-functional-theory (DFT) calculations were generated by running geometry optimizations employing the semi-empirical PM3 Hamiltonian. The DFT calculations were performed on the basis of the p*BP*/DN model. Nonlocal corrections as proposed by *Becke* and *Perdew* (*BP*) were introduced perturbationally (p) after convergence of the local density model (SVWN). The *BP* functional was combined with a numerical split-valence basis set (DN). All DFT calculations were performed without imposing symmetry or geometrical constraints. Molecular orbital plots were generated with the SPARTAN graphics module.

Support by the *Swiss National Science Foundation*, the *U.S. National Institutes of Health* (R01-GM59716), the *US National Science Foundation* (CHE-0135786), the German *Fonds der Chemischen Industrie*, and a *TALENT stipend* (*M. J. v. E.*) of the *Netherlands Organization for Scientific Research* (*NWO*) is gratefully acknowledged. We thank Dr. *L. E. Echegoyen* and Dr. *A. Ceresa* for their help and advice, and Dr. *C. Thilgen* for assistance with the nomenclature.

REFERENCES

[1] C. Thilgen, A. Herrmann, F. Diederich, *Angew. Chem.* **1997**, *109*, 2362; *Angew. Chem., Int. Ed.* **1997**, *36*, 2268; C. Thilgen, F. Diederich, *Top. Curr. Chem.* **1998**, *199*, 135.

[2] A. Hirsch, 'The Chemistry of the Fullerenes', Thieme, Stuttgart, 1994; F. Diederich, C. Thilgen, *Science* 1996, *271*, 317; A. Hirsch, *Top. Curr. Chem.* **1998**, *199*, 1; R. Taylor, 'Lecture Notes on Fullerene Chemistry', Imperial College Press, London, 1999; S. R. Wilson, D. I. Schuster, B. Nuber, M. S. Meier, M. Maggini, M. Prato, R. Taylor, in 'Fullerenes: Chemistry, Physics, and Technology', Eds. K. M. Kadish, R. S. Ruoff, Wiley-Interscience, New York, 2000, pp. 91–176.

[3] R. Taylor, *J. Chem. Soc., Perkin Trans. 2* **1993**, 813; P. R. Birkett, A. G. Avent, A. D. Darwish, H. W. Kroto, R. Taylor, D. R. M. Walton, *J. Chem. Soc., Chem. Commun.* **1995**, 683.

[4] A. Herrmann, F. Diederich, C. Thilgen, H.-U. ter Meer, W. H. Müller, *Helv. Chim. Acta* **1994**, *77*, 1689.

[5] a) C. Bingel, H. Schiffer, *Liebigs Ann. Chem.* **1995**, 1551; b) C. Bingel, *Chem. Ber.* **1993**, *126*, 1957.

[6] A. Herrmann, M. Rüttimann, C. Thilgen, F. Diederich, *Helv. Chim. Acta* **1995**, *78*, 1673.

[7] S. R. Wilson, Q. Lu, *J. Org. Chem.* **1995**, *60*, 6496.

[8] F. Langa, P. de la Cruz, A de la Hoz, W. Espíldora, F. P. Cossío, B. Lecea, *J. Org. Chem.* **2000**, *65*, 2499.

[9] R. C. Haddon, L. T. Scott, *Pure Appl. Chem.* **1986**, *58*, 137; R. C. Haddon, *Acc. Chem. Res.* **1988**, *21*, 243; R. C. Haddon, *Science* **1993**, *261*, 1545.
[10] R. C. Haddon, *Chem. Phys. Lett.* **1986**, *125*, 231; R. C. Haddon, *J. Am. Chem. Soc.* **1986**, *108*, 2837.
[11] J. M. Hawkins, A. Meyer, M. A. Solow, *J. Am. Chem. Soc.* **1993**, *115*, 7499; J. M. Hawkins, A. Meyer, *Science* **1993**, *260*, 1918.
[12] J. Baker, P. W. Fowler, P. Lazzeretti, M. Malagoli, R. Zanasi, *Chem. Phys. Lett.* **1991**, *184*, 182.
[13] A. Rathna, J. Chandrasekhar, *Fullerene Sci. Technol.* **1995**, *3*, 681.
[14] A. Herrmann, M. W. Rüttimann, T. Gibtner, C. Thilgen, F. Diederich, T. Mordasini, W. Thiel, *Helv. Chim. Acta* **1999**, *82*, 261.
[15] X. Zhang, C. S. Foote, *J. Am. Chem. Soc.* **1995**, *117*, 4271.
[16] A. L. Balch, J. W. Lee, M. M. Olmstead, *Angew. Chem.* **1992**, *104*, 1400; *Angew. Chem., Int. Ed.* **1992**, *31*, 1356.
[17] A. L. Balch, L. Hao, M. M. Olmstead, *Angew. Chem.* **1996**, *108*, 211; *Angew. Chem., Int. Ed.* **1996**, *35*, 188.
[18] H. P. Spielmann, G.-W. Wang, M. S. Meier, B. R. Weedon, *J. Org. Chem.* **1998**, *63*, 9865.
[19] A. Hirsch, I. Lamparth, T. Grösser, H. R. Karfunkel, *J. Am. Chem. Soc.* **1994**, *116*, 9385; A. Hirsch, I. Lamparth, G. Schick, *Liebigs Ann. Chem.* **1996**, 1725; F. Djojo, A. Herzog, I. Lamparth, F. Hampel, A. Hirsch, *Chem. Eur. J.* **1996**, *2*, 1537.
[20] P. R. Birkett, A. G. Avent, A. D. Darwish, H. W. Kroto, R. Taylor, D. R. M. Walton, *Chem. Commun.* **1996**, 1231.
[21] L. Isaacs, R. F. Haldimann, F. Diederich, *Angew. Chem.* **1994**, *106*, 2434; *Angew. Chem., Int. Ed.* **1994**, *33*, 2339.
[22] F. Diederich, R. Kessinger, *Acc. Chem. Res.* **1999**, *32*, 537; F. Diederich, R. Kessinger, in 'Templated Organic Synthesis', Eds. F. Diederich, P. J. Stang, Wiley-VCH, Weinheim, 2000, pp. 189–218.
[23] E. Nakamura, H. Isobe, H. Tokuyama, M. Sawamura, *Chem. Commun.* **1996**, 1747; T. Ishi-i, K. Nakashima, S. Shinkai, *Chem. Commun*. **1998**, 1047.
[24] M. Taki, S. Sugita, Y. Nakamura, E. Kasashima, E. Yashima, Y. Okamoto, J. Nishimura, *J. Am. Chem. Soc.* **1997**, *119*, 926.
[25] G. A. Burley, P. A. Keller, S. G. Pyne, G. E. Ball, *Chem. Commun.* **2000**, 1717.
[26] T. Da Ros, M. Prato, V. Lucchini, *J. Org. Chem.* **2000**, *65*, 4289.
[27] M. J. van Eis, R. J. Alvarado, L. Echegoyen, P. Seiler, F. Diederich, *Chem. Commun.* **2000**, 1859.
[28] M. J. van Eis, I. Pérez Núñez, L. A. Muslinkina, R. J. Alvarado, E. Pretsch, L. Echegoyen, F. Diederich, *J. Chem. Soc., Perkin Trans. 2* **2001**, *5*, 1890.
[29] a) J.-P. Bourgeois, L. Echegoyen, M. Fibbioli, E. Pretsch, F. Diederich, *Angew. Chem.* **1998**, *110*, 2203; *Angew. Chem., Int. Ed.* **1998**, *37*, 2118; b) J.-P. Bourgeois, P. Seiler, M. Fibbioli, E. Pretsch, F. Diederich, L. Echegoyen, *Helv. Chim. Acta* **1999**, *82*, 1572; c) J.-P. Bourgeois, C. R. Woods, F. Cardullo, T. Habicher, J.-F. Nierengarten, R. Gehrig, F. Diederich, *Helv. Chim. Acta*, **2001**, *84*, 1207.
[30] Y. Nakamura, A. Asami, S. Inokuma, T. Ogawa, M. Kikuyama, J. Nishimura, *Tetrahedron Lett.* **2000**, *41*, 2193.
[31] F. Diederich, U. Jonas, V. Gramlich, A. Herrmann, H. Ringsdorf, C. Thilgen, *Helv. Chim. Acta* **1993**, *76*, 2445; J. Osterodt, M. Nieger, P.-M. Windscheif, F. Vögtle, *Chem. Ber.* **1993**, *126*, 2331; D. A. Leigh, A. E. Moody, F. A. Wade, T. A. King, D. West, G. S. Bahra, *Langmuir* **1995**, *11*, 2334; U. Jonas, F. Cardullo, P. Belik, F. Diederich, A. Gügel, E. Harth, A. Herrmann, L. Isaacs, K. Müllen, H. Ringsdorf, C. Thilgen, P. Uhlmann, A. Vasella, C. A. A. Waldraff, M. Walter, *Chem. – Eur. J.* **1995**, *1*, 243; F. Arias, L. A. Godínez, S. R. Wilson, A. E. Kaifer, L. Echegoyen, *J. Am. Chem. Soc.* **1996**, *118*, 6086; P. R. Ashton, F. Diederich, M. Gómez-López, J.-F. Nierengarten, J. A. Preece, F. M. Raymo, J. F. Stoddart, *Angew. Chem.* **1997**, *109*, 1611; *Angew. Chem., Int. Ed.* **1997**, *36*, 1448; S. Wang, R. M. Leblanc, F. Arias, L. Echegoyen, *Langmuir* **1997**, *13*, 1672; A. Ikeda, C. Fukuhara, S. Shinkai, *Chem. Lett.* **1997**, 407; M. Kawaguchi, A. Ikeda, S. Shinkai, *J. Chem. Soc., Perkin Trans. 1*, **1998**, 179; Z. Guo, Y. Li, J. Xu, Z. Mao, Y. Wu, D. Zhu, *Synth. Commun.* **1998**, *28*, 1957; F. Diederich, L. Echegoyen, M. Gómez-López, R. Kessinger, J. F. Stoddart, *J. Chem. Soc., Perkin Trans. 2* **1999**, 1577; S.-G. Liu, L. Echegoyen, *Eur. J. Org. Chem.* **2000**, 1157.
[32] F. Diederich, M. Gómez-López, *Chem. Soc. Rev.* **1999**, *28*, 263.
[33] C.-H. Hung, J.-S. Shih, *J. Chin. Chem. Soc.* **2000**, *47*, 1095.
[34] CS Chem3D Pro, Version 5.0, *CambridgeSoft Corporation*, Cambridge, 1999.
[35] A. E. Howard, U. C. Singh, M. Billeter, P. A. Kollman, *J. Am. Chem. Soc.* **1988**, *110*, 6984; T. P. Straatsma, J. A. McCammon, *J. Chem. Phys.* **1989**, *91*, 3631; Y. Sun, P. A. Kollman, *J. Chem. Phys.* **1992**, *97*, 5108.

[36] Y. L. Ha, A. K. Chakraborty, *J. Phys. Chem.* **1991**, *95*, 10781; Y. L. Ha, A. K. Chakraborty, *J. Phys. Chem.* **1993**, *97*, 11291.
[37] a) D. Bright, M. R. Truter, *J. Chem. Soc.* B **1970**, 1544; b) M. A. Bush, M. R. Truter, *J. Chem. Soc. B* **1971**, 1440; c) P. Dapporto, P. Paoli, I. Matijasic, L. Tusek-Bozic, *Inorg. Chim. Acta.* **1996**, *252*, 383; d) P. Dapporto, P. Paoli, I. Matijasic, L. Tusek-Bozic, *Inorg. Chim. Acta.* **1998**, *282*, 76.
[38] J.-F. Nierengarten, T. Habicher, R. Kessinger, F. Cardullo, F. Diederich, V. Gramlich, J.-P. Gisselbrecht, C. Boudon, M. Gross, *Helv. Chim. Acta* **1997**, *80*, 2238.
[39] H. Ajie, M. M. Alvarez, S. J. Anz, R. D. Beck, F. Diederich, K. Fostiropoulos, D. R. Huffman, W. Krätschmer, Y. Rubin, K. E. Schriver, D. Sensharma, R. L. Whetten, *J. Phys. Chem.* **1990**, *94*, 8630; R. Taylor, J. P. Hare, A. K. Abdul-Sada, H. W. Kroto, *J. Chem. Soc., Chem. Commun.* **1990**, 1423.
[40] A. L. Balch, V. J. Catalano, J. W. Lee, M. M. Olmstead, S. R. Parkin, *J. Am. Chem. Soc.* **1991**, *113*, 8953.
[41] P. Cui, L. Li, K. Tang, X. Jin, *J. Chem. Res.* **2001**, 240.
[42] P. Seiler, A. Herrmann, F. Diederich, *Helv. Chim. Acta* **1995**, *78*, 344.
[43] M. Toyota, M. Tori, K. Takikawa, Y. Shiobara, M. Kodama, Y. Asakawa, *Tetrahedron Lett.* **1985**, *26*, 6097; E. A. Couladouros, I. C. Soufli, *Tetrahedron Lett.* **1995**, *36*, 9369; E. A. Couladouros, I. C. Soufli, V. I. Moutsos, R. K. Chadha, *Chem. – Eur. J.* **1998**, *4*, 33.
[44] F. H. Kohnke, J. F. Stoddart, B. L. Allwood, D. J. Williams, *Tetrahedron Lett.* **1985**, *26*, 1681; B. L. Allwood, F. H. Kohnke, A. M. Z. Slawin, J. F. Stoddart, D. J. Williams, *J. Chem. Soc., Chem. Commun.* **1985**, 311.
[45] F. Wada, H. Hirayama, H. Namiki, K. Kikukawa, T. Matsuda, *Bull. Chem. Soc. Jpn.* **1980**, *53*, 1473.
[46] D. A. Grossie, W. H. Watson, F. Vögtle, W. M. Müller, *Acta Crystallogr., Sect. B* **1982**, *38*, 3157; W. H. Watson, J. Galloy, D. A. Grossie, F. Vögtle, W. M. Müller, *J. Org. Chem.* **1984**, *49*, 347; D. Britton, M. K. Chantooni Jr., I. M. Kolthoff, *Acta Crystallogr., Sect. C* **1988**, *44*, 303; L. Parenteau, F. Brisse, *Can. J. Chem.* **1989**, *67*, 1293; A. Albert, D. Mootz, *Z. Naturforsch. B* **1998**, *53*, 242.
[47] P. J. Dutton, F. R. Fronczek, T. M. Fyles, R. D. Gandour, *J. Am. Chem. Soc.* **1990**, *112*, 8984; B. Belamri, C. Bavoux, A. Thozet, *J. Inclusion Phenom. Mol. Recognit. Chem.* **1990**, *8*, 383; D. Mootz, A. Albert, S. Schaefgen, D. Stäben, *J. Am. Chem. Soc.* **1994**, *116*, 12045.
[48] S. D. Burke, Q. Zhao, *J. Org. Chem.* **2000**, *65*, 1489.
[49] P. Hodge, J. Waterhouse, *J. Chem. Soc., Perkin Trans 1* **1983**, 2319.
[50] R. Ungaro, B. El-Haj, J. Smid, *J. Am. Chem. Soc.* **1976**, *98*, 5198.
[51] A. Hirsch, I. Lamparth, H. R. Karfunkel, *Angew. Chem.* **1994**, *106*, 453; *Angew. Chem., Int. Ed.* **1994**, *33*, 437.
[52] L. Isaacs, P. Seiler, F. Diederich, *Angew. Chem.* **1995**, 107, 1636; *Angew. Chem., Int. Ed.* **1995**, *34*, 1466.
[53] a) A. F. Kiely, R. C. Haddon, M. S. Meier, J. P. Selegue, C. P. Brock, B. O. Patrick, G.-W. Wang, Y. Chen, *J. Am. Chem. Soc.* **1999**, *121*, 7971; b) M. S. Meier, G.-W. Wang, R. C. Haddon, C. P. Brock, M. A. Lloyd, J. P. Selegue, *J. Am. Chem. Soc.* **1998**, *120*, 2337.
[54] Spartan SGI Version 5.1.3, *Wavefunction, Inc.*, 18401 Von Karman Ave., Irvine, CA 82715, 1998.
[55] E. Bakker, P. Bühlmann, E. Pretsch, *Chem. Rev.* **1997**, *97*, 3083.
[56] E. Bakker, E. Pretsch, *Anal. Chem.* **1998**, *70*, 295.
[57] E. Bakker, E. Pretsch, P. Bühlmann, *Anal. Chem.* **2000**, *72*, 1127.
[58] Y. Mi, E. Bakker, *Anal. Chem.* **1999**, *71*, 5279.
[59] A. Ceresa, E. Pretsch, *Anal. Chim. Acta* **1999**, *395*, 41.
[60] C. Boudon, J.-P. Gisselbrecht, M. Gross, A. Herrmann, M. Rüttimann, J. Crassous, F. Cardullo, L. Echegoyen, F. Diederich, *J. Am. Chem. Soc.* **1998**, *120*, 7860.
[61] S. R. Miller, D. A. Gustowski, Z.-H. Chen, G. W. Gokel, L. Echegoyen, A. E. Kaifer, *Anal. Chem.* **1988**, *60*, 2021.
[62] T. Da Ros, M. Prato, M. Carano, P. Ceroni, F. Paolucci, S. Roffia, *J. Am. Chem. Soc.* **1998**, *120*, 11645.
[63] J. Zheng, K. Tashiro, Y. Hirabayashi, K. Kinbara, K. Saigo, T. Aida, S. Sakamoto, K. Yamaguchi, *Angew. Chem.* **2001**, *113*, 1909; *Angew. Chem., Int. Ed.* **2001**, *40*, 1857.
[64] a) C. Boudon, J.-P. Gisselbrecht, M. Gross, L. Isaacs, H. L. Anderson, R. Faust, F. Diederich, *Helv. Chim. Acta* **1995**, *78*, 1334; b) F. Cardullo, P. Seiler, L. Isaacs, J.-F. Nierengarten, R. F. Haldimann, F. Diederich, T. Mordasini-Denti, W. Thiel, C. Boudon, J.-P. Gisselbrecht, M. Gross, *Helv. Chim. Acta* **1997**, *80*, 343.
[65] P. C. Meier, *Anal. Chim. Acta* **1982**, *136*, 363.
[66] G. G. Guilbault, R. A. Durst, M. S. Frant, H. Freiser, E. H. Hansen, T. S. Light, E. Pungor, G. Rechnitz, N. M. Rice, T. J. Rohm, W. Simon, J. D. R. Thomas, *Pure Appl. Chem.* **1976**, *48*, 127.
[67] E. Bakker, *Anal. Chem.* **1997**, *69*, 1061.

[68] A. Altomare, G. Cascarano, C. Giacovazzo, A. Guagliardi, M. C. Burla, G. Polidori, M. Camalli, *J. Appl. Crystallogr.* **1994**, *27*, 435.
[69] G. M. Sheldrick, SHELXL-97 Program for the Refinement of Crystal Structures, University of Göttingen, Germany, 1997.
[70] G. M. Sheldrick, SHELXS-97 Program for the Solution of Crystal Structures, University of Göttingen, Germany, 1997.

Received April 3, 2002